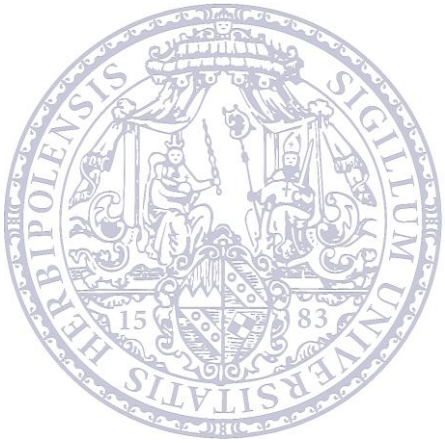

Oxidative stress: Role in genomic damage and disease

Oxidativer Stress: Bedeutung für genomische Schäden und Krankheit

Doctoral thesis for a doctoral degree at the Graduate School of Life Sciences, Julius-Maximilians-Universität Würzburg, Section Biomedicine

Submitted by

Gnana Oli Rajaraman

from

Kanchipuram

Wuerzburg 2011

Submitted on: ……..……..

Members of the *Promotionskomitee:*

Chairperson: …… Prof. Dr. Ulrike Holzgrabe

Primary Supervisor: ……..……..Prof. Dr. Helga Stopper

Supervisor (Second): ……..PD Dr. Tcholpon Djuzenova

Supervisor (Third): ……PD Dr. Alois Palmetshofer

Date of Public Defence: ……..……

Date of Receipt of Certificates: ……..

Contents

Abbreviations

ACE i	Angiotensin converting enzyme inhibitors
ACN	acetonitril
Ald	Aldosterone
Ang II	Angiotensin II
AT1R	Angiotensin II type 1 receptor
BSA	Bovine serum albumin
CE	Collision energy
COMT	Catecholamine-O-methyltransferase
CXP	Collision cell exit potential
DAT	Dopamine transporters
DFO	Deferoxamine
dG	Deoxyguanine
^{15}N-dG	Stable isotope labeled deoxyguanine
DHE	Dihydroethidium
DNA	Deoxyribonucleic acid
DOCA	Deoxycorticosterone acetate
DP	Declustering potential
EDTA-Na_2	Ethylenediamine-tetraacetic acid disodium salt
EtOH	Ethanol
ESCODD	European standard committee on oxidative DNA damage
ESCULA	European standard committee on urinary oxidative DNA lesion analysis
FBS	Fetal bovine serum
FDA	Food and drug administration
FOH	Farnesol
FPP	Farnesol pyrophosphate
FP	Focusing potential
FRAP	Ferric reducing antioxidant property
GC-MS	Gas chromatography –mass spectrometer
GGOH	Geranylgeraniol

GPx	Glutathione peroxidase
GR	Glutathione reductase
GSS	Glutathione synthatase
GSH	Glutathione reduced form
$^{13}C_2$-^{15}N-GSH	Glycine labeled glutathione reduced form
GSSG	Glutathione oxidized form
$^{13}C_2$-^{15}N-GSSG	Glycine labeled glutathione oxidized form
h	Hour
H_2O_2	Hydrogen peroxide
HPLC	High performance liquid chromatography
HPLC-UV	High performance liquid chromatography-ultra violet
HPLC-ECD	High performance liquid chromatography-electro chemical detector
HPLC-FL	High performance liquid chromatography-fulorescence
HMG-CoA	3-hydroxy-3-methylglutarylcoenzyme A
iMAEC	Immortalized mouse aortic endothelial cells
L-DOPA	levodopa
LAT1	L-type amino acid transporter
LC-MS	Liquid chromatography-mass spectrometry
LC-ESI-MS/MS	Liquid chromatography-electro spray ionization mass spectrometry
LLC-PK1	Porcine kidney cell line
LOD	Limit of detection
LOQ	Limit of quantification
M	Mol per liter
MAO	Monoamino oxidase
µM	Micromole per liter
min	Minute
MeOH	Methanol
MN	Micronuclei
MRM	Multiple reaction monitoring
m/z	Mass to charge ratio
NADH	Nicotinamide adenine dinucleotide, reduced form

NADPH	Nicotinamide adenine dinucleotide phoshate, reduced form
NaCl	Sodium chloride
NaOH	Sodium hydroxide
NEM	N-ethylmaleimide
NOXO1	NOX1 organizer subunit
8-NitroG	8-nitroguanine
nm	Nanometer
nM	Nanomole per liter
NOX	NADPH oxidase
NO	Nitric oxide
$^{1}O_2$	Singlet oxygen
O_2	Molecular oxygen
$O_2^{\bullet -}$	Superoxide anion
$^{\bullet}OH$	Hydroxyl radical
$ONOO^-$	Peroxynitrite
8-oxodG	8-oxo-deoxyguanosine
8-OHdG	8-hydroxyguanine
^{15}N-8-oxodG	Stable isotope labeled 8-oxo-deoxyguanosine
PBMC	Peripheral blood monocyte cells
PD	Parkinson’s disease
pM	Picomol per liter
p22phox	Membrane subunit of NOX enzyme
p40phox	Cytosolic subunit of NOX enzyme
p67phox	Activator subunit of NOX enzyme
p47phox	Organizer subunit of NOX enzyme
p47phox$^{-/-}$	p47phox knockout
p47phox$^{-/-}$ Y	p47phox knockout young
p47phox$^{-/-}$O	p47phox knockout old
Rac	Member of a family of hydrolases that bind and hydrolyze GTP
RAAS	Renin-angiotensin-aldosterone system
RIA	Radio immune assay
RNA	Ribonucleic acid

ROS	Reactive oxygen species
RSV	Rosuvastatin
%RSD	Percent relative standard deviation
RT	Retention time
rpm	Rounds per minute
RPMI	Roswell Park Memorial Institute medium
SEM	Standard error of the mean
SOD	Superoxide dismutase
±SE	Plus or minus standard error
SPE	Solid phase extraction
S/N	Signal to noise ration
WT	Wild type: C57BL/6 background wild type mice
WTY	Wild type young: C57BL/6J background wild type young mice
WTO	Wild type old: C57BL/6J background wild type old mice

1 Introduction

1.1 The NADPH oxidases (NOX)

The NADPH Oxidase (NOX) enzymes are transmembrane electron transporters. They transport electrons from the cytoplasmic electron donor NADPH to molecular oxygen and, which is reduced to superoxide anion radicals [1, 2]. The function of each NADPH oxidase requires the interaction of at least two cytosolic proteins, including GTPases, phox proteins, and proteins of the cytoskeleton. In mammalian cells seven NOX proteins have been identified, namely NOX1, NOX2, NOX3, NOX4, NOX5 and DUOX1 and DUOX2. All of these proteins differ in their mode of activation, expression, and interaction with other proteins and possibly in the type of ROS formed [3].

1.2 NOX1

Superoxide generation by NOX1 depends on subunits, such as small membrane bound protein p22phox, cytosolic subunits NOXO1 (NOX organizer 1= p47phox homolog) and NOXA1 (NOX activator 1 = p67phox homolog) and small GTPase binding protein Rac (see Figure 1) [2, 4]. NOX1 is highly expressed in colon but also found in intermediate-to- low amounts in smooth muscle, endothelium, fibroblasts, prostate and uterus [1, 5, 6]. The Best known function of NOX1 is in the vascular system, where it plays a prohypertensive role, particularly after angiotensin II stimulation [7].

1.3 NOX2

NOX2 is the prototype NOX, also known as gp91phox. Activation of NOX2 requires membrane bound p22phox, cytosolic proteins p47phox, p67phox and p40phox. p22phox helps to stabilize the NOX proteins. The organizer protein p47phox is phosphorylated upon cell activation and translocated to the membrane p22phox along with activator p67phox, the GTP binding protein Rac and modulator protein p40phox. After translocation of p67phox to the membrane, it directly interacts with NOX2 and activates the enzyme [1, 2]. NOX2 is most abundant in phagocytes [1, 2, 6, 8] and lower but quantitatively significant amounts are found in kidney [9], smooth muscle cells, and

fibroblast [8]. The well known function of NOX2 is microbial killing [8]. In addition NOX2 might be involved in ageing, particularly through an inflammatory process [10].

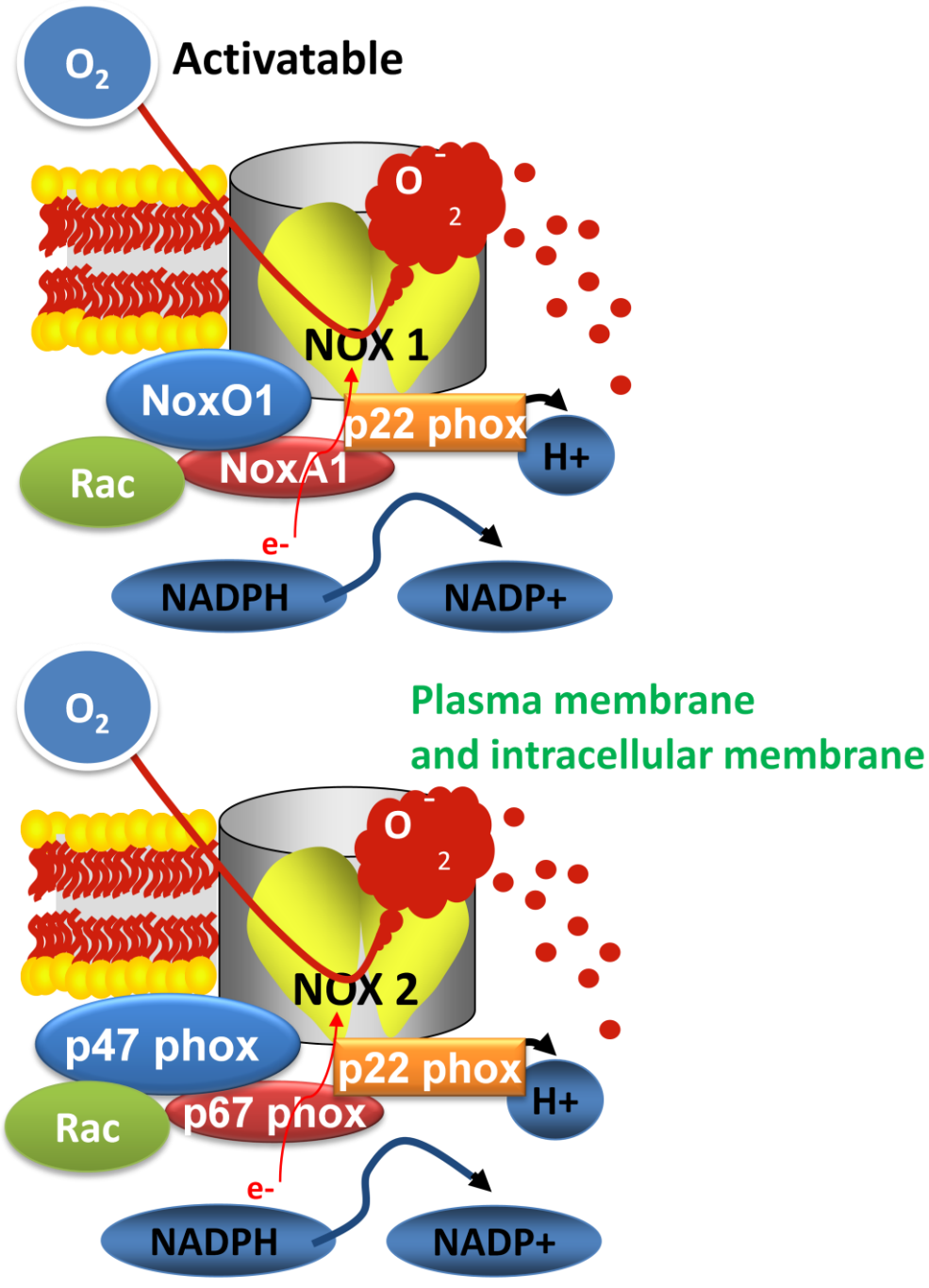

Figure 1: Schematic diagram of NOX1 and NOX2 and activation by their cytosolic subunits

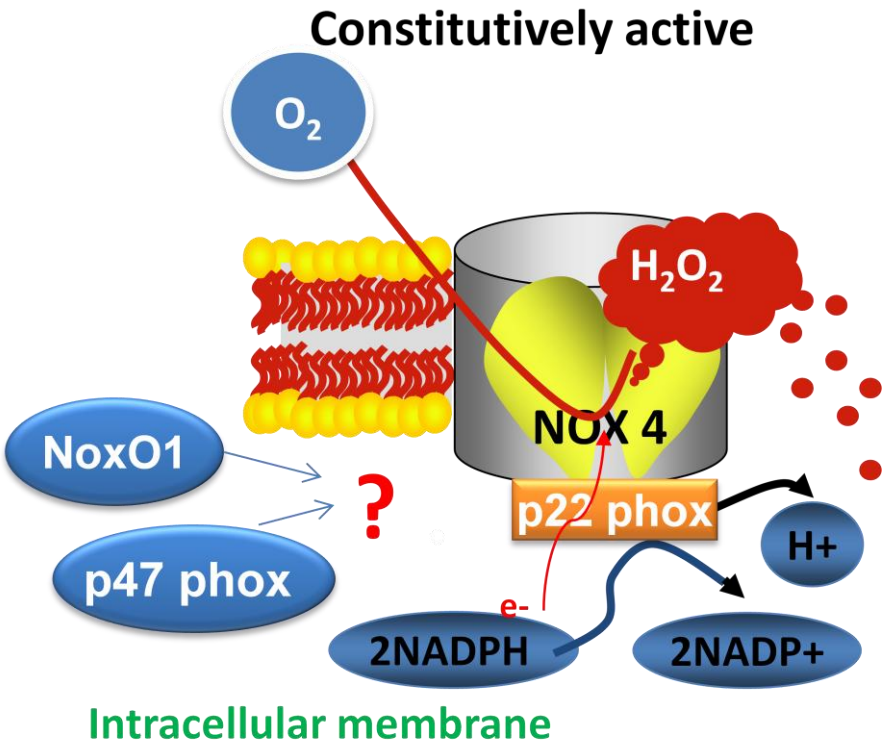

Figure 2: Schematic diagram of NOX4 and activation by its cytosolic subunits.

1.4 NOX3

NOX3 activation needs the stabilizer protein p22phox, but it is not clear whether cytosolic proteins are involved. NOX3 probably exhibits the most specific and restricted tissue expression. It is essentially found in the inner ear, both the vestibular and the auditive part [11, 12].

1.5 NOX4

NOX4 shares only about 39% identity with NOX2. NOX4 activation requires p22phox but most likely no cytosolic proteins such as p47phox, p67phox and p40phox. This enzyme is highly expressed in the kidney and endothelial cells [2] and also present in embryonic stem cells, fibroblasts, osteoclasts and neurons [1]. NOX3, NOX5, DUOX1 and DUOX2 are calcium dependent and produce hydrogen peroxide.

1.6 The organizer protein p47phox

p47phox [13, 14] is a cytosolic organizer protein for NOX2 [2] and it shares about 25% sequence identity to its homolog NOXO1 (organizer for NOX1). Both organizer subunits play a similar function for their target enzymes. However, p47phox has an autoinhibitory region, which inhibits the translocation to the plasma membrane, which is absent in NOXO1. Phosphorylation of the autoinhibitory domain in p47phox allows association with p22phox [2]. p47phox is highly expressed in myeloid cells [14], and also in glomerular mesangial cells [15], endothelial cells [16], vascular smooth muscle cells, testis, inner ear, neurons, hepatocytes and lung [2].

1.7 DNA as the oxidation target

When there is imbalance between ROS and endogenous antioxidants the oxidative stress is increased (Figure 3). The free radical theory of ageing was first proposed by Denham Harman [17]. There is an emerging consensus that oxidative damage is of central importance. Lipid, protein and DNA are the key targets for oxidation. Although oxidation of lipids and proteins accumulates with age, only DNA oxidation leads to altered genomic information [18].

Many types of base and sugar damage occur in DNA after an attack by ROS. Some of these result in disruptions of the phosphodiester backbone, which give rise to single stranded (ss) DNA nicks of various configurations [19]. Among the chemical events that can affect DNA is an oxidation of guanine to 7,8-dihydro-8-oxo-2-deoxyguanosine (8-oxodG) [10]. Similar to the other types of damage, this lesion is efficiently repaired by at least two pathways of base excision repair. The steady-state level of 8-oxodG events is 100 – 1,000 per cell in mice, but the number of these events that fail to be repaired and become point mutations is less clear. Some studies report that there is no detectable increase in the steady-state level of nuclear 8-oxodG with age [10, 20], although others have reported an increase [21, 22]; detailed information can be found in a recent review [23]. Another report indicates that there is an accumulation of failed repair sites for 8-oxodG in aged mice [24].

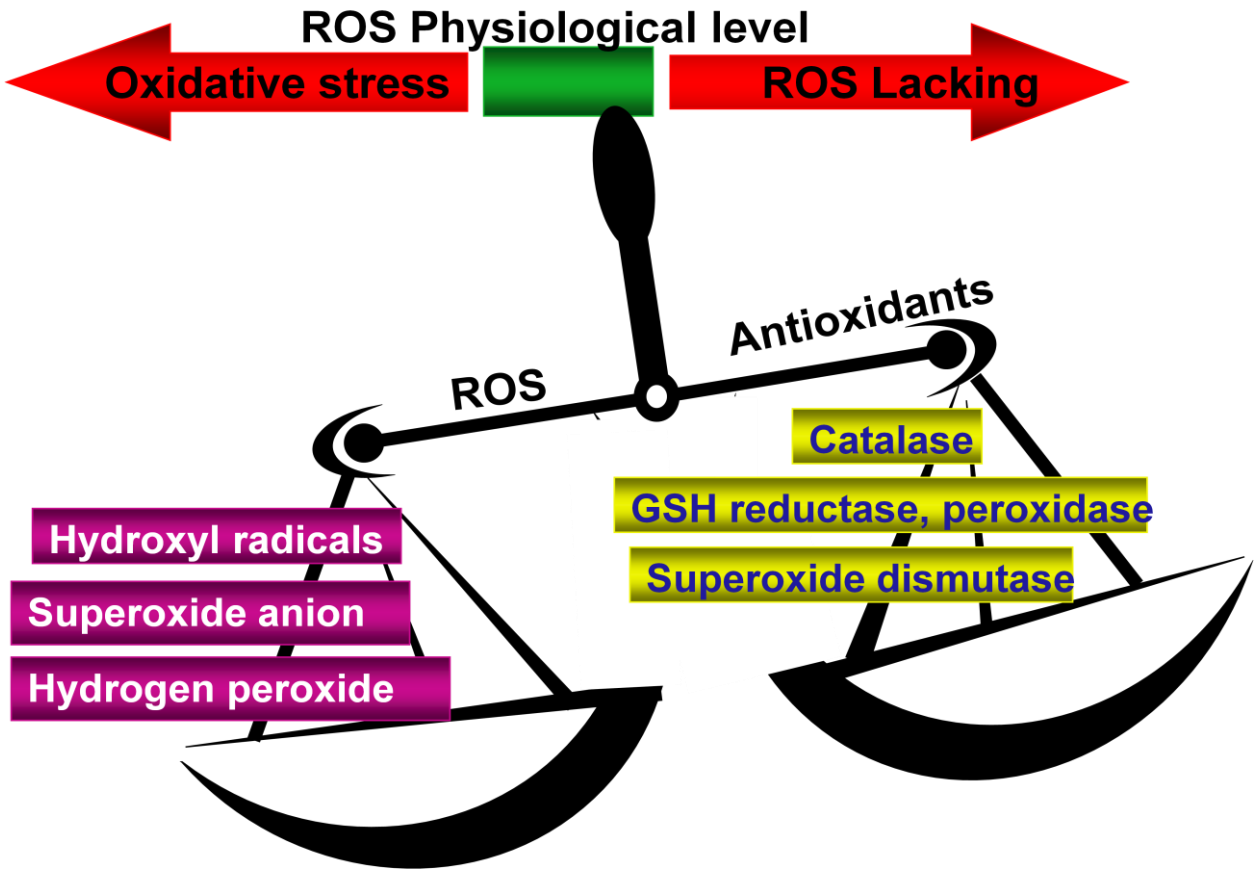

Figure 3: Oxidative stress by an imbalance between ROS and endogenous antioxidants.

1.8 Formation of 8-oxodG

Superoxide, the primary product of NOX, is produced physiologically via a one-electron reduction of molecular oxygen. Superoxide is highly reactive and short lived and can dismutate to a second oxidant intermediate, H_2O_2, spontaneously or enzymatically via superoxide dismutase (SOD). Hydrogen peroxide is more stable than superoxide and is also capable of crossing biological membranes [25]. Reduction of hydrogen peroxide to water is accomplished by catalase and glutathione peroxidase. However, in the presence of transition metals such as iron or copper, hydrogen peroxide is reduced to hydroxyl radicals(•OH) which is the most deleterious ROS [26, 27]. Kasai and Nishimura (1986) were the first to report that the reaction of •OH with nucleobases of the DNA strand, such as guanine, leads to the formation of 8-oxo-7,8-dihydro-2'-deoxyguanosine. Initially, the reaction of the •OH addition leads to the generation of

radical adducts, then by one electron abstraction, 8-hydroxy-2'-deoxyguanosine (8-OHdG) is formed (Figure 4). 8-OHdG undergoes keto-enol tautomerism, and turns into the oxidized product 8-oxodG (Figure 4 and 5) [28]. The mechanistic models of one-electron oxidation reactions of the guanine base in isolated DNA and chemical reactions in the context of •OH radical, singlet oxygen, and two-quantum photoionization processes were reviewed recently [29-31]. The formation of 8-oxodG can lead to chromosomal aberrations and the induction of mutations, which mainly involve GC to TA transversions [32, 33].

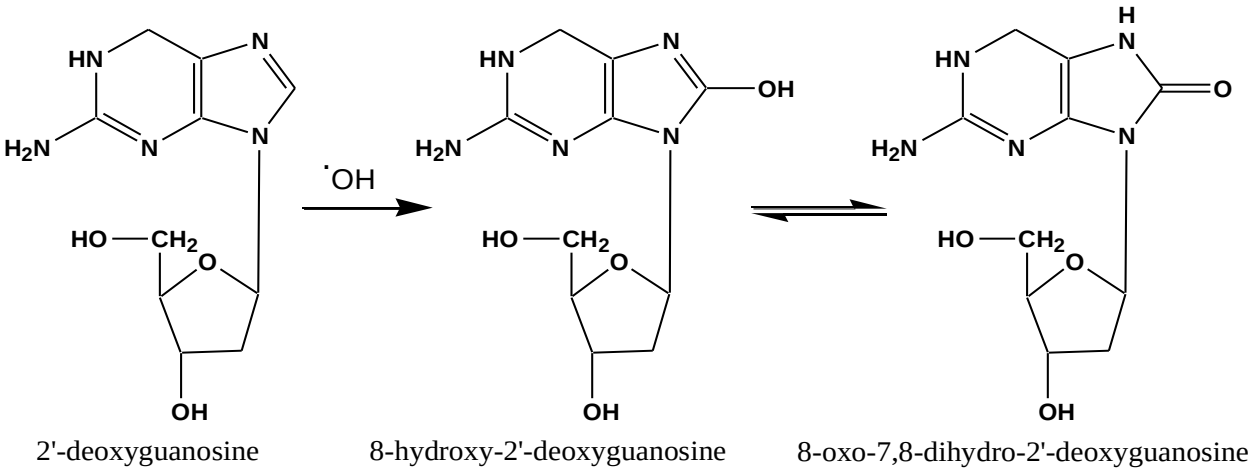

Figure 4: The oxidation of deoxyguanine by hydroxyl radicals leads to the generation of 8-hydroxy-2'-deoxyguanosine (8-OHdG) which undergoes keto-enol tautomerism, and turns into the oxidized product 8-oxo-7,8-dihydro-2'-deoxyguanosine (8-oxodG).

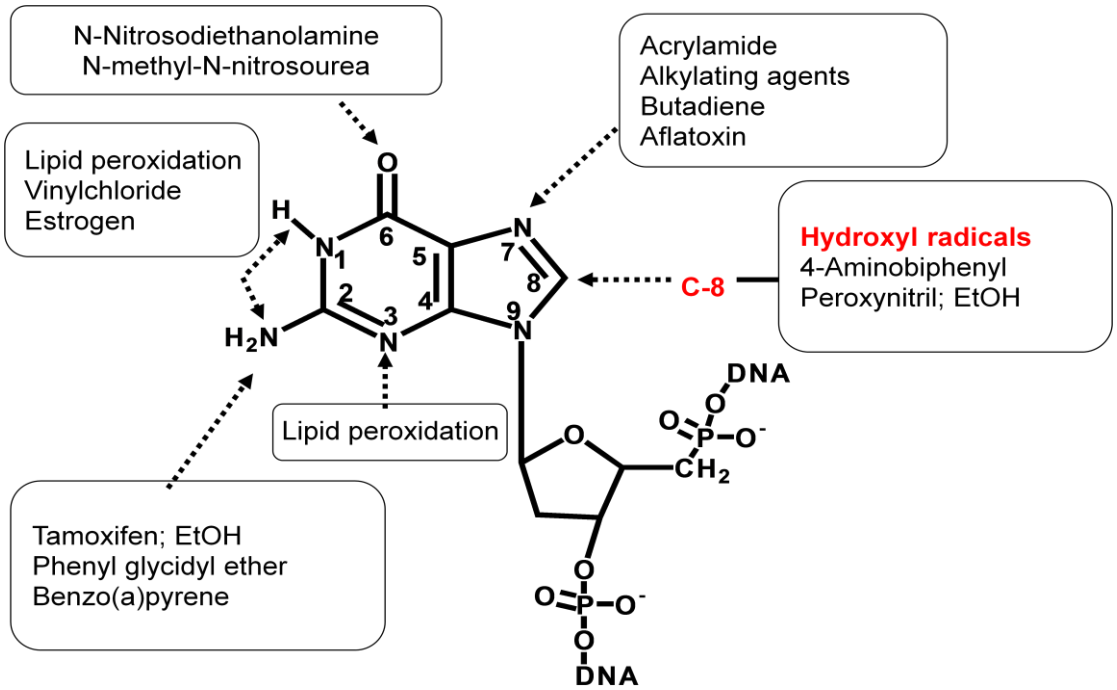

Figure 5: Possible adducts formed by different radicals with guanine; the hydroxyl radical at the 8th position is most favorable and it is an important pro-mutagenic biomarker. (The modified figure was adopted from Singh et al [34] with permission from Oxford University Press, 2006).

1.9 Cellular 8-oxodG

Cellular 8-oxodG is a direct biomarker for oxidative DNA damage and has been extensively analyzed in humans (leukocytes), rats (liver, lung, kidney, brain, heart, colon and testis), mice (liver, lung, kidney, brain, heart, aorta, mammary gland, uterus and small intestine) and cultured cells. 8-oxodG is quantified using high performance liquid chromatography coupled to an electrochemical detector (HPLC-ECD), mass spectrometry (HPLC-MS), or tandem mass detection (HPLC-MS/MS), immunoassays, ^{32}P-postlabeling and a modified single-cell gel electrophoresis (comet) assay. In the 1990's HPLC and gas chromatography coupled with mass spectrometer (GC-MS) were commonly used for the analysis of 8-oxodG. The reported values for normal human cellular 8-oxodG varied up to 1000 fold depending on the method of analysis. The question of artifact formation of 8-oxodG during the analytical procedure was raised [35]. To resolve the possible methodological problems for cellular 8-oxodG analysis, the European Standard Committee on Oxidative DNA Damage (ESCODD) was set up in 1997.

1.10 Artifact formation during 8-oxodG analysis

In the ESCODD validation trial, a variety of methods (HPLC, HPLC-ECD, HPLC-MS/MS, GC-MS and enzymatic assays) were used to minimize the artifactual formation of 8-oxodG. As a result of the trial, it became acknowledged that artifact formation occurs during DNA isolation and sample preparation [36]. In 2002, Ravanat et. al. reported that the use of desferrioxamine (a transition metal chelator), in the extraction buffers and of sodium iodide (a chaotropic agent which helps in DNA precipitation), could minimize the artifact formation [37]. Other ESCODD trials found that the HPLC-ECD method is an accurate method for analyzing 8-oxodG, but that the background levels vary considerably. This was recognized to be due to uncontrolled sample preparation (DNA hydrolysis) [38]. Singh et al., [39] introduced the immunoaffinity column combined with tandem mass spectrometry, as well as the use of the stable isotope $^{15}N_5$-8-oxodG as an internal standard. The advantage of this method is that it is more specific because of the affinity of the antibody to 8-oxodG. Furthermore, the addition of the internal standard $^{15}N_5$-8-oxodG can account for loss during the sample preparation. After a lot of inter-laboratory trials, ESCODD concluded with some difficulty that the background 8-oxodG level in human lymphocytes is between 0.3 and 4.2/10^6dG [40].

Concerning HPLC-MS/MS based methods, the online sample extraction using a column-switching device has proven to be an extremely useful technique for sample preparation from biological matrices [41]. Its advantages include automatic sample preparation and less ion suppression as well as higher sensitivity, plus selectivity due to a direct measurement of DNA adducts in crude hydrolysates [42]. In the case of 8-oxodG analysis, the artifactual oxidation of dG occurs especially during DNA preparation, which by use of online extraction could be minimized. Chao et al attempted to minimize the artifactual production of 8-oxodG during DNA preparation and the electrospray ionization process, using an isotope-dilution LC–MS/MS method coupled with an online solid-phase extraction (SPE) system for the direct and simultaneous analysis of 8-oxodG and dG in crude DNA hydrolysates [43]. The method proposed by

Chao et al gave a low level of 8-oxodG/10^6 dG [44], We found 2.0 8-oxodG/10^6 dG in rat liver DNA, 1.1 in human leukaemia HL-60 cells, and 2.6 in neuronal PC-12 cells (Figure 6). The relative standard deviation of replicates was 20%. Positive controls (HL-60 cells incubated for 10 min with 10 µg/mL methylene blue in the presence of a 60 W lamp at 10 cm distance) showed 32 8-oxodG/10^6 dG (Figure 6). The values of 8-oxodG analyzed by this method were within the limit of ESCODD-suggested levels between 0.5 and 5 lesions per 10^6 dG bases [45].

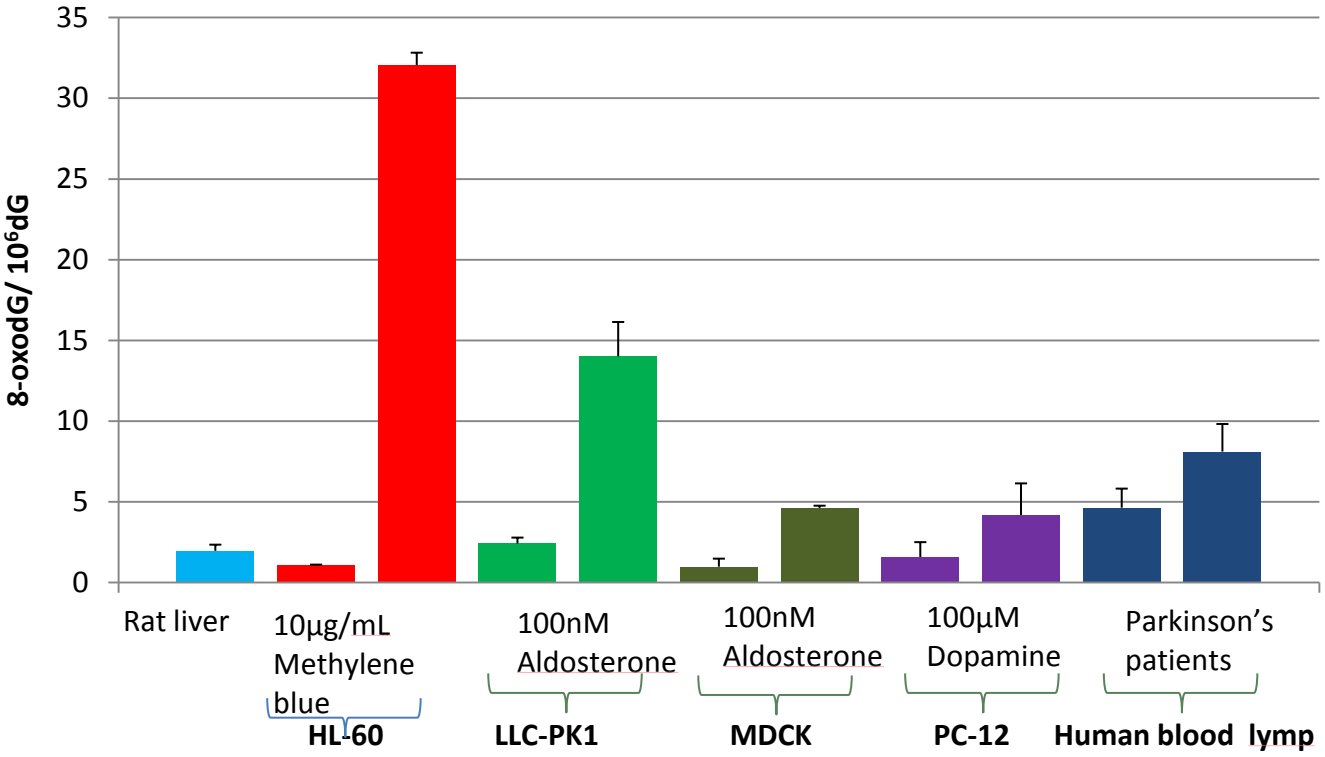

Figure 6: The histogram displays the background level of 8-oxodG in rat, and different cell line and lymphocyte DNA. HL= Human promyelocytic leukemia cells; LLC-PK1= pig kidney proximal tubule cells; MDCK= Madin-Darby canine kidney cell line; PC-12= pheochromocytoma of the rat adrenal medulla.

1.11 Urinary 8-oxodG

Urine is the most frequently examined matrix for 8-oxodG, because of the non-invasive nature, easy sampling and storage (stable for more than 10 years) and the possibility to conduct large studies. However, there is a considerable debate about the possible

sources of extracellular oxidatively modified DNA lesions. DNA repair, diet, cell death or cell turnover, mitochondrial turnover, cellular uptake and re-utilisation of damage products are possible contributions to urinary 8-oxodG (see recent reviews) [46, 47].

1.12 Reduced and oxidized glutathione

Glutathione (GSH γ-L-glutamyl-L-cysteinylglycine), and its oxidized form disulfide glutathione (GSSG) (Figure 7) comprise the most abundant cellular redox system, playing a fundamental role in cell homeostasis. It is also involved in signaling processes associated with programmed cell death. Alteration of the redox balance causes oxidative damage [48]. The biologically active site of GSH is represented by the thiol group on the cystine residue (Figure 8). The de novo biosynthesis of GSH requires two ATP-dependent enzymes. Glutamic acid and cystein get converts into γ-glutamyl-cysteine in the presence of γ-glutamyl-cysteine synthetase. This step can be blocked by dl-Buthionine-sulfoximine (BSO). The γ-glutamyl-cysteine is converted into GSH by glutathione synthase [49]. Both, direct and glutathione peroxidase-mediated enzymatic oxidation of GSH lead to the formation of GSSG. Reduction of GSSG leads to GSH formation in the presence of glutathione reductase (GR) as NADPH dependent reaction (Figure 9) [50, 51]. The activity of GR and availability of NADPH are sufficient to maintain the molar ratio of GSSG: GSH about 1:100. However, if the level of stress is increased or the GR activity is limited, then there is accumulation of GSSG and the molar ratio of the GSSG/GSH increases [48, 52].

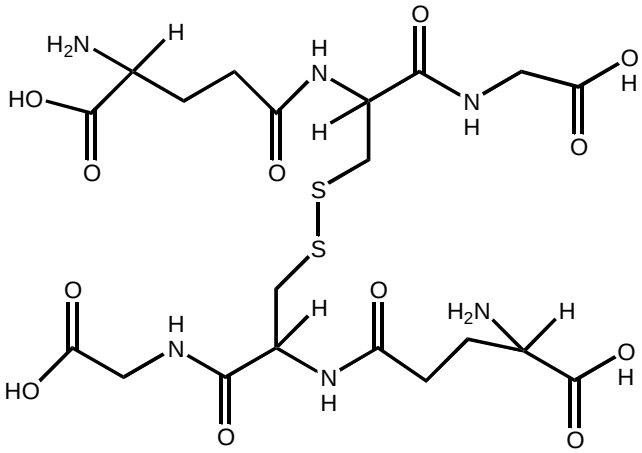

Figure 7: Structure of oxidized glutathione (GSSG)

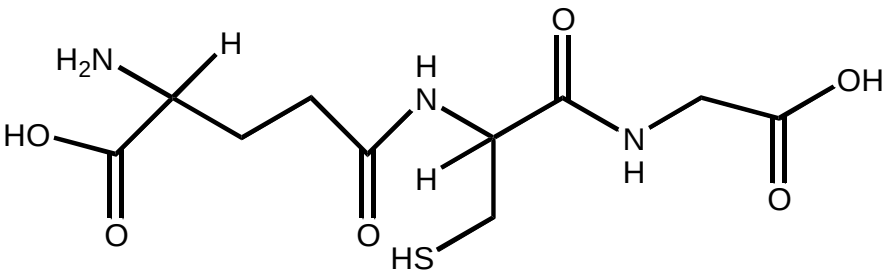

Figure 8: Structure of reduced glutathione (GSH)

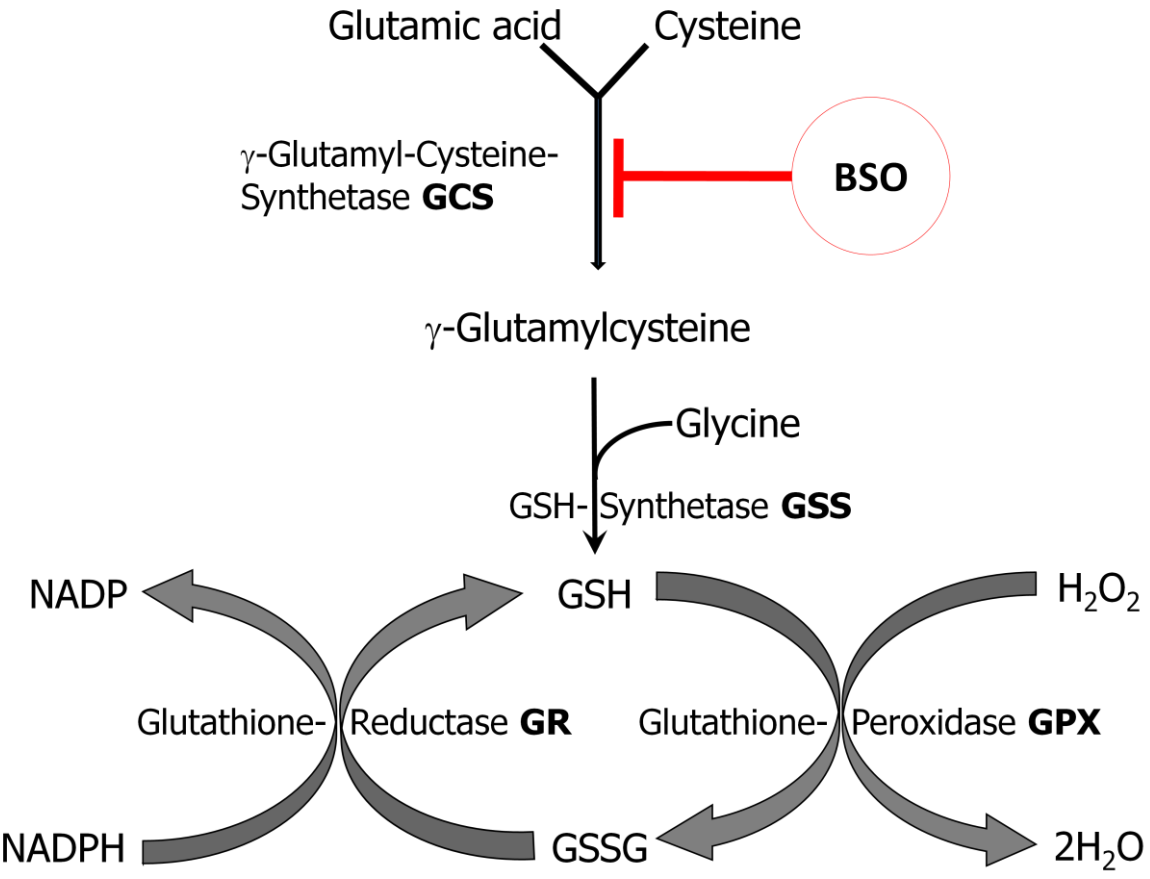

Figure 9: Biosynthetic pathway for reduced (GHS) and oxidized glutathione (GSSG). GCS= gltamylcysteine synthetase; GSS= glutathione synthetase; GR= glutathione reductase; GPX= glutathione peroxydase; GCS= gltamylcysteine synthetase; BSO= dl-Buthionine-sulfoximine

1.13 8-isoprostaglandin F2α (8-isoPGF2α)

8-isoPGF2α (Figure 10) is a specific and stable lipid peroxidation product. 8-isoPGF2α has received more attention than all other 64 isomers. Because it has been shown to act as a potent renal and pulmonary vasoconstrictor, platelet aggregation modulator, inflammatory mediator [53-55]. National Institute of Health (NIH) organized Biomarkers of Oxidative Stress Study (BOSS) concluded 8-isoPGF2α is a most accurate biomarker of oxidative stress [56].

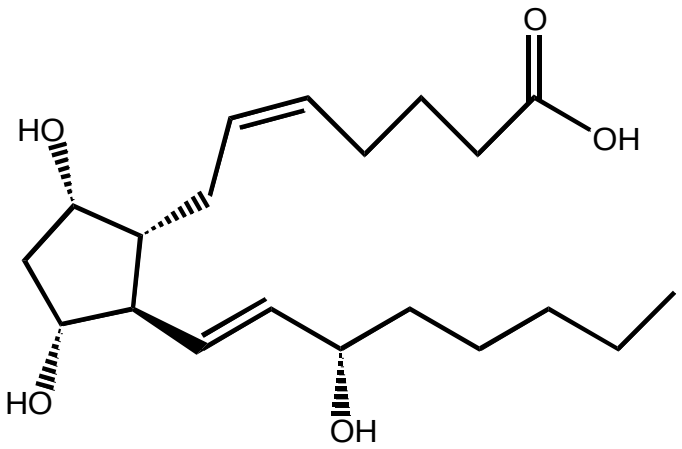

Figure 10: Structure of 8-isoprostaglandin (8-isoPGF2α)

1.14 8-Nitroguanine (8-nitroG)

8-Nitroguanine (8-nitroG) is known to be a mutagenic product from the guanine base of DNA that induces GC to AT transversion mutation. Nitric oxide (NO) reacts with superoxide to form highly reactive peroxynitrite (ONOO−), which causes the nitrative DNA lesion 8-nitroguanine (Figure 11) [57, 58].

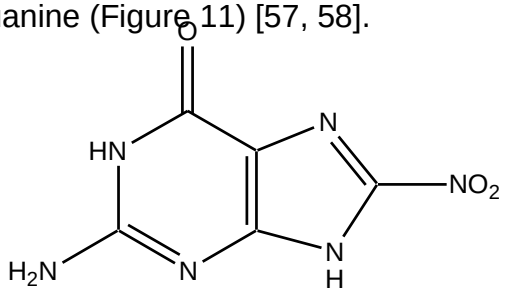

Figure 11: Structure of 8-nitroguanine (8-nitroG)

1.15 Creatinine

Creatinine (Figure 12) is a cyclic derivative of creatine. Creatinine clearance determines the quantitative kidney damage. Creatinine clearance can be measured by calculating the amount of serum creatinine filtered by the glomerulus at a unit of time [59]. Creatinine is a breakdown product of creatinine phosphate, and the amount depends on the muscle tissue in the body and the renal function. The creatinine rate of excretion is relatively constant over time. Therefore, most of the urinary markers are commonly normalized to creatinine [60].

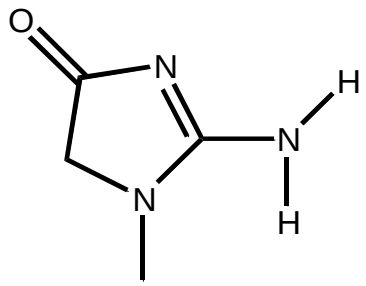

Figure 12: Chemical structure of creatinine

1.16 NOX activation by Ang II

Ang II (Figure 13) activates NOX in cardiovascular, kidney and central nervous systems. In general, Ang II binds to its receptor AT1R, activates NOX (Figure 14) and produces ROS. However, the complete mechanisms of NOX activation by Ang II are complex and still incompletely understood [61].

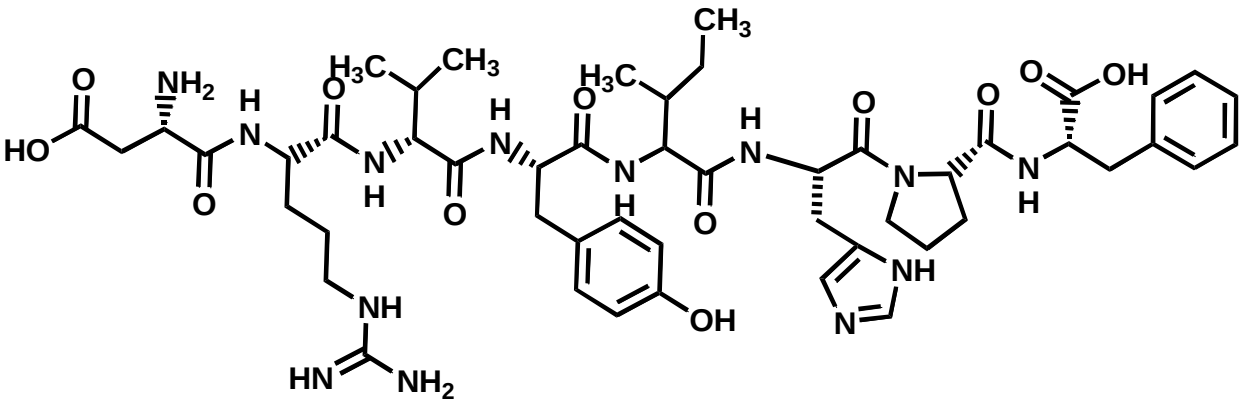

Figure 13: Chemical structure of Ang II

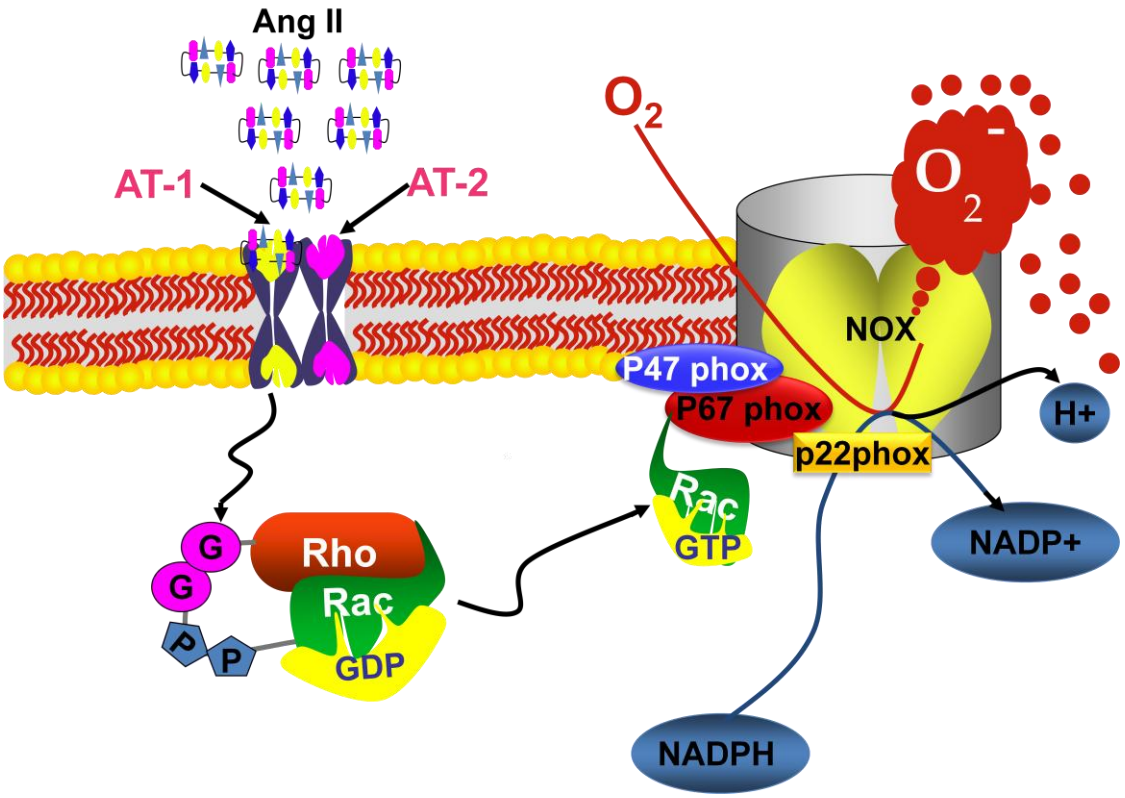

Figure 14: Nox activation by Ang II via AT1 receptor and production of superoxide anion radicals

1.17 Aldosterone

Aldosterone (Figure 15) is synthesized from cholesterol in the zona glomerulosa (ZG) of the adrenal cortex. A number of factors have been shown to stimulate or inhibit aldosterone production. However, the major regulator of aldosterone synthesis and secretion is Ang II [62]. Aldosterone causes oxidative stress via upregulation of the expression of the NOX subunits [63]. It induces a genotoxic effect in LLC-PK1 cells via production of superoxide anion and hydrogen peroxide [64, 65].

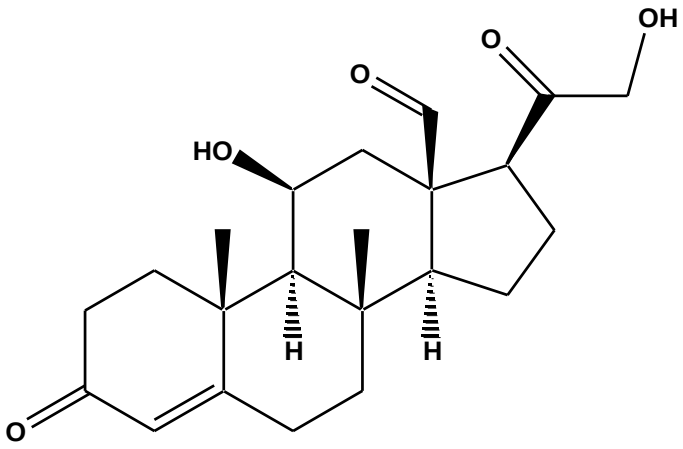

Figure 15: Chemical structure of aldosterone

1.18 Rosuvastatin

The structural formula of rosuvastatin shown in Figure 16.

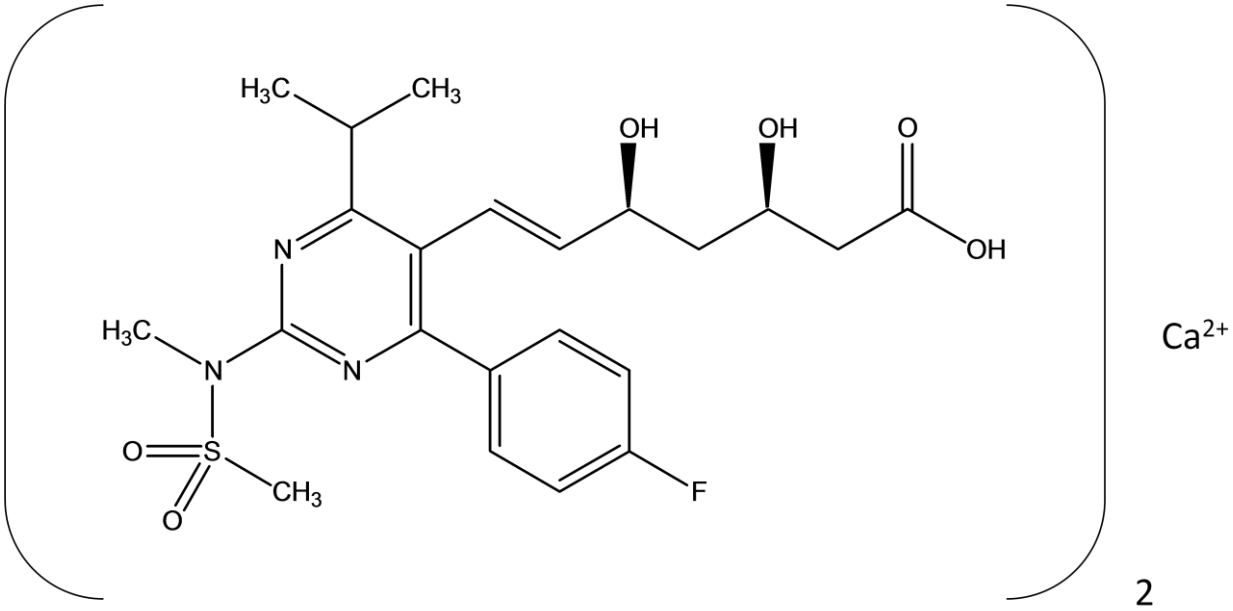

Figure 16: Chemical structure of rosuvastatin calcium salt

Statins are lipid lowering drugs. They inhibit 3-hydroxy-3methylglutaryl-coenzyme A (HMG-CoA) reductase which catalyses the rate limiting step for cholesterol biosynthesis [66]. In addition to the lipid lowering effect, statins shows pleiotropic actions including anti-inflammatory, anti-thrombotic and antioxidant effects. Recently we have shown that rosuvastatin exerts antioxidative effects, and it prevents from oxidative stress induced DNA damage. This anti-oxidant effect is, probably mediated via up-regulation of glutathione synthesis [67]. Moreover, rosuvastatin reduces an elevated level of angiotensin II type 1 receptor (AT1R) and protects the vascular system [68].

1.19 Parkinson's Disease and oxidative DNA damage

Parkinson's disease (PD) is the most common neurodegenerative movement disorder affecting approximately 2% of the human population aged 65 and above [69]. While the full clinical syndrome of PD is a complex disorder, the characteristic motor symptoms associated with the sporadic and all genetic forms of this disorder result from the degeneration of the dopamine-producing neurons of the substantia nigra (SN). This is

the rationale for the dopamine-substitution therapies, including treatment with L-3,4-dihydroxyphenylalanine, levodopa (L-DOPA) and peripheral aromatic amino acid decarboxylase- and catecholamine-O-methyltransferase inhibitors, selective monoamine oxidase type B inhibitors, dopamine receptor agonists and drugs which indirectly improve dopaminergic functions (for example, glutamate antagonists). While the trigger for this relatively selective neuronal vulnerability remains unknown. The cascade of degenerative events leading to cell death is beginning to be understood. The major hypotheses believed to contribute to the eventual demise of dopamine producing cells in the SN include protein aggregation, oxidative stress, disturbed iron metabolism, mitochondrial dysfunction and dysfunction of proteasomal pathways [70-74].

L-DOPA has been the most frequently prescribed drug for alleviating symptoms of PD in the last three decades. However, the contribution of L-DOPA therapy to oxidative damage is still debated. There is evidence for the toxic properties of L-DOPA to neuronal cells in vitro [75, 76], however this toxicity has not been confirmed in healthy rodents [77], nonhuman primates [78] or humans [79]. Moreover, the recent clinical trials did not supply proof for toxic effects of L-DOPA which would contribute to PD progression [80].

In the postmortem SN of PD patients concentrations of the oxidized DNA-base 8-oxodG are markedly increased compared to controls [81, 82]. Migliore, et al. reported an increased frequency of micronuclei, a subset of chromosomal aberrations, and of single strand breaks and oxidized purine bases in the peripheral blood leukocytes of patients with untreated PD [83]. Recently, large cohort studies revealed a correlation between frequencies of chromosomal aberrations or micronuclei in peripheral lymphocytes and cancer risk [84, 85]. In addition, even sublethal damage of cellular nucleic acids or genomic damage may contribute to the further degeneration of neuronal cells, thus enhancing the progression of the disease [86-88].

1.20 Electro Spray Ionisation (ESI) and Multiple Reaction Monitoring (MRM) in Liquid Chromatography-Tandem Mass Spectrometry (LC-MS/MS)

1.20.1 Electro Spray Ionisation (ESI)

Electrospray ionization (ESI) is a popular technique in mass spectroscopy for ionizing biological or chemical molecules. ESI works well with many different types of compounds. This technique works well with larger and small molecules; therefore, it is used in proteomics (analysis of proteins), lipidomic (analysis of lipids) and metabolomics (analysis of metabolites). The working process of ESI consists of two stages (Figure 17) [89].

First, the sample or analytes are dissolved in a mobile phase which consists of organic solvents and acidified water or buffer. This analytes are separated in a HPLC and introduced into a vessel, called a capillary, that ends in a very fine tip. A very high voltage is applied to this tip, which charges the analytes molecule in the solvent. The charged analytes are entered into the evaporation chamber. Then the molecules repel one another almost violently. When the charged liquid first exits the tip, it briefly forms a cone shape known as a Taylor cone. The charged cone shape liquid droplets burst away from each other into a fine spray [89, 90].

Second, the charged droplets in the spray go through a series of divisions. This occurs because the solvent within these droplets gradually evaporates with the assistance of nitrogen gas pumped into the chamber and forms smaller droplet ions. When these ions are pushed close enough together, they will repel each other this behavior is known as the Coulomb force and causing the droplets to divide into two smaller droplets. This process repeats itself until the solvent is completely evaporated and the droplets have split up to the point that each is a single, charged molecule. The single charged molecules enter into the mass detector. One of the advantages of this ionization method is that the molecules remain intact and will not be broken apart, that is why this ionization is called soft ionization technique [89, 90].

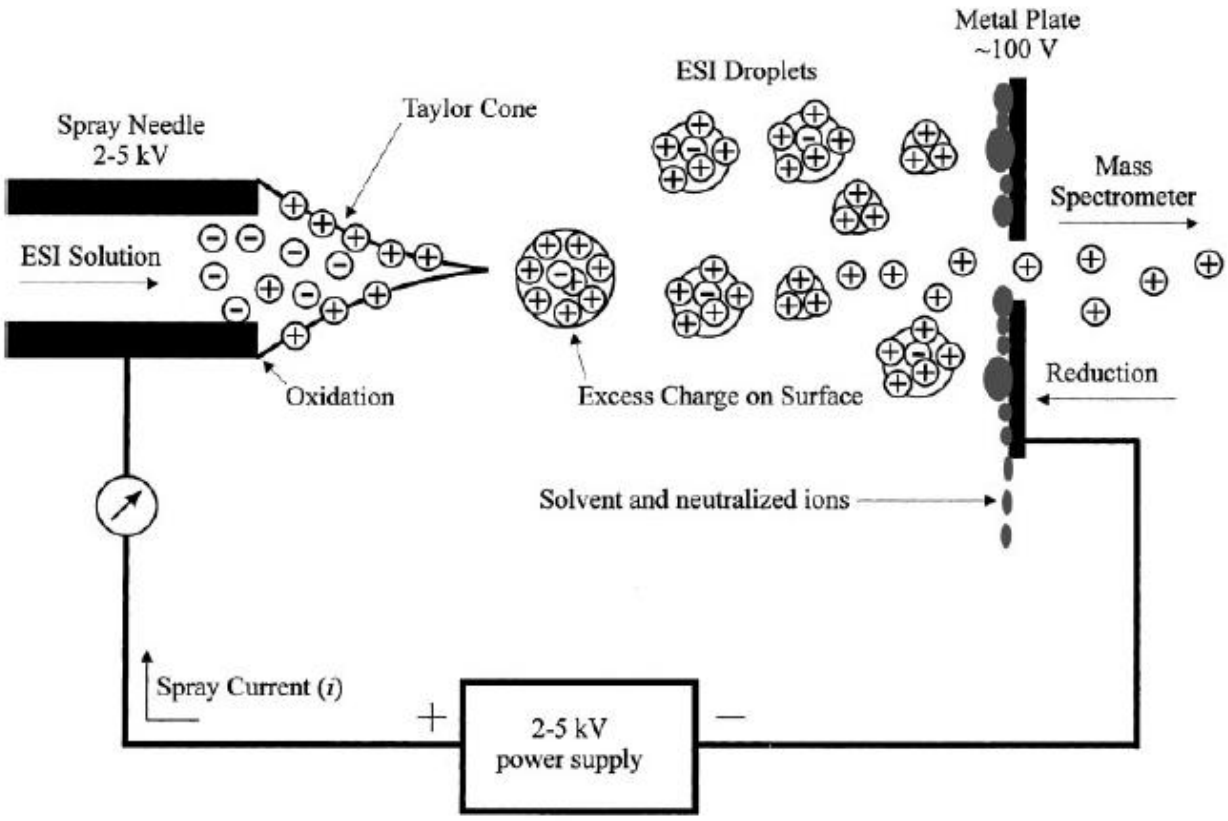

Figure 17: Electro spray ionization process in LC-MS/MS. The schematic diagram with the permission of Cech and Enke [89] (copy right permission from John Wiley and Sons, 2001).

1.20.2 Multiple reaction monitoring (MRM)

Multiple reaction monitoring (MRM) coupled with stable isotope dilution mass spectrometry using a triple quadrupole mass spectrometer is a powerful tool for quantitative measurement of target molecule in metabolomics, proteomics [91], lipidomics etc. [34, 92-94].

In MRM mode, two stages (Figure 18) of mass filtering are employed on a triple quadrupole mass spectrometer [94]. In the first stage, the ionized m/z of a precursor ion is filtered in the first quadrupole (Q1). The selected precursor ion is dispersed into several fragment ions in the second quadrupole (Q2) by collision excitation with a neutral gas in a pressurized collision cell. In the second stage, only the interesting m/z mass of the fragment ions can pass into the third quadrupole (Q3) [92]. Therefore the intensities of these ions are measured and converted to concentrations. The MRM triple quadrupole LC-MS/MS measures up to 2500 transitions in a single assay [92, 93].

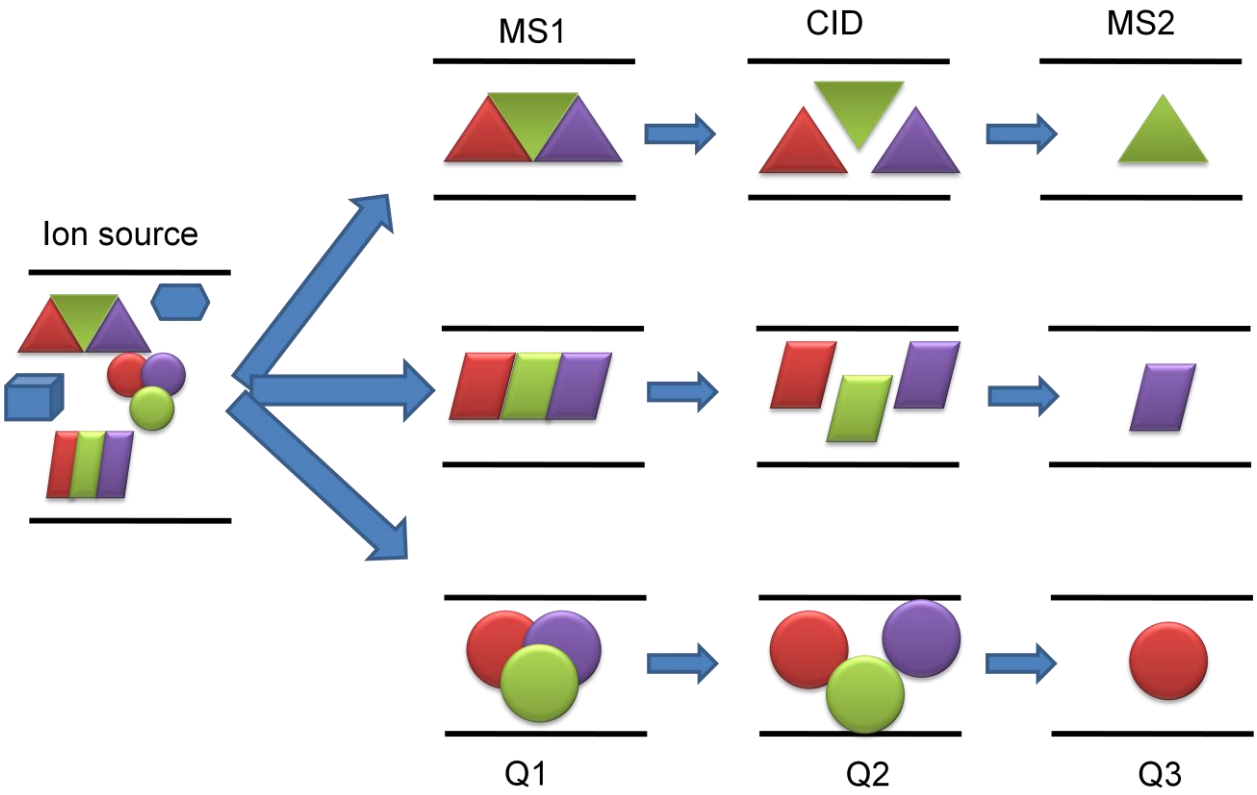

Figure 18: Multiple reaction monitoring process in triple quadrupole mass analysis. The precursor ions from the ion source are pushed into first (Q1) quadrupole (MS1 level) and selectively allows only the targeted parent ions to pass into second (Q2) quadrupole for collision-induced dissociation (CID) fragmentation. The third (Q3) quadrupole (MS2 level) selectively allows only a specific pre-identified fragment ion to pass to detector [94].

2 Objectives

NADPH oxidase (NOX) produces reactive oxygen species (ROS). The imbalance between ROS and endogenous antioxidants leads to oxidative stress. Since Harman proposed the "free-radical theory of aging", more than 50 years ago oxidative stress has been postulated to be a major fundamental factor for ageing and age related diseases. There is an emerging consensus that oxidative damage is of central importance. Lipid, protein and DNA are the key targets for oxidation. Although oxidation of lipids and proteins accumulates with age, only DNA oxidation leads to altered genomic information.

I). Nowadays there are a lot of reports suggesting that oxidative stress-induced oxidative DNA damage is accumulated in animal organs during the ageing process [23].

- We wanted to study the influence of NADPH oxidase (NOX) derived reactive oxygen species (ROS) induced oxidative DNA damage. Therefore we compared WT mice (C57BL/6J) with p47phox$^{-/-}$ (deletion of NOX organizer subunit p47phox) mice.
- To study the role of NOX derived ROS in ageing, we compared young and older WT mice (C57BL/6J) with p47phox$^{-/-}$ mice in the context of oxidative stress and oxidative DNA damage.

To analyze oxidative stress and oxidative DNA damage markers, we developed a new isotope- diluted-LC-ESI-MS/MS method and validated it to analyze 8-oxodG, 8-isoPGF2α, GSH, GSSG, Ang II, Aldosterone and creatinine in a single sample preparation.

Using this method, we analyzed the oxidative DNA damage marker 8-oxodG in urine and kidney. The oxidative stress markers, urinary and plasma 8-isoPGF2α and the oxidized, reduced glutathione (GSSG/GSH ratio) from plasma were also analyzed by LC-ESI-MS/MS. The DNA strand breaks were analyzed in cells from liver, kidney, using the comet assay.

II). Statins are lipid lowering drugs. They inhibit 3-hydroxy-3methylglutaryl-coenzyme A (HMG-CoA) reductase which catalysis the rate limiting step for cholesterol biosynthesis [66]. In addition to the lipid lowering effect, statins shows pleiotropic actions including anti-inflammatory, anti-thrombotic and antioxidant effects. Recently we have shown that rosuvastatin exerts antioxidative effects, and it prevents DNA damage from oxidative stress. The antioxidant effect of rosuvastatin acts via up-regulation of glutathione synthesis [67]. Moreover, rosuvastatin reduces elevated levels of angiotensin II type 1 receptor (AT1R) and protects the vascular system [68].

- Therefore we wanted to study the protective effect of rosuvastatin on Ang II induced oxidative stress and genomic damage in the pig kidney cell line LLC-PK1.

We analyzed genomic damage in the comet assay, 8-oxodG, micronuclei frequency, and endogenous antioxidant enzyme expressions such as glutathione synthetase, glutathione reductase and glutathioneperoxidase.

III). Parkinson's disease (PD) is a neurodegenerative movement disorder affecting about 2% of the human population at old age. L-3,4-Dihydroxyphenylalanine (L-DOPA) in combination with a peripheral aromatic amino acid decarboxylase inhibitor is the most frequently prescribed drug for alleviating symptoms of PD, but a potential contribution of L-DOPA therapy to further neurodegeneration via oxidative stress is still debated.

- We intended to elucidate, whether oxidative stress is elevated in chronically L-DOPA-treated PD patients, and whether this leads to elevated genomic damage.

Therefore we analyzed 8-oxodG in lymphocyte DNA of PD patients and matched controls. In addition, we assessed the antioxidant capacity of plasma, and the micronucleus frequency in peripheral lymphocytes.

Overall to analyze oxidative DNA damage and oxidative stress markers, we applied both new and European Standards Committee on Oxidative DNA damage (ESCODD) approved isotope-diluted-LC-ESI-MS/MS methods. Further we used comet assay, micronuclei frequency test for genomic damage assessment.

3 Materials and methods

3.1 Materials

3.1.1 Chemicals

If not mentioned otherwise all chemicals were purchased from sigma-Aldrich. N-methyl-D3-creatinine, 98% from Cambridge Isotope Laboratory, Inc. MA, USA; ^{15}N-dG, 98% from Silantes, Germany; Glycine-$^{13}C_2$,^{15}N-glutathione, >90%, from Cambridge isotope Laboratories, MA, USA;8-Nitroguanine from Santa cruz, CA, USA; ^{13}C-^{15}N labeled Ang II, >98% from Eurisotop, Germany; aldosterone-d7, >98, Isosciences, PA, USA; 8-isoPGF2α and 8-isoPGF 2α-d4, 99% from Cayman chemicals, MI, USA. HPLC-grade methanol and water for liquid chromatography were purchased from Roth, Karlsruhe, Germany;

3.1.2 Animals

p47phox knockout (p47phox$^{-/-}$) and C57BL/6 wild type (WT) mice were kindly provided by Prof. Dr. Rolf Schulte-Hermann (Institute for Cancer research, University of Vienna, Borschkegasse 8a, A-1090, Vienna, Austria). p47phox$^{-/-}$ mice were originally produced from embryonic stem cell 129/Sv-derived sperm and C57BL/6-derived eggs. All mice were bred in the breeding facilities of the Institute of Pharmacology and Toxicology, University of Wuerzburg, Germany. The animals were confirmed from ear DNA sequenced by PCR (Phire Animal Tissue Direct PCR kit; experiment was done by Simone Weissenberger, Department of Toxicolog, University of Wuerzburg, Germany). Additionally C57BL/6 wild type mice were purchased from Fa. Janvier, France. The mice were housed in Scantainers and care was provided according to the institutional animal care. In aging p47phox$^{-/-}$ mice granular structures (chronic granulomatous disease) are deposited in the lungs. However, even without antibiotics survival is possible for more than 14 months [95]. In our case the percent of animals which died spontaneously at our animal facility was 15.62%.

Urine was collected at the age of 12-13 weeks (13 weeks 5 days for WT; 12 weeks for p47phox-/- mice) and the plasma and tissue were collected at the age of 21-23 weeks (23 weeks 4 days for WT; 21 weeks 2 days for p47phox-/- mice). This was considered as young group. Urine, plasma and tissue from old WT mice were collected at the age of 52- 53 weeks (considered as old group) and the results were compared with relatively old phox-/- mice at the age of 30-32 weeks. For urine collection two animals were placed in a metabolic cage overnight, adequate food and water was supplied and the urine was collected and stored at -20°C. LLC-PK1 cells were cultured at 37°C, 5% (v/v) CO_2 in Dulbecco's Modified Eagle Medium (DMEM) low glucose (1g/l) supplemented with 10 % (v/v) fetal bovine serum (FBS), 1% (w/v) L-glutamine, 2.5% (w/v) HEPES and antibiotics (50 U/ml penicillin, 50 µg/ml streptomycin).

3.1.3 Extraction of primary kidney cells

Freshly obtained mouse kidneys were minced on ice to small pieces, which were suspended in 3 ml buffer consisting of RPMI 1640, 15 % DMSO, 1.8 % (w/v) NaCl. The extracted primary rat kidney cells were sifted through a cell strainer with a mesh pore size of 100 µm (BD, Heidelberg, Germany), centrifuged for 5 minutes at 1000 rpm and at 4 °C and were finally resuspended in 1 ml Dulbecco's Modified Eagle Medium (DMEM) low glucose (1g/l) supplemented with 10 % (v/v) fetal bovine serum (FBS), 1% (w/v) L-glutamine, 2.5% (w/v) HEPES and antibiotics (50 U/ml penicillin, 50 µg/ml streptomycin) [96].

3.1.4 Cell line

LLC-PK1 cells from pig kidney, which resemble proximal tubule cells, were obtained from the American Type Culture Collection (Manassas, VA, USA). Cell culture media and reagents were obtained from PAA Laboratories GmbH (Pasching, Austria). LLC-PK1 cells were grown at 37°C in a humidified atmosphere of 5% CO2 in Dulbecco's modified Eagle's medium (DMEM) with 1000 mg/L glucose supplemented with 10% fetal calf serum (FCS; Gibco-BRL), 25 mM HEPES, 1% L-glutamine and 0.2% antibiotics (50U/mL penicillin, 50µg/mL streptomycin). Cells were routinely split twice a

week to keep the under-exponential-growth conditions. They were cultured for no more than 10 passages after thawing them from stock [97].

3.1.5 Subjects

18 PD patients were enrolled in this study. Patient characteristics are summarized in table 7. Patients were treated with L-DOPA in a dose range of 188 to 1850 mg/day and dopa decarboxylase inhibitor, either carbidopa (25 to 425 mg/day) or benserazide (47 to 187 mg/day) or both. Further medications included catechol-O-methyl transferase (COMT) inhibitors, dopamine agonists, antipsychotic drugs, and MAO inhibitors (Table 8). Life-partners of PD patients were also enrolled in this study, yielding a matched control group. The study was approved by the University of Wuerzburg ethics committee and was carried out according to the declaration of Helsinki. A written consent was obtained from all patients prior to participation in the study.

3.1.6 Collection of blood samples

Blood samples were collected from patients and healthy controls for 8-oxodG and FRAP assay (1x7.5 ml), micronucleus analysis and L-DOPA quantification (1x7.5 ml). Blood samples were taken via an indwelling cannula and collected in coded tubes containing heparin. Samples were transported from the Leopoldina Hospital, Schweinfurt (Germany) to the Department of Toxicology at the University of Wuerzburg (Germany) at room temperature within 2-3 h and processed immediately.

3.2 Analytical methods

3.2.1 A new LC-ESI-MS/MS method development and validation for analysis of 8-oxodG, 8-isoPGF2α, 8-nitroG, GSH, GSSG, dG, angiotensin II, aldosterone, and creatinine (analytes or markers)

3.2.1.1 Synthesis of stable isotope labeled internal standards

3.2.1.1.1 Synthesis of ^{15}N-^{13}C-GSSG

Isotopically labeled GSSG was prepared using commercially available glycine-labeled GSH ([glycine 1,2-$^{13}C_2$,^{15}N]-GSH). For this, a solution of 2mM labeled GSH was treated with an equal volume of 16mM H_2O_2. The oxidant was gradually added to the reactant while the solution was stirred. The reaction was carried out at 25°C for 6h. ^{13}C-^{15}N-GSSG was isolated using HPLC-UV with a Reprosil pur (150x4.6 mm; 5µm), column with a mobile phase of 10% MeOH in 0.1% TFA. The isocratic run time was 15 min and the flow rate 400µL/min, the analytes were detected at 210nm. The nature of the purified glycine-labeled GSSG was confirmed by mass spectrometry and quantified in the above mentioned HPLC-UV method using unlabeled GSSG standard [98, 99].

3.2.1.1.2 Synthesis of ^{15}N-^{13}C-GSH-NEM

GSH was detected and quantified as GSH-NEM alkylated adduct. To prepare the adduct, a 5-fold molar excess of *N*-ethylmaleimide (NEM) was added to GSH and left for 30 min. NEM and GSH were dissolved in PBS (pH 7.4), and the reaction gives a stoichiometric conversion to the adduct. In the same manner the glycine-labeled GSH-NEM adduct was synthesized from commercially available glycine 1,2-^{13}C, ^{15}N-GSH. Labeled and unlabeled adducts were confirmed by mass spectrometry [99].

3.2.1.1.3 Synthesis of ^{15}N-8-oxodG

The stable isotope labeled 8-oxodG was synthesized based on the method reported by Singh et al. [39]. A 1 mg/mL solution of $^{15}N_5$-dG (>98% ^{15}N, Silantes, Germany) was dissolved in a Chelex-treated 20 mM sodium phosphate buffer, pH 7.0. Then, sequentially, copper II sulphate, sodium ascorbate, hydrogen peroxide (final

concentrations 1.2, 170, and 370 mM, respectively) were added to the above solution and the reaction mixture incubated at ambient temperature for 20 min. The reaction was terminated by addition of 300 µL, 1mg/mL catalase. $^{15}N_5$-8-oxodG was identified based on mass spectrometry and comparison of the retention time with authentic unlabelled standard. Isotopically labelled 8-oxodG was purified on a HPLC-UV (245nm), using a Hypersil ODS (250mm × 4. 6mm; 5µm, Phenomenex) column. The mobile phase was 10% methanol in water, the total run time was 15 min at the rate of 1mL flow per minute. The retention times were 9.5 and 12.5 for $^{15}N_5$-dG and $^{15}N_5$-8-oxodG, respectively. Purified $^{15}N_5$-8-oxodG was confirmed by mass spectrometry. The pooled fractions were dried on centrifugal vacuum evaporator and reconstituted in water. Finally, the concentration was determined by using a calibration curve with unlabelled standard 8-oxodG.

3.2.1.2 Identification of fragmentation pattern for the analytes by mass spectrometry

All the analytes and respective internal standards were individually dissolved in 10 % methanol in 0.1% formic acid. The analytes were manually tuned/scanned for the fragmentation pattern in both, positive and negative mode. From the manual tune, the base peak was identified, then the quantitative mass transitions were identified using Analyst 1.4.2 software.

3.2.1.3 Separation of the analytes by LC and detection by ESI-MS/MS

20 µl of standards/sample were injected onto a reversed phase column Reprosil Pur ODS, 150 x 2.0 mm, 3 µm (Maisch, Ammerbuch, Germany). The gradient method with solvent A containing 0.1% formic acid in water and solvent B containing 100% methanol used a flow rate of 250µL/min. The total run time was divided into two periods. First 25 min of positive mode was applied for detection. Second, from 25 min until the end of the run, the negative mode was used for detection (Table 1).

Table 1: The gradient method for the LC-ESI-MS/MS analysis

Step	Total Time (min)	Flow Rate (µl/min)	Solvent A (%) 0.1% formic acid in water	Solvent B (%) 100% MeOH
0	0	250	90	10
1	10	250	80	20
2	30	250	10	90
3	35	250	90	10
4	60	250	90	10

3.2.1.4 Alternative method with 25 min run time

In order to reduce the run time of the analysis, the gradient method was modified as given below (Table 2). By this method creatinine, GSSG, GSH, dG, 8-nitroG, 8-oxodG, can be separated and quantified. The other three markers Ang II, Aldo and 8-isoPGF2α cannot be analyzed. Moreover, only a positive mode mass spectrometry detection is possible.

Table 2: The gradient method for 25min LC-ESI-MS/MS analysis

Step	Total Time (min)	Flow Rate (µl/min)	Solvent A (%) 0.1% formic acid in water	Solvent B (%) 100% MeOH
0	0	250	90	10
1	10	250	80	20
2	11	250	50	50
3	13	250	50	50
4	15	250	90	10
5	25	250	90	10

3.2.1.5 Validation of the method

The validation of the method was carried out according to the Food and Drug Administration (FDA) and ICH guidelines for bio-analytical method validation. So the linearity, accuracy, precision, LOD, LOQ and recovery were determined for the new LC-ESI-MS/MS method [100].

3.2.1.5.1 Linearity

The linearity was checked with various concentrations of the standard solution. For preparation of the stock solution, the calculated amount of all the analytes was mixed into one stock. From the stock solution a further serial dilution 1:1 ratio with mobile phase (10%MeoH in 0.1% formic acid) was performed to get the lowest concentration (Table 3). All the concentrations were mentioned in pmol, and the injection volume was 20µL.

Table 3: Concentrations of standard for linearity assesment

s.no	Creatinine (pmol)	GSSG (pmol)	dG (pmol)	8-nitroG (pmol)	8-oxodG (pmol)	GSH-NEM (pmol)	Ang II (pmol)	Aldo (pmol)	8-isoPGF2a (pmol)
1	5000.00	100.00	45.00	1060.00	21.20	500.00	20.00	10.00	10.00
2	2500.00	50.00	22.50	530.00	10.60	250.00	10.00	5.00	5.00
3	1250.00	25.00	11.25	265.00	5.30	125.00	5.00	2.50	2.50
4	625.00	12.50	5.63	132.50	2.65	62.50	2.50	1.25	1.25
5	312.50	6.25	2.81	66.25	1.33	31.25	1.25	0.625000	0.625000
6	156.25	3.13	1.41	33.13	0.662500	15.63	0.625000	0.312500	0.312500
7	78.13	1.56	0.703125	16.56	0.331250	7.81	0.312500	0.156250	0.156250
8	39.06	0.781250	0.351563	8.28	0.165625	3.91	0.156250	0.078125	0.078125
9	19.53	0.390625	0.175781	4.14	0.082813	1.95	0.078125	0.039063	0.039063
10	9.77	0.195313	0.087891	2.07	0.041406	0.976563	0.039063	0.019531	0.019531
11	4.88	0.097656	0.043945	1.04	0.020703	0.488281	0.019531	0.009766	0.009766
12	2.44	0.048828	0.021973	0.517578	0.010352	0.244141	0.009766	0.004883	0.004883
13	1.22	0.024414	0.010986	0.258789	0.005176	0.122070	0.004883	0.002441	0.002441
14	0.610352	0.012207	0.005493	0.129395	0.002588	0.061035	0.002441	0.001221	0.001221
15	0.305176	0.006104	0.002747	0.064697	0.001294	0.030518	0.001221	0.000610	0.000610
16	0.152588	0.003052	0.001373	0.032349	0.000647	0.015259	0.000610	0.000305	0.000305
17	0.076294	0.001526	0.000687	0.016174	0.000323	0.007629	0.000305	0.000153	0.000153
18	0.038147	0.000763	0.000343	0.008087	0.000162	0.003815	0.000153	0.000076	0.000076
19	0.019073	0.000381	0.000172	0.004044	0.000081	0.001907	0.000076	0.000038	0.000038
20	0.009537	0.000191	0.000086	0.002022	0.000040	0.000954	0.000038	0.000019	0.000019
21	0.004768	0.000095	0.000043	0.001011	0.000020	0.000477	0.000019	0.000010	0.000010
22	0.002384	0.000048	0.000021	0.000505	0.000010	0.000238	0.000010	0.000005	0.000005
23	0.001192	0.000024	0.000011	0.000253	0.000005	0.000119	0.000005	0.000002	0.000002
24	0.000596	0.000012	0.000005	0.000126	0.000003	0.000060	0.000002	0.000001	0.000001
25	0.000298	0.000006	0.000003	0.000063	0.000001	0.000030	0.000001	0.000001	0.000001
26	0.000149	0.000003	0.000001	0.000032	0.000001	0.000015	0.000001	0.000000	0.000000

3.2.1.5.2 Accuracy

Accuracy is determined by replication of the analysis of a known concentration of the analyte. Three different concentrations were used, and five determinations of each concentrations were analyzed. The percentages of the relative standard deviations (%RSD) were checked for the peak area of the respective analytes.

3.2.1.5.3 Limit of quantification (LOQ) and limit of detection (LOD)

To determine the LOQ, the lowest range of the linearity solutions was used. The signal to noise (S/N) ratio was checked using Analyst1.4.2 software. The S/N ratio should be more than 5. For determination of LOD, the LOQ solution was further diluted, injected using the same method and checked for detectable peaks. The S/N ratio should be 3-5 for LOD.

3.2.1.5.4 Recovery

Recovery studies were carried out using samples with or without spiking of a known concentration of standards. The difference between spiked and non-spiked sample is the recovered amount.

3.2.1.6 Urine sample preparation

200 µL of urine sample were treated with 20 µL of 200 nM freshly prepared *N*-ethylmaleimide. Then, a fixed amount of stable isotope labeled internal standard was added. The final concentration of the internal standards was 10pmol d3-creatinine, 5pmol ^{13}C-^{15}N-GSSG, 67.5pmol ^{15}N-dG, 2.82pmol ^{15}N-8-oxodG, 10pmol ^{13}C-^{15}N-GSH-NEM, 0.51pmol ^{15}N-^{13}C-Ang II, 0.8pmol d7-Aldosterone and 1. 12pmol d4-8-isoPGF2α per injection. The sample was incubated for 20 min and centrifuged at room temperature. The prepared sample solution was transferred into a HPLC vial. 25 µL of mobile phase (10% MeOH in 0.1% formic acid) was added and vortexed for a few seconds to mix and to remove the air bubbles. Aliquots of 20 µL were injected into the HPLC using an auto sampler.

3.2.1.7 Plasma sample preparation

Plasma sample preparation was carried out using Waters C-18 solid phase extraction (SPE) cartridges, as previously described [101] with little modification. 300µL fresh plasma were treated with 30 µL of 200 mM freshly prepared *N*-ethylmaleimide (final concentration of 20 mM) [98, 99] and spiked with a fixed amount of stable isotope labeled internal standard mixture. Final concentrations of the internal standards per injection were four X 10pmol d3-creatinine, 5pmol ^{13}C-^{15}N-GSSG, 67.5pmol ^{15}N-dG, 2.82pmol ^{15}N-8-oxodG, 10pmol ^{13}C-^{15}N-GSH-NEM, 0.51pmol ^{15}N-^{13}C-Ang II, 0.8pmol d7-Aldosterone and 1. 12pmol d4-8-isoPGF2α. The above solution was incubated for 20 min. The sample solutions were applied to the Waters C18 SPE cartridge that had been preconditioned with 5 mL of methanol and 15 mL of HPLC water, respectively. After loading the sample, the cartridge was washed with 3 mL of HPLC water. Vacuum was applied to dry the column which helps to eliminate the water from the eluent. The analytes or markers were eluted from the cartridge using 10 ml of methanol. The column elutes were collected and dried under nitrogen gas. Finally, the dried samples were re-dissolved in 60µL of mobile phase, then centrifuged at 14000 rpm for 15 min at 4°C and transferred to a HPLC sample vial for LC-MS/MS analyses.

3.2.2 Analysis of 8-oxodG from DNA by LC-ESI-MS/MS

3.2.2.1 DNA isolation

The leukocyte layer was used for DNA isolation. The genomic DNA was isolated from animal tissues/cultured cells/ leukocyte using a minor modification of a recently developed protocol designed to minimize artefacts of DNA-oxidation during isolation (chaotropic protocol; [37, 43]. This protocol has also been adopted by the European Standards Committee on Oxidative DNA damage (ESCODD). Whole blood was centrifuged at 2500 x g for 10 min at room temperature, yielding three layers. The upper layer is plasma; the intermediate layer contains concentrated leukocytes; and the bottom layer consists of erythrocytes. The animal tissues/cultured cell/ leukocyte pellets were homogenized with 3 ml of buffer A (320 mmol/L sucrose, 5 mmol/L MgCl2, 10 mmol/L Tris/HCl, pH 7.5, 0.1 mmol/L desferrioxamine, and 1% (v/v) Triton X-100). After homogenization, the sample was centrifuged at 1500g for 10 min. washed with 1.5 ml of

buffer A and centrifuged again (1500g for 10 min). A total of 600 µl of buffer B (10 mmol/L Tris/HCl, pH 8, 5 mmol/L EDTA–Na2, 0.15 mmol/L desferrioxamine) and 35 µl of 10%(w/v) sodium dodecyl sulfate were added, and the sample was agitated vigorously. After 30 µl of RNase A (1 mg/ml) in RNase buffers (10 mmol/L Tris/HCl, pH 7.4, 1 mmol/L EDTA, and 2.5 mmol/L DFO) and 8 µl of RNase T1 (1U/µl in RNase buffer) were added, the samples were incubated at 37 °C for 1 h to remove contaminating RNA from the DNA. Then, 30 µl of proteinase K (20 mg/ml) was added and the samples were incubated at 37 °C for 1 h. Subsequently, 1.2 ml of NaI solution (7.6 M NaI, 40 mmol/L Tris/HCl, pH 8.0, 20 mmol/L EDTA–Na_2, 0.3 mmol/L desferrioxamine) and 2 ml of 2-propanol were added. The sample was gently shaken until the DNA had precipitated completely and then centrifuged at 5000g for 15 min. The DNA pellet was washed with 1 ml of 40% (v/v) 2-propanol. After centrifugation (5000g for 15 min) the DNA pellet was washed with 1 ml of 70% (v/v) ethanol. Finally, the DNA pellet was collected by centrifugation and dissolved in 0.1 mmol/L desferrioxamine overnight. DNA concentration was measured by the absorbance at 260 nm. Protein contamination was checked using the absorbance ratio A260/A280; an absorbance ratio over 1.6 was acceptable.

3.2.2.2 Enzymatic hydrolysis of DNA

DNA hydrolysis was performed as described by Chao et al.[43]. DNA samples (about 20 µg) from human blood were spiked with 2.82 pmol of $^{15}N_5$-8-oxodG and 84.3 pmol of $^{15}N_5$-dG. Then 10µL of 1 U/µL nuclease P1 (in 300 mmol/L sodium acetate and 1 mmol/L ZnSO4, pH 5.3) was added to the DNA solutions and the DNA was incubated at 37 °C for 2 h. Thereafter, 10 µL of 10× alkaline phosphatase buffer (500 mmol/L Tris/HCl, pH 8, 1 mmol/L EDTA) containing 0.2 µL of alkaline phosphatase was added and the incubation was continued at 37 °C for 2 h. Finally 10µL of 0.1 M HCl was added to neutralize the solution. The neutralized DNA hydrolysates were filtered through a cut-off filter tube (Ultrafree 5000 NMWL, Millipore, Germany) and centrifuged at 4°C and 7000×g for 45 min then measured by online LC–MS/MS.

3.2.2.3 Automated solid-phase extraction

The detailed column switching operation method is schematically described elsewhere (Figure 19) [43, 102]. The column-switching system consisted of a switching valve (two-position microelectric actuator; Valco) and an Inertsil, ODS-3 column (50mm × 4.6mm; 5µm). 100 µL of prepared DNA sample was loaded on to the trap column using auto sampler (Agillent 1100 series) with the switching valve at position B. The loading and washing buffer, 0.1% formic acid in 5% (v/v) methanol at a flow rate of 1mL/min was delivered by quaternary pump (Agillent 1100 series). The trap column was run with loading buffer for 3.6 min, followed by the valco valve changing to position A to transfer into the LC system. At 5 min after injection, the valve was switched back to injection position B, and the trap column was washed using a mobile phase with linear gradient from 100% of 0.1% formic acid in 5% (v/v) methanol to 100% of 0.1 % formic acid in 50% methanol for 7 min. This was followed by 100% of 0.1% formic acid in 5% (v/v) methanol for 3 min equilibration of the trap column. The valco valve was controlled by analyst® software 1. 4. 2 (Applied Biosystems) and the total run time was 15 min. After 3.6 min, the sample was automatically transferred onto a polyamine-II endcapped HPLC column (YMC; 150mm × 4.6mm, 5µm) entering from the opposite direction. The isocratic method was used to achieve the desired sample separation using 85% (v/v) methanol with 0.1% formic acid at a flow rate of 1mL/min. The eluted sample from the HPLC system was introduced into the turbo ion spray source of an API 3000 triple-quadrupole mass spectrometer (Applied Biosystem), operating in the positive ion mode, using nitrogen as the nebulizing gas and with the turbo gas temperature set at 475 °C. The multiple reaction monitoring conditions were obtained for the fragmentation of 8-oxodG (284 to 168 m/z), $^{15}N_5$-8-oxodG (289 to 173 m/z), 2'-dG (268 to 152 m/z), and $^{15}N_5$-2'-dG (273 to 157 m/z). Nebulizer and curtain gas flow rate were set at 12 arbitrary units. Collision assisted dissociation gas and turbo gas were set at 4 arbitrary units for both. The collision energy was set at 17eV and 21eV for dG and 8-oxodG respectively, nitrogen used as a collision gas. The separated 8-oxodG and dG were quantified using the respective internal standard (Figure 20).

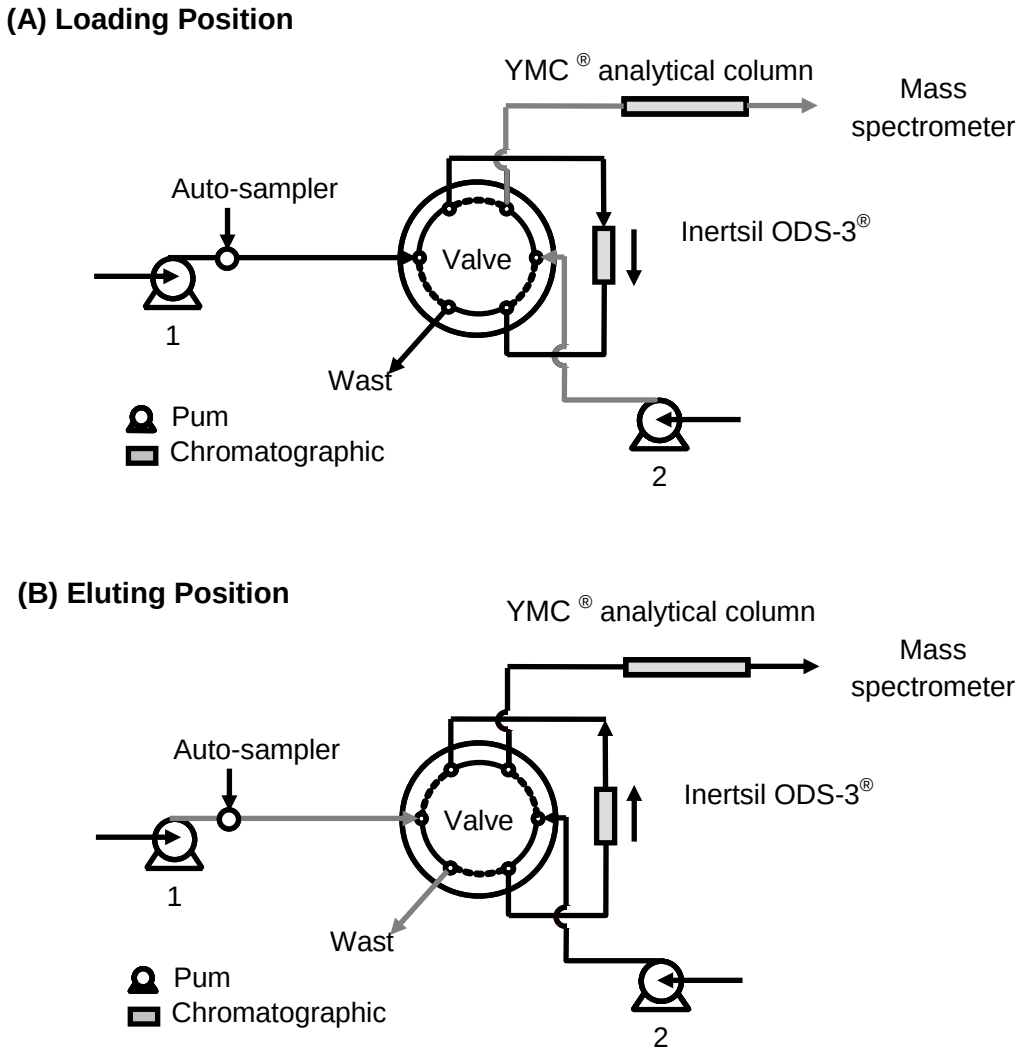

Figure 19: Schematic configuration and valve positions of the on-line extraction LC-MS/ MS system. (a) Sample loading position and (b) sample back flush and elution position. Modified schematic diagram with permission from Brink et al. [102](copyright 2006, Elsevier Limited).

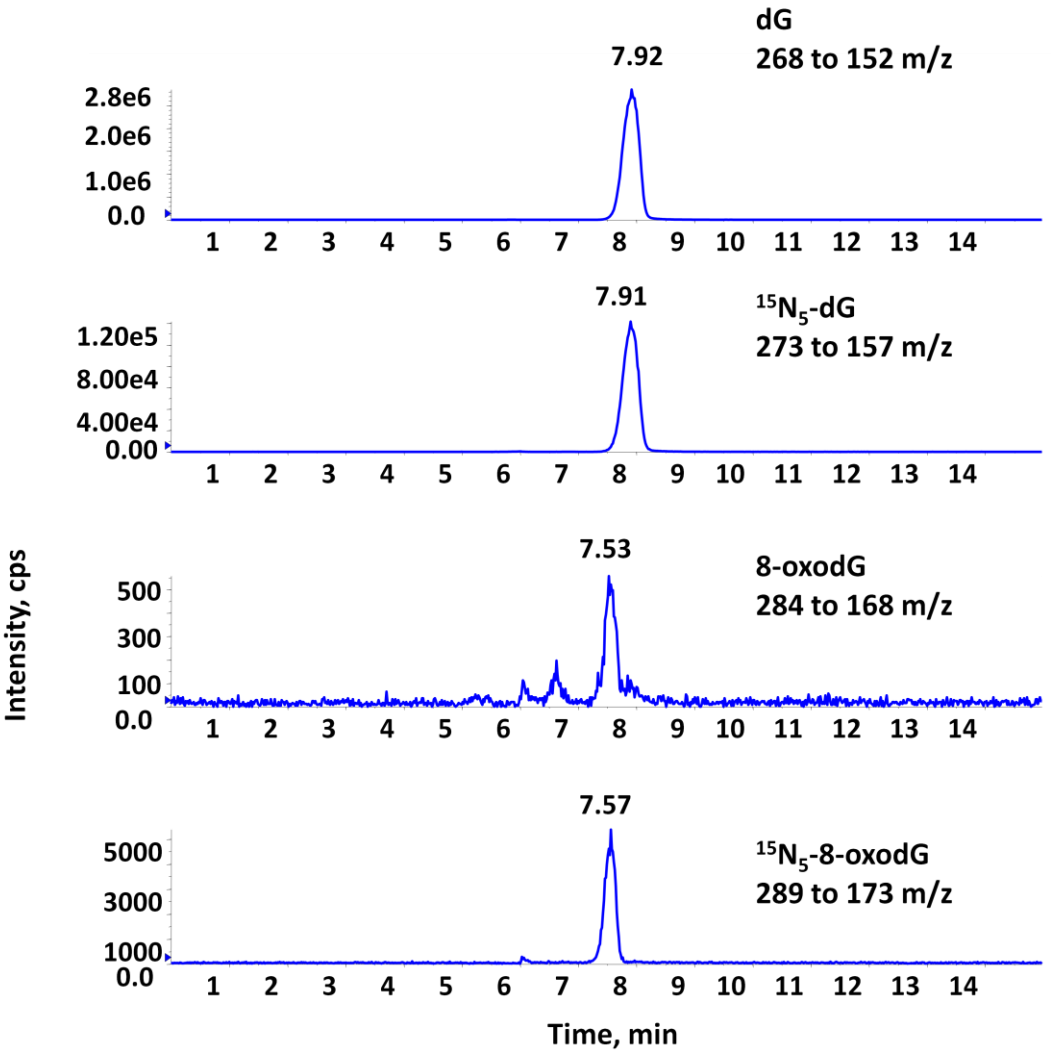

Figure 20: LC-MS/MS chromatogram for analysis of 8-oxodG from DNA

3.2.3 Total glutathione measurement by spectrophotometer

dl-Buthionine-sulfoximine (BSO) (500 µM) was added for 24 h to achieve partial glutathione-depletion and thus enhance cellular sensitivity. Test substances were then added for 3 h. After incubation, cells were washed twice with PBS and resuspended in 400 µl 1% sulfosalicylic acid. After 15 min incubation on ice, cells were centrifuged (5000 × g). 20 µl of the supernatant was mixed with 260 µl of 100 mM phosphate buffer, 20 µl of 2.5 mM dithiobis-2-nitrobenzoic acid and 300 µl glutathione reductase (1.3 units glutathione reductase/ml, 50 mM phosphate

buffer, 0.5 mM EDTA, 0.3 mM NADPH) solution. The kinetics was determined at 410 nm using a U-2000 Spectrophotometer (Hitachi, Tokyo, Japan) [67].

3.2.4 Ferric Reducing -Ability of Plasma/ -Antioxidant Power- (FRAP) Assay

This method determines the reduction of a ferric tripyridyltriazine complex to its ferrous, coloured form, in the presence of plasma antioxidants. The antioxidative capacity of plasma/substances were determined as described by [103]. Briefly, 20µl of plasma/sample (which had been stored at -20°C) were added to 180 µl of water. Next, 600 µl of the FRAP reagent was added and a photometric reading at 593 nm was taken immediately (data not shown), after 15min and after 30 min (not shown). The FRAP reagent consists of a 1:1:10 mixture of 10 mmol/L ferric-tripyridyltriazine, 20 mmol/L ferric chloride and 300 mmol/L acetate buffer. Three determinations from each sample were made at each time point. Results are given as ferric tripyridyltriazine complex reduction equivalents (µmol/L) [104].

3.3 Biological methods

3.3.1 Superoxide measurement

$2x10^5$ cells were seeded on coverslips the day before treatment. After the end of the treatment the medium was removed and cells were washed twice with PBS. Fresh medium was added containing 5 µM dihydroethidium (Merck Biosciences GmbH) and the cells were incubated for 30 min at room temperature in the dark. After washing with PBS, pictures of the cells were taken using an Eclipse 55i microscope (Nikon GmbH) and a Fluoro Pro MP 5000 camera (Intas Science Imaging Instruments GmbH) at 200-fold magnification. Quantification was done by measuring grey values of 200 cells per treatment with ImageJ (http://rsb.info.nih.gov/ij/)[105].

3.3.2 Comet assay

The isolated mouse kidney was minced to small pieces in 3 mL buffer [RPMI 1640, 15% DMSO, 1.8% (w/v) NaCl], filtered through a cell strainer with a mesh pore size of 100 µm (Becton Dickinson), precipitated at 1,000 rpm and 4°C for 5 min (Heraeus Labofuge 400e), and re-suspended in 1 mL buffer. In the case of LLC-PK1 cells (3.5×10^5), they

were seeded the day before in small culture flasks, treated for 4 h with test substances in 5 mL medium then harvested. Isolated kidney cells or LLC-PK1 cells (20µL) were suspended in 180µL of low-melting-point agarose (0.5% diluted in calcium and magnesium-free PBS), and 45 µL of the suspension was embedded on the frosted microscope slides coated with a layer of high-melting-point agarose (1.5%, diluted in calcium and magnesium-free PBS). For lysis, slides were immersed in a jar containing fresh cold lysing solution (1% Triton X-100, 10% DMSO, and 89% lysis buffer containing 10 mM Tris, pH 10; 1% Na-sarcosine; 2.5 M NaCl; and 100 mM Na2EDTA) and incubated at 4°C in a dark chamber for 1 h. Next, slides were placed into a horizontal electrophoresis tank with fresh alkaline electrophoresis buffer (300 mM NaOH and 1 mM Na_2-EDTA, pH 13), and left for 20 min at 4°C in the dark, to allow DNA unwinding and alkali-labile damage expression. Electrophoresis was carried out, at 4°C in the dark, for 20 min in a 25-V and 300-mA electrical field. Afterward, the slides were neutralized for 5 min in 0.4 M Tris (pH 7.5) and then the DNA was stained by adding 20 µL of 20 µg/mL propidium iodide (CAS Nr. 25535-16-4) to each slide. A fluorescence microscope at ×200 and a computer-aided image analysis system (Komet 5; Kinetic Imaging, Bromborough, UK) was used for analysis. Fifty cells in total were analyzed; the mean tail DNA (percentage of intensity in the tail region) is given [106-108].

3.3.3 Micronucleus frequency assay

Micronuclei (MN) are expressed in dividing cells that either contain chromosome breaks (resulting from unrepaired double-strand breaks) and/or by whole chromosomes that are unable to travel to the spindle poles during mitosis. They are observed in cells with completed nuclear division and are scored in the binucleated stage of the cell cycle by using the cytokinesis inhibitor, cytochalasin B. The micronucleus frequency test was performed as described earlier [107, 109]. Cells were incubated for 4 h with the tested compounds, then 3 µg/ml cytochalasin B was added for 24 h to obtain binucleated (BN) cells. The frequency of micronuclei was obtained after scoring 1000 BN cells on each of two slides at a 400-fold magnification.

3.3.4 RNA isolation and semi quantitative reverse transcriptase PCR

Total RNA was isolated from treated cells with the RNeasy mini kit (Qiagen, Hilden, Germany) and 2.5 µg of RNA was used for cDNA synthesis using RevertAidTM First Strand cDNA Synthesis Kit (Fermentas GmbH, St. Leon-Rot, Germany). cDNA was amplified by polymerase chain reaction (PCR) using REDTaqTM ReadyMixTM PCR Reaction Mix (Sigma-Aldrich, Taufkirchen, Germany) for 35-40 cycles using the primers depicted further down.

The following primers with the respective GenBank accession number and predicted size were used for amplification: β-actin (NM_001101; 591 bp) 5'-TCCCTGGAGAAGAGCTACGA- 3' (sense), 5'-GTCACCTTCACCGTTCCAGT-3' (antisense); glutathione peroxidase (GPX, NM_000581; 538 bp) 5'-CCAGTCGGTGTATGCCTT-CT-3'(sense), 5'-GATGTCAGGCTCGATGTCAA-3' (antisense); glutathione reductase (GR, NM_00637; 453) 5'-GATCCCAAGCCCACAATAGA-3' (sense), 5'-CAGGCAGTCAACATCTGGAA-3'(antisense); glutathione synthase (GSS, NM_00-0178; 494 bp) 5'-CAGCGTGCCATAGAGAATGA-3' (sense), 5'-TTCAGGGC-CTGTACCATTTC-3' (antisense). PCR products were resolved on a 1.5% agarose gel, stained with ethidium bromide. Results were related to the β-actin and subsequently normalised to the control. For quantification of the mRNA, the density of the bands was measured using Gel Doc 2000 with the software Multi-Analyst Version 1.0.2 (Bio-Rad, Hercules, CA, USA) [67].

3.3.5 Statistics

Mann-Whitney test was used to determine significance between two groups and Kruskal-Wallis test was used to determine significance between multiple groups (GraphPad InStat 3.05 software). Values are given as means ± standard error mean (SEM) or as means ± standard deviation (SD). A p value ≤0.05 was considered statistically significant.

4 Results

4.1 LC-ESI-MS/MS method development and validation: Analysis of 8-oxodG, 8-isoPGF2α, 8-nitroG, GSH, GSSG, dG, angiotensin II, aldosterone, and creatinine within a single run.

4.1.1 Synthesis of stable isotope labeled internal standards

4.1.1.1Synthesis of ^{15}N-^{13}C-GSSG

After synthesis the pure ^{15}N-^{13}C-GSSG was isolated using a HPLC-UV method (Figure 21-22). The synthesized glycine-labeled GSSG was scanned in the positive mode mass spectrometry in the range of 100 to 1000 m/z and the molecular ion was observed at 619. 20^{H+} and the product ions were 361 and 490 m/z.

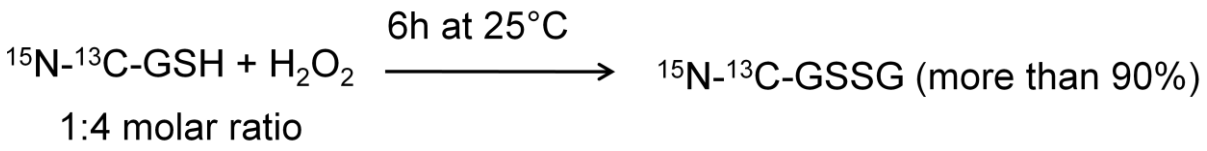

Figure 21) Chemical reaction of labeled GSSG from labeled GSH. A solution of 2mM labeled GSH was treated with an equal volume of 16mM hydrogen peroxide. The reaction was carried out at 25°C for 6h

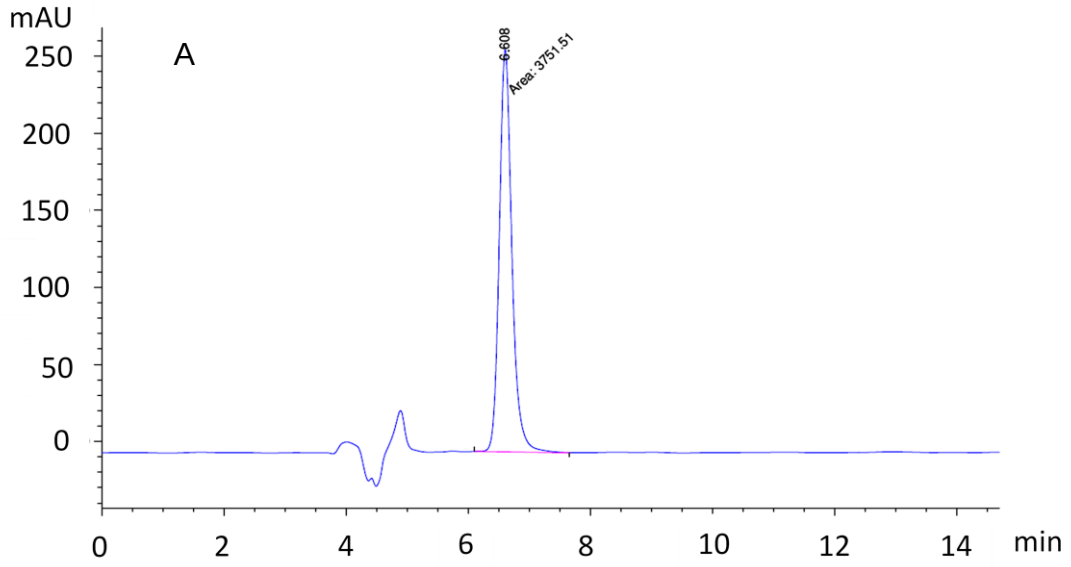
A
mAU
250
200
150
100
50
0
6.608
Area: 3751.51
0
2
4
6
8
10
12
14
min

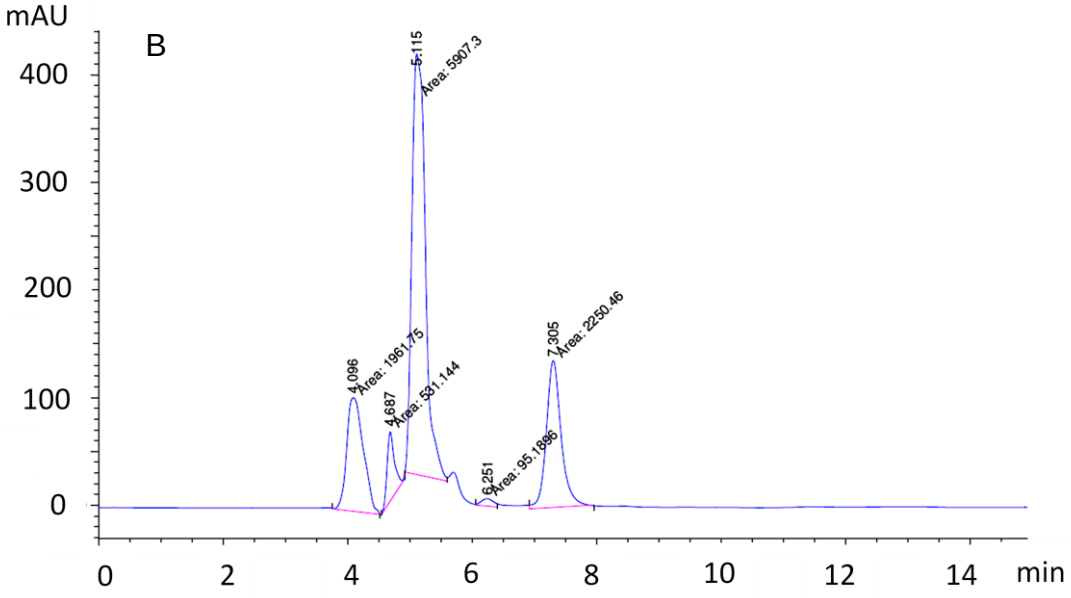
B
mAU
400
300
200
100
0
5.115
Area: 5907.3
4.096
Area: 1961.75
4.687
Area: 531.144
6.251
Area: 95.1886
7.305
Area: 2250.46
0
2
4
6
8
10
12
14
min

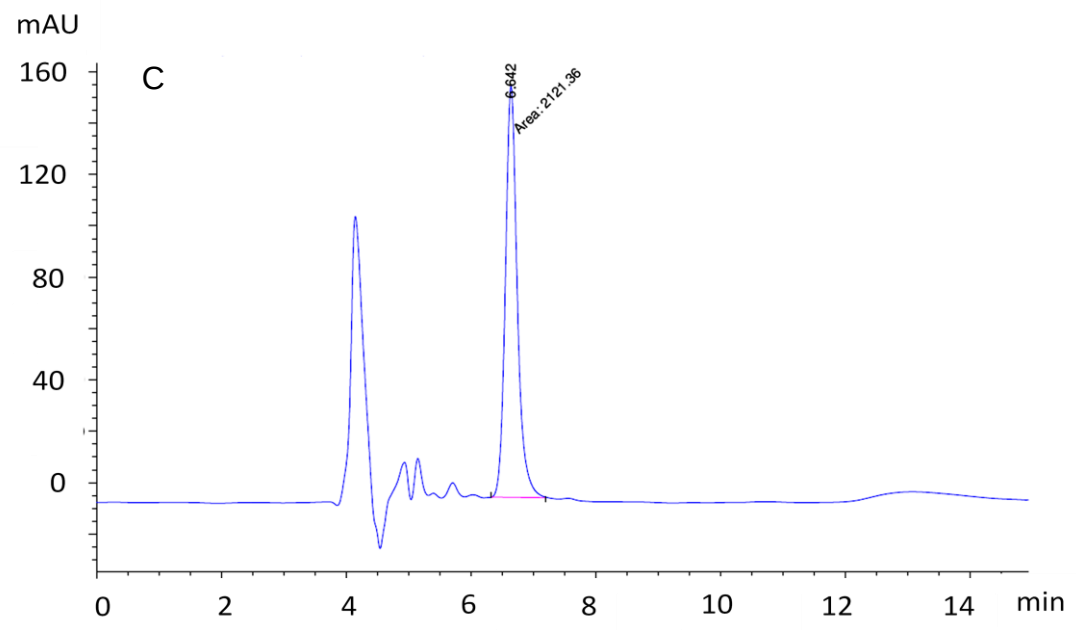

Figure 22: ^{13}C-^{15}N-GSSG was isolated using HPLC-UV with a Reprosil pur (150 x4.6 mm; 5µm), column with a mobile phase of 10% MeOH in 0.1% TFA. The isocratic run time was 15 min and the flow rate 400µL/min, the analytes were detected at 210nm. HPLC-UV chromatogram of B) GSSG standard peak, C) Reaction mixture peaks, D) Pure isolated 15N-13C-GSSG peak.

4.1.1.2 Synthesis of ^{15}N-^{13}C-GSH-NEM

GSH was detected as the GSH-NEM adduct. In order to prevent the artifactual oxidation of GSH to GSSG during sample preparation, it is very important to block the thiol group of GSH with NEM. Furthermore the NEM adduct is more easily detectable by positive electro spray ionization [99]. The synthesized labeled GSH-NEM adducts showed molecular ion at 436 m/z and product ion at 307 m/z mass spectrometer.

4.1.1.3 Synthesis of ^{15}N-8-oxodG

Figure 23 shows a typical chromatogram obtained when an aliquot of the reaction was separated by semi preparative HPLC. The identity of the peak corresponding to $^{15}N_5$-8-oxodG was confirmed by LC/MS analysis. Contamination due to the peak from $^{15}N_5$-dG was detected. To remove this contamination, the $^{15}N_5$-8-oxodG fraction was re-injected onto the HPLC system. The concentration of $^{15}N_5$-8-oxodG was determined by UV

spectrometry. The purified $^{15}N_5$-8-oxodG (Figure 24), which is five mass higher than that of unlabelled standard was confirmed by mass spectrometry (Figure 25).

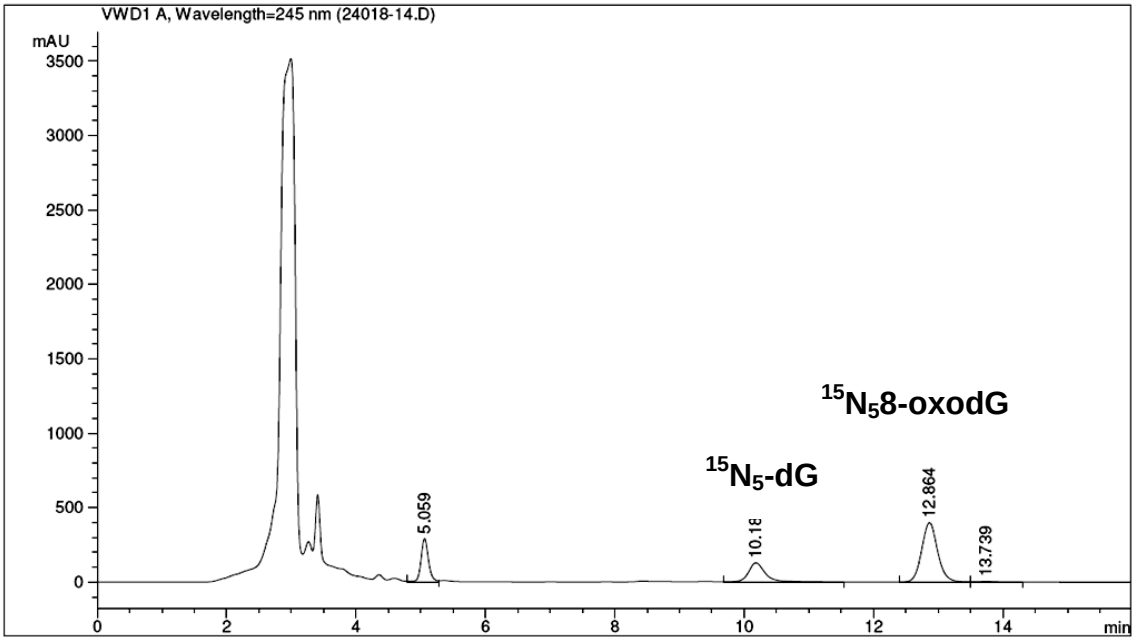

Figure 23: HPLC-UV chromatogram for the reaction mixture for synthesis of $^{15}N_5$-8-oxodG from $^{15}N_5$-dG

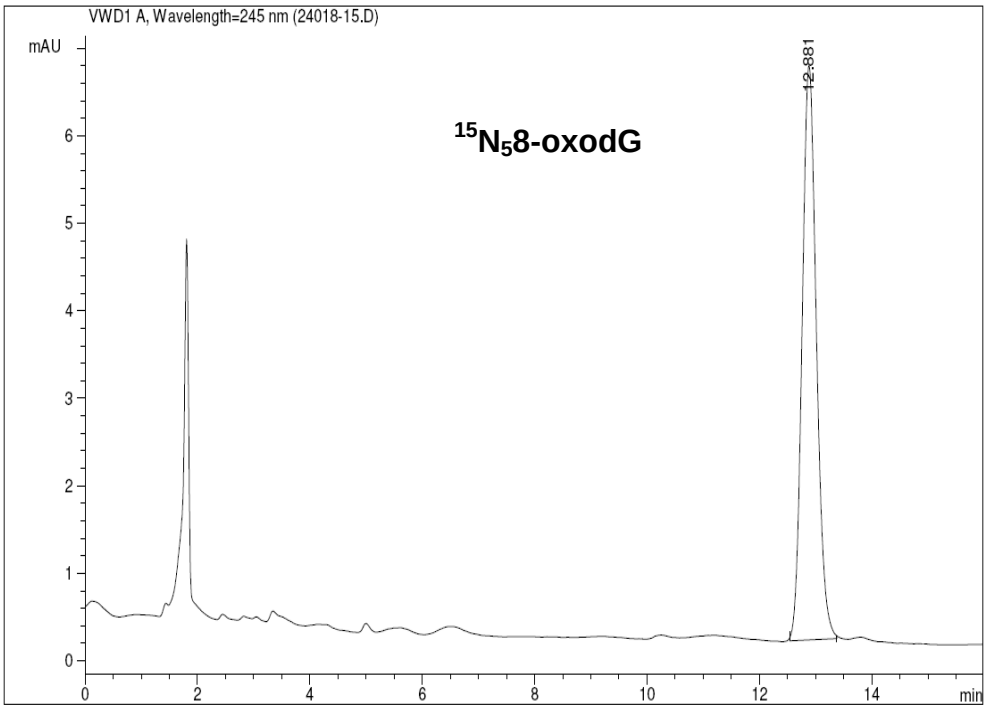

Figure 24: HPLC-UV chromatogram for the purified $^{15}N_5$-8-oxodG from $^{15}N_5$-dG reaction mixture

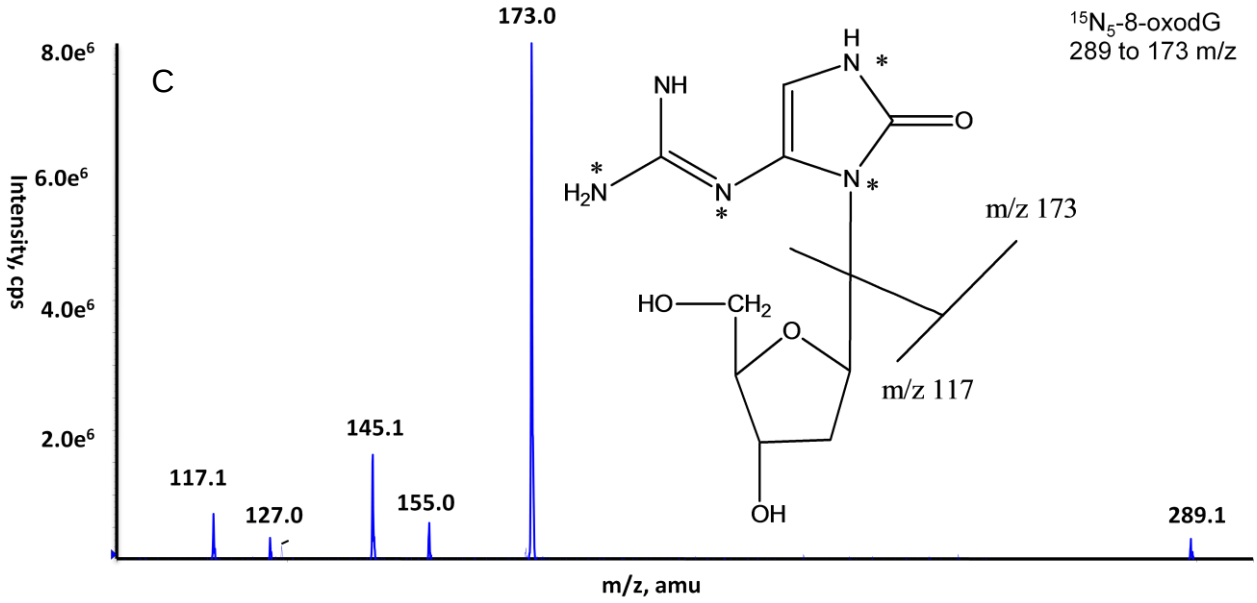

Figure 25: Mass fragmentation of $^{15}N_5$-8-oxodG (the asterisks indicate the labeled sites in the internal standard) in positive mode. The MS/MS spectrum for $^{15}N_5$-8-oxodG is shown corresponding to the product ion for $^{15}N_5$-8-oxoG at m/z 173 formed from the $[M+H]^+$ ion at m/z 289.

4.1.2 Mass spectrometer parameters

A triple-stage quadrupole mass spectrometer (API 3000, Applied Biosystems, Darmstadt, Germany) equipped with a Turbo Ionspray source was used. The ion spray voltage was 3500 V, the source temperature 400°C. The analytes were monitored in the positive and negative multiple reaction monitoring (MRM) mode simultaneously. For optimum sensitivity, specific product ions and optimal instrument settings were obtained by infusion of authentic standards and using the quantitative optimization function of the Analyst 1.4.2 software (Applied Biosystems, Darmstadt, Germany). Table 4 provides the details of the instrumental settings. Two transitions for each analytes were monitored. Peak areas of the most sensitive transitions were used for quantification. Creatinine, GSSG, GSH-NEM, dG, 8-nitroG, 8-oxodG and Ang II were analyzed using positive MRM mode. Aldosterone and 8-isoPGF2α were analyzed using negative MRM mode.

Table 4. Multiple reaction monitoring parameters for the analytes.

Analytes	Precursor ion Q1	Product ion Q3	DP	FP	CE	CXP	
Creatinine	114	44*	16	90	17	15	Positive mode detection
		86	16	90	17	15	
d3-creatinine	117	89*	16	90	17	15	
GSSG	613.20	335.16*	20	200	30	15	
		484	16	130	5	24	
^{13}C-^{15}N-GSSG	619.20	361.16*	20	200	30	15	
		490	20	200	30	15	
dG	268.20	152.10*	16	90	17	14	
15N-dG	273.20	157.10*	16	90	17	14	
8-nitroG	197.23	151.00	86	300	21	16	
8-oxodG	284	168*	21	110	21	16	
^{15}N-8-oxodG	289	173*	21	110	21	16	
GSH-NEM	433.31	304.09*	20	200	30	15	
		201.10	20	200	30	15	
^{13}C-^{15}N-GSH-NEM	436	307*	20	200	30	15	
Ang II	523.95	263.10*	41	210	31	26	
		110.10	41	210	57	10	
^{15}N-^{13}C-Ang II	528.84	273.20*	61	150	31	24	
		110.20	61	150	61	18	
Aldo	359.28	188.80*	-56	-	-26	-9	Negative mode detection
		331	-56	-	-24	-19	
d7-Aldo	366.15	192.80*	-61	-	-28	-9	
		338	-61	-	-24	-17	
8-isoPGF2α	353	193.05*	-61	-	-36	-17	
		273	-61	-	-30	-17	
d4-8-isoPGF2α	357	197*	-20	-	-30	-15	

*Transitions used for quantification
DP: declustering potential [V]; FP: focusing potential [V]; CE: collision energy [V]; CXP: collision cell exit potential [V].

4.1.3 Separation of analytes by LC and detection by ESI-MS/MS

To achieve the final separation method of these compounds took numerous trials. Reduced flow rates and the selection of the appropriate mobile-phase composition are key factors for high sensitivity in LC-ESI-MS, because the ion formation process in ESI involves the ionization of sample molecules in the liquid phase. In general, a solvent

with low surface tension, low viscosity, and low heat of vaporization would increase the production of gas-phase ions. For those reasons, ESI measurements usually employ acidified solutions of acetonitrile (ACN)/water or methanol (MeOH)/water. A study reported that MeOH as the organic modifier represents a better mobile-phase system for nano LC-ESI-MS/MS, especially analysis of peptide mixtures [110]. Moreover, methanol is less expensive and less toxic than ACN, therefore, we used methanol as an organic modifier in our method.

We used a simple mobile phase consisting of 0.1% formic acid in water and 100% methanol. The gradient started with 10% methanol and increased 2% per min until 10 min. In this period creatinine, GSSG, dG and 8-nitroG were separated. After 10 min methanol was increased up to 3.5% per min until 30 min to separate GSH-NEM, 8-oxodG and Ang II. When the gradient contained about 65% methanol, Ang II eluted. After 30 min the methanol amount was reversed to 10% until the end of the run at 60 min (Figure 26 - 32).

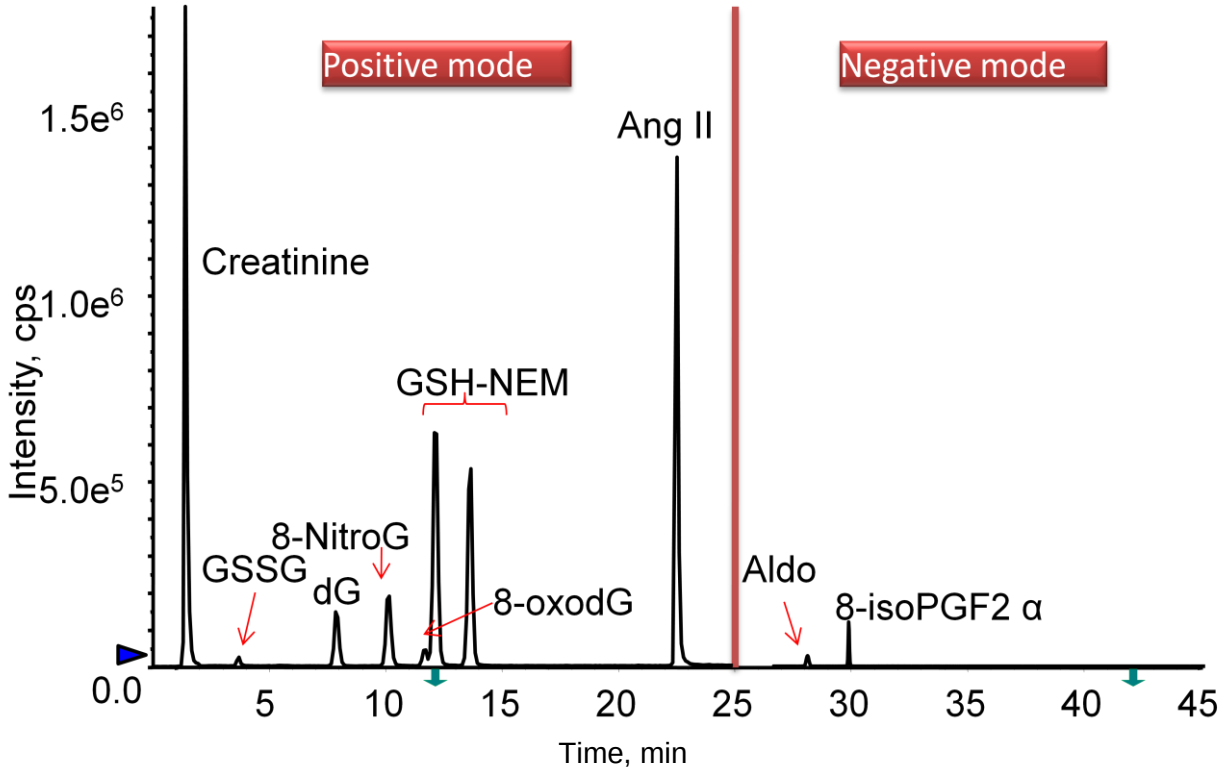

Figure 26: Total ion chromatogram for the analyzed markers were detected using positive and negative mode.

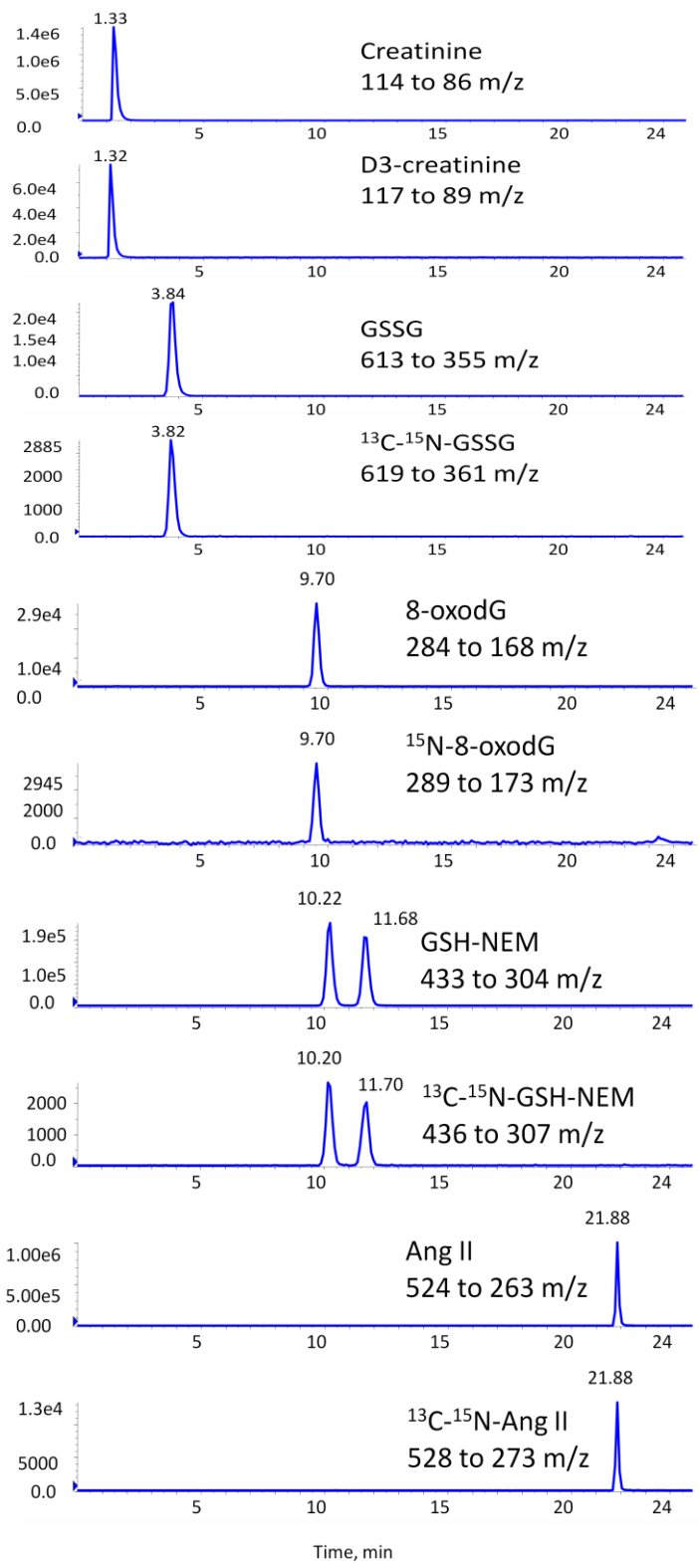

Figure 27: Multiple reaction monitoring (MRM) chromatograms for individual analytes (Positive mode)

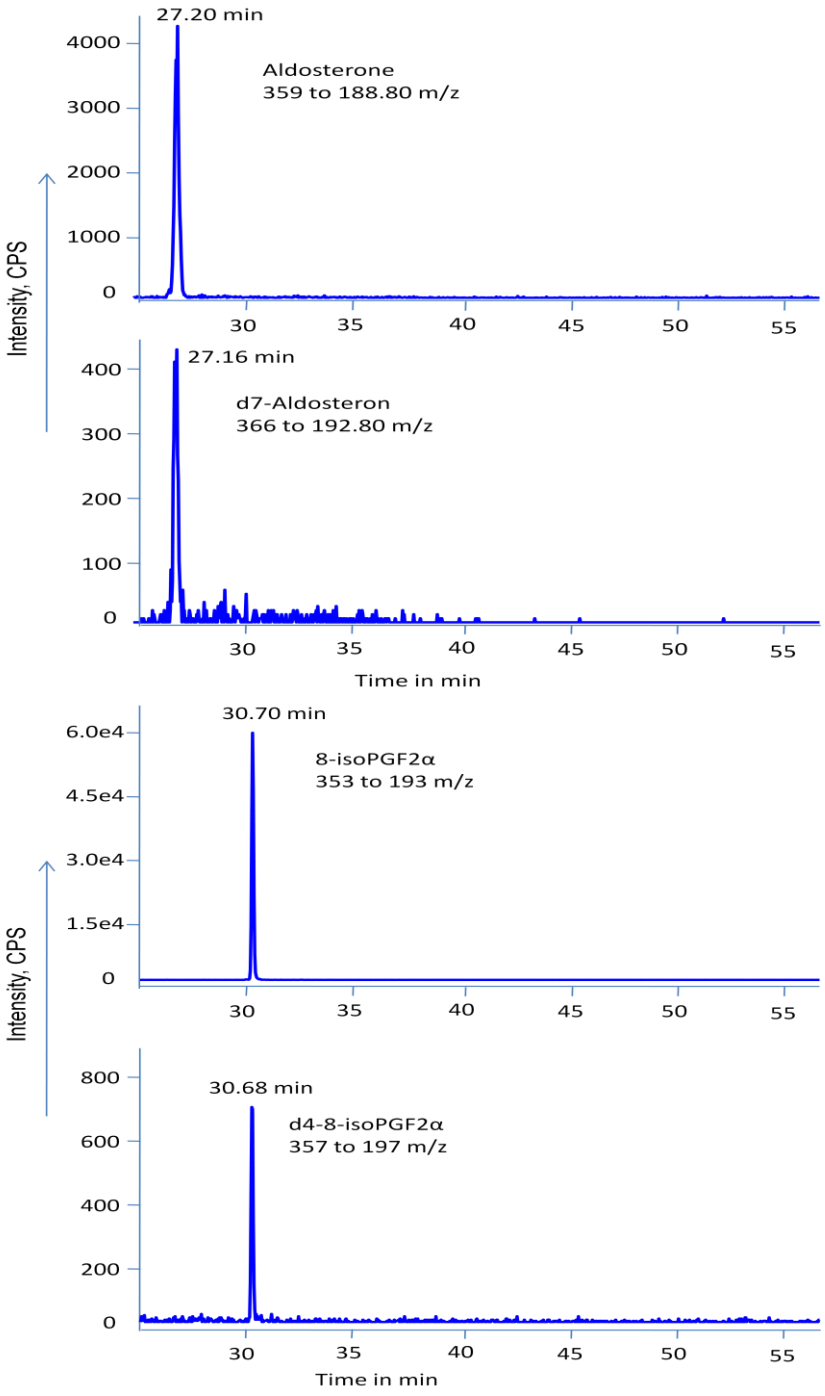

Figure 28: Multiple reaction monitoring (MRM) chromatograms for individual analytes (negative mode)

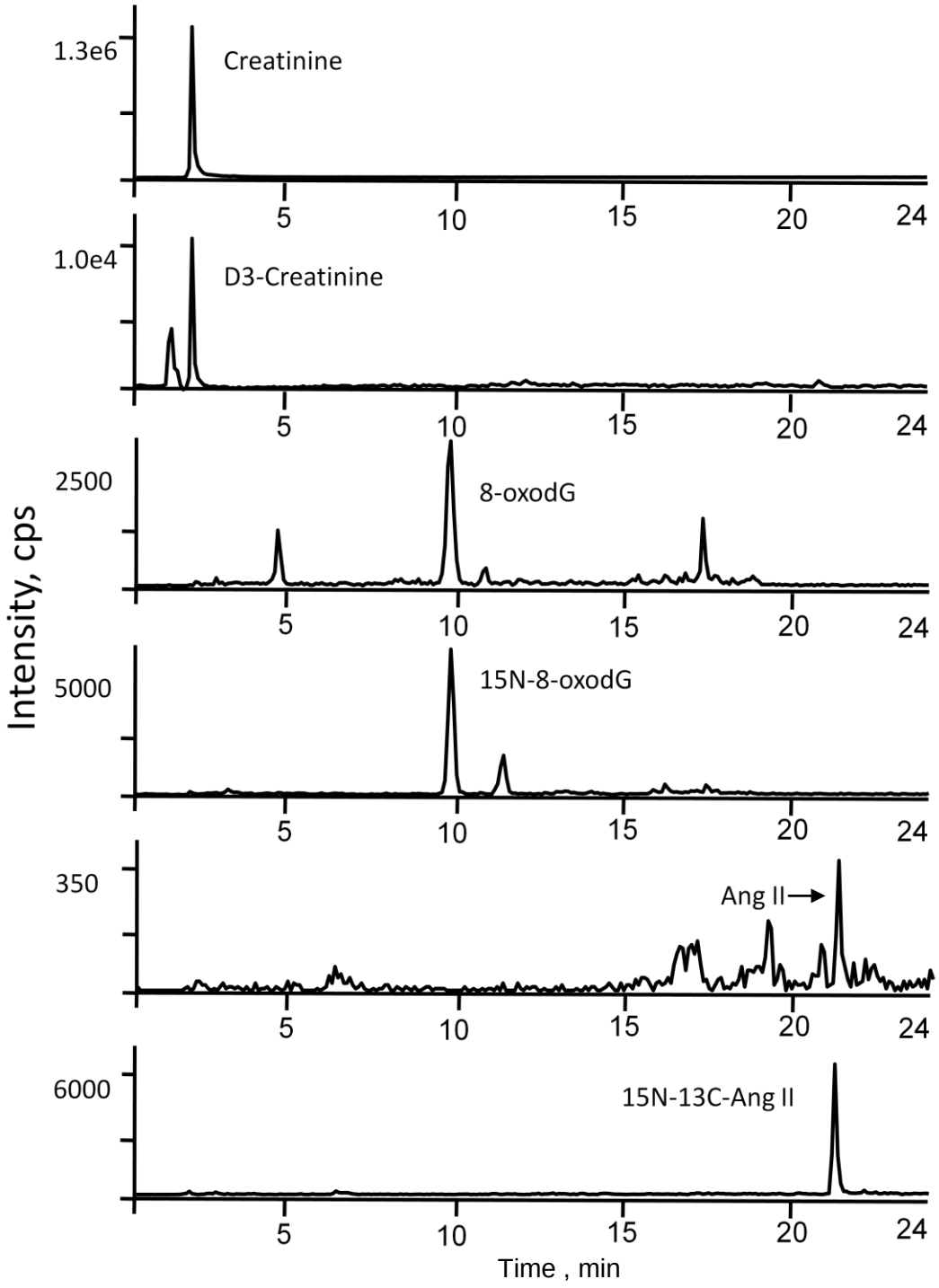

Figure 29: Multiple reaction monitoring (MRM) chromatograms from a representative sample of WT young mice (12-13 weeks) showing urinary analytes and respective stable isotope internal standards (Positive mode)

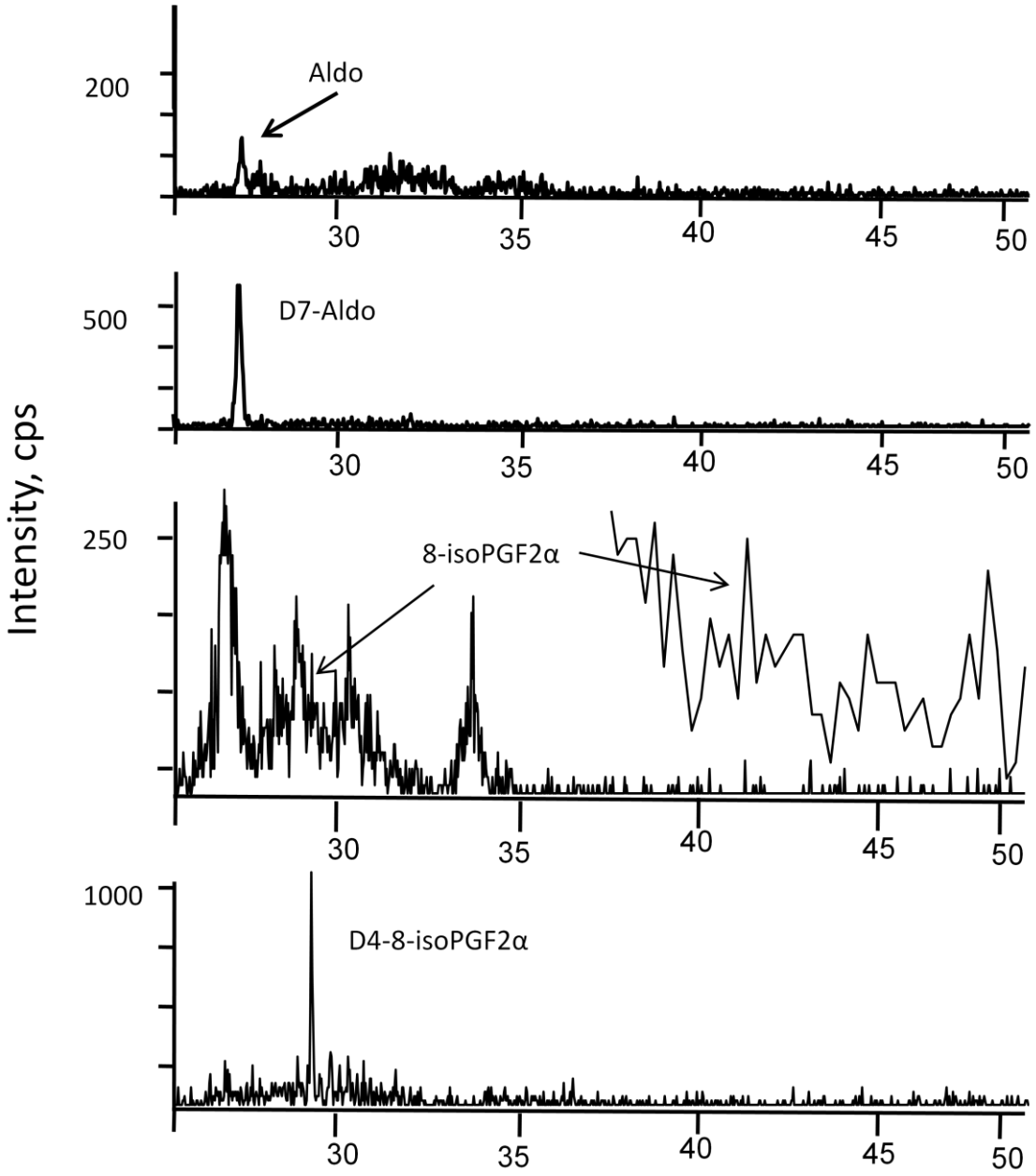

Figure 30: Multiple reaction monitoring (MRM) chromatograms from a representative sample of WT young mice (12-13 weeks) showing urinary analytes and respective stable isotope internal standards (negative mode).

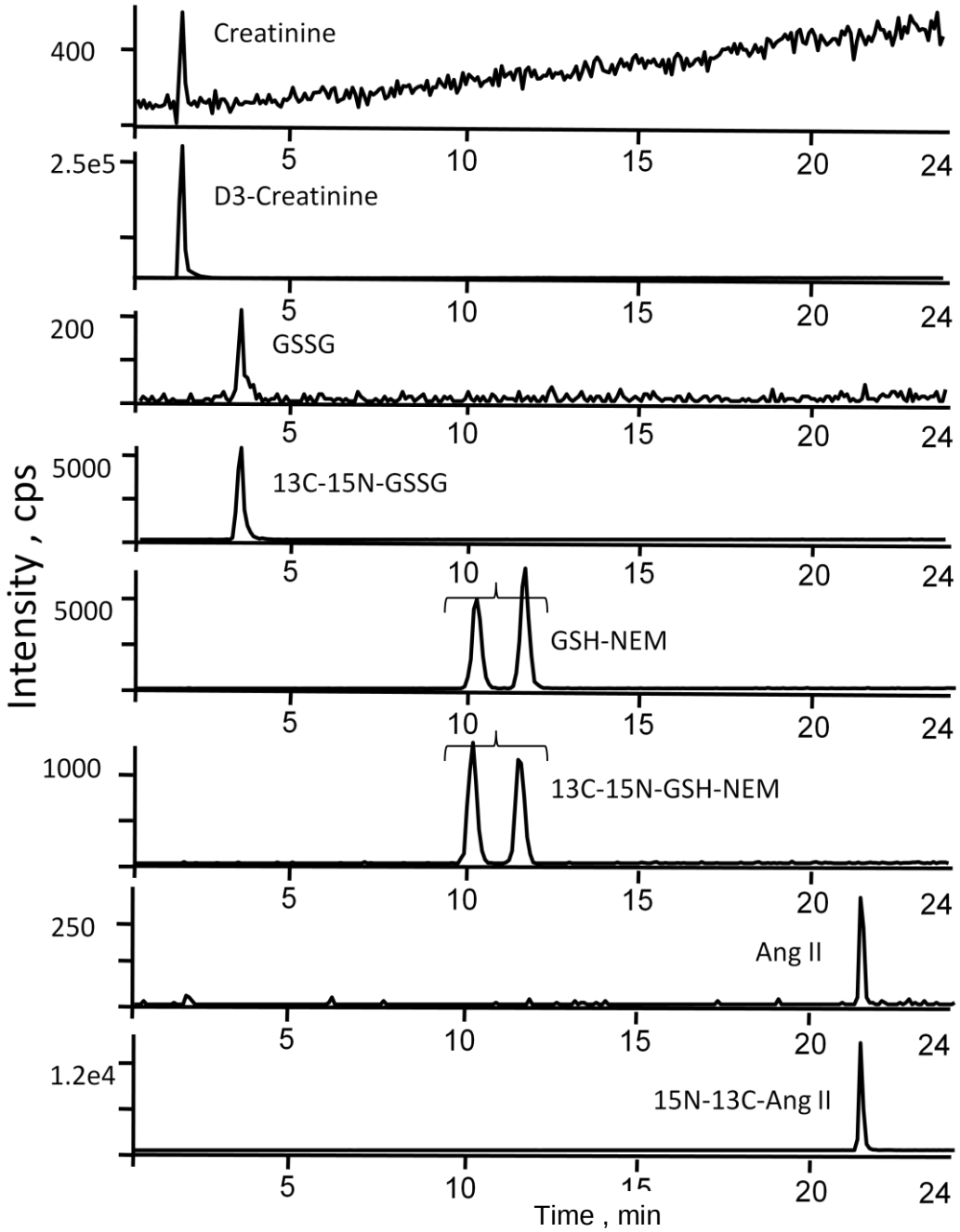

Figure 31: Multiple reaction monitoring (MRM) chromatograms from a representative sample of WT young mice (12-13 weeks) showing plasma analytes and respective stable isotope internal standards (positive mode).

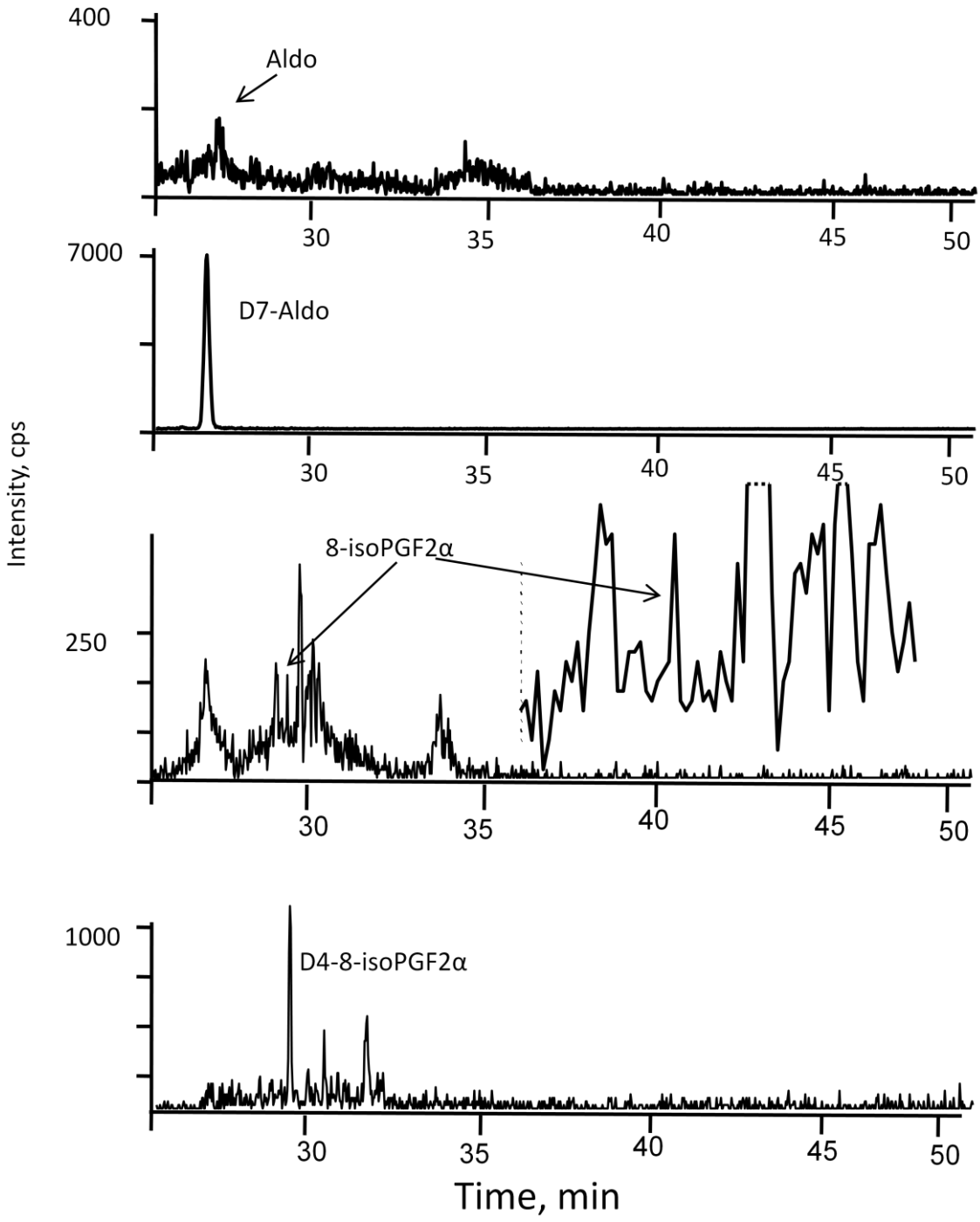

Figure 32: Multiple reaction monitoring (MRM) chromatograms from a representative sample of WT young mice (12-13 weeks) showing plasma analytes and respective stable isotope internal standards (negative mode).

4.1.4 Method validation

The method was validated according to the U.S. Department of Health and Human Services, Food and Drug Administration guidelines for bioanalytical method [100]. The limit of quantification (LOQ) was defined as the lowest concentration of analytes that could be reliably and reproducibly measured for accuracy, intraday precision, and interday imprecision. The determined LOQs were 9.7 pmol for creatinine, 0.04pmol for 8-oxodG, 0.24pmol for GSH-NEM, 6.2 pmol for GSSG, and for 8-isoPGF2α less than 0.01pmol. Ang II and aldosterone yielded less than 0.01pmol on the column. The limit of detection (LOD), defined as the lowest concentration that gave a signal-to-noise ratio of at least 3, was found to show acceptable values for all analytes (Table 5). The linearity of the analytes was not less than 0.977, which is acceptable according to the FDA guidelines.

Table 5: Linearity, LOQ, LOD and recovery for the analytes.

Markers	Linearity r =	LOQ pmol	LOD pmol (S/N)	Recovery in %	
				Lower range	Higher range
Creatinine	0.9987	9.7	2.5 (3.9)		
8-oxodG	0.9917	0.04	0.01 (3)		
GSH-NEM	0.9954	0.24	0.0076 (4)	46.005	33.731
GSSG	0.9779	6.2	6.2 (14.5)	113.83	102.7175
Ang II	0.9904	0.0012	0.0000048 (12.5)	103	93.2875
Aldo	0.9875	0.0048	0.00015 (13.5)		
8-isoPGF2α	0.9899	0.0012	0.0000024 (186)	107.75	71.775

The accuracy of the method was checked with low, middle and high concentration of the analytes standards and the % relative standard deviations (%RSD) were calculated. The accuracy was also checked for the method variation using a run time of 25 min. The % RSDs for all analytes and both methods were within the acceptable limit (Table 6).

Table 6: Listed markers in two different methods

Markers	Accuracy 60 min run time % rsd			Accuracy 25 min run time % rsd		
	low	middle	High	low	middle	High
Crea	7.31	4.92	2.01	2.55	4.40	3.83
8-oxodG	4.34	2.75	1.72	3.33	1.63	0.93
GSH-NEM	7.45	8.31	3.79	6.38	3.24	5.43
Ang II	6.21	3.80	2.34	8.51	8.42	5.14
Aldo	6.53	4.92	5.25			
8-isoPGF2α	14.26	6.44	7.89			

In the following parts of this thesis is, this optimized method was applied for the analysis of urine samples from WT and p47phox$^{-/-}$ mice. 8-oxodG, Ang II, aldosterone, and 8-isoPGF2α were quantified. GSSG and GSH were detected but not quantified, because these markers have no biological relevant in urine. 8-nitroG was not detectable and dG was not considered in these samples (refer to section 4.2).

Furthermore, plasma samples from WT and p47phox$^{-/-}$ mice were analyzed. GSSG and GSH, Ang II, Aldosterone and 8-isoPGF2α were quantified. dG, 8-oxodG and 8-nitroG were not detected (refer to section 4.2).

4.2 Role of the NOX subunit p47phox on oxidative DNA and lipid damage

4.2.1 Role of p47phox in the formation of oxidative DNA damage

To investigate whether p47phox is necessary for ROS induced oxidative DNA damage during ageing, we compared young and old WT and p47phox $^{-/-}$ mice. The level of DNA damage determined by comet assay analysis in the liver and kidney is shown in figure 33 A and B. There was no statistically significant difference between young WT and p47phox$^{-/-}$ mice. However, in kidneys from old mice there was a significant difference between the groups (Figure 33 A and B). The DNA damage in the kidneys from old WT animals was about three fold higher than in young WT mice. The difference in livers from WT and p47phox $^{-/-}$ mice was not significant (Figure 33 B), but showed a trend for elevated damage in WT mice.

To characterize further the DNA damage, we analyzed the oxidative DNA base modification 8-oxodG, from kidney DNA of young and old WT versus p47phox$^{-/-}$ mice. The level of 8-oxodG is expressed as adducts per millions of dG. There was an accumulation of 8-oxodG in kidney with age in WT but not in p47phox$^{-/-}$ mice (Figure 34). And there were statistically significant differences between WT and p47phox-/- mice with WT mice showing more 8-oxodG in both age groups.

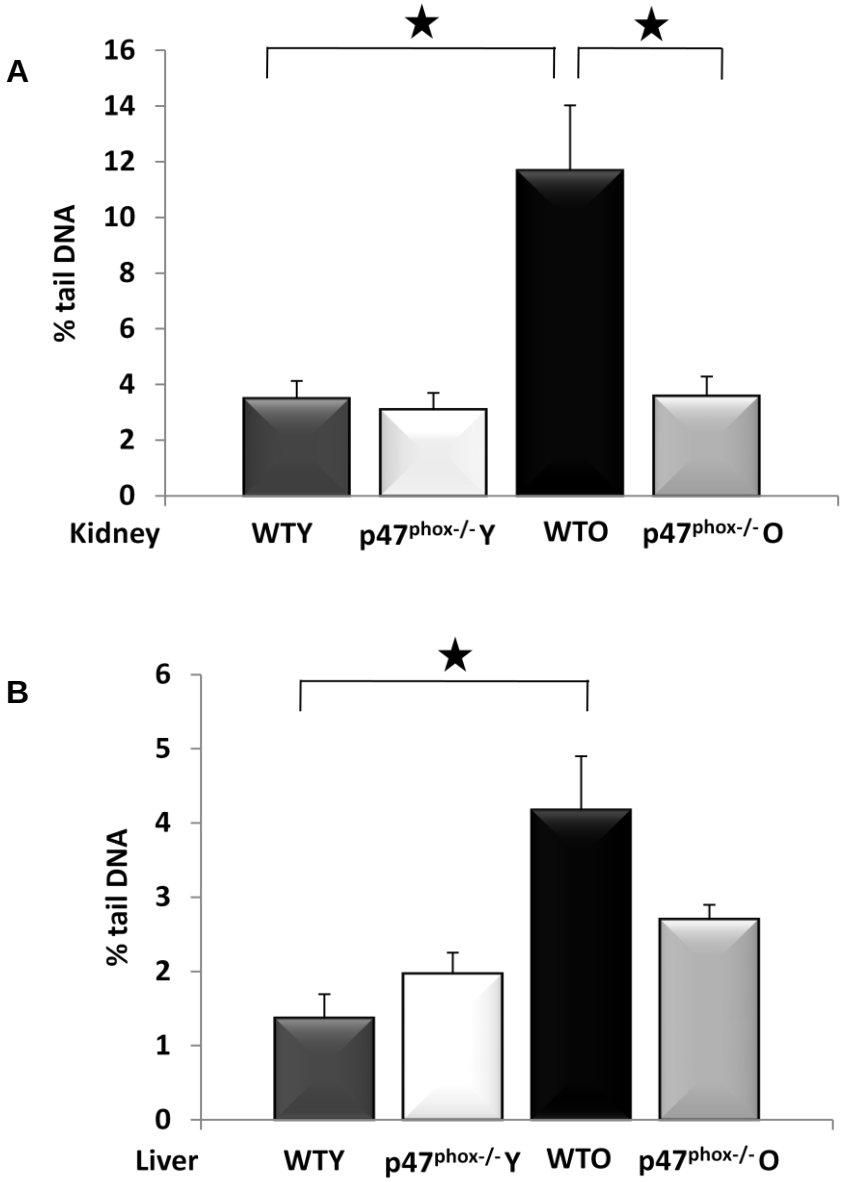

Figure 33: DNA damage measured by the comet assay **A)** mouse kidney cells from WTY (n=6, female, 21-23 weeks), p47phox$^{-/-}$Y (n=5, female, 21-23 weeks), WTO (n=9, 5 male, 4 female, 52-53 weeks), p47phox$^{-/-}$O (n=4, female, 30 weeks); **B)** mouse liver cells from WTY (n=6, female, 21-23 weeks), p47phox$^{-/-}$Y (n=5, female, 21-23 weeks), WTO (n=9, 5 male, 4 female,

52-53 weeks), p47phox$^{-/-}$O (n=4, female, 30 weeks); n= number of samples analyzed; WTY= wild type young; WTO= wild type old; p47$^{phox-/-}$Y= p47phox knockout mice young; p47$^{phox-/-}$O= p47phox knockout mice old. Values are expressed in mean ± SE; ★P≤ 0.05 considered significant.

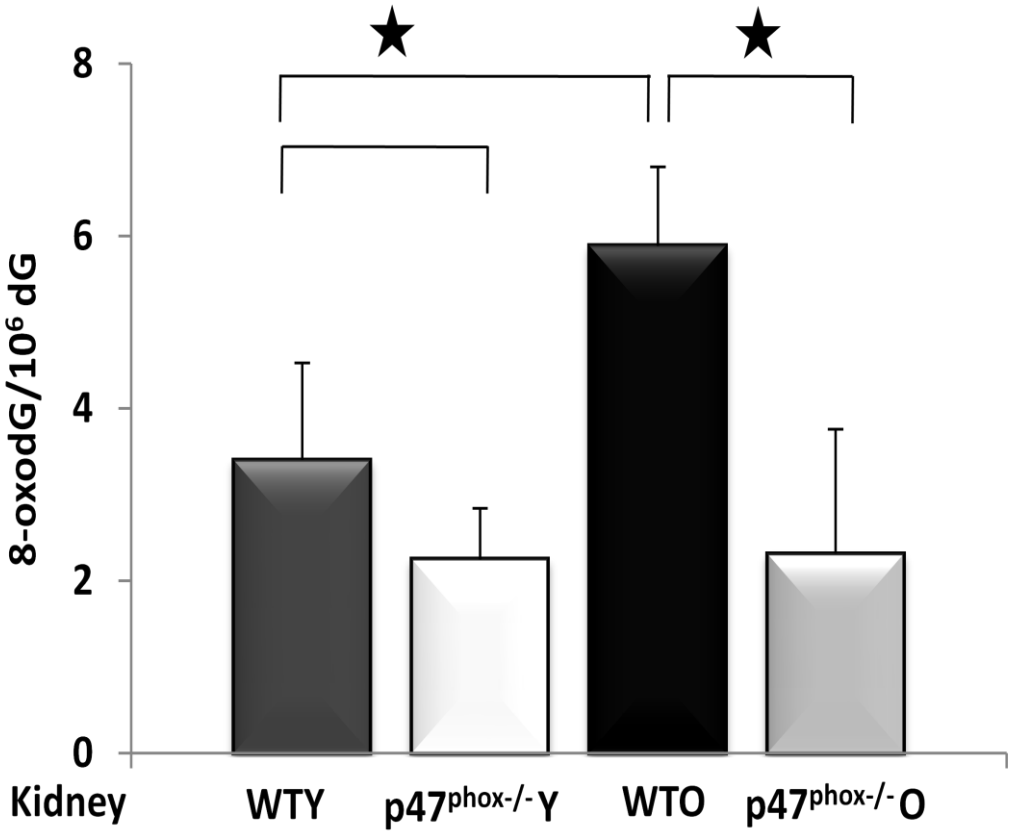

Figure 34: Oxidative modification of DNA by LC-MS/MS. 8-oxodG from mouse kidney WTY (n=6, female, 21-23 weeks), p47phox$^{-/-}$Y (n=5, female, 21-23 weeks), WTO (n=9, 5 male, 4 female, 52-53 weeks), p47phox$^{-/-}$O (n=4, female, 30 weeks); n= number of samples analyzed; WTY= wild type young; WTO= wild type old; p47$^{phox-/-}$Y= p47phox knockout mice young; p47phox$^{-/-}$O= p47phox knockout mice old. Values are expressed in mean ± SE; ★P≤ 0.05 considered significant.

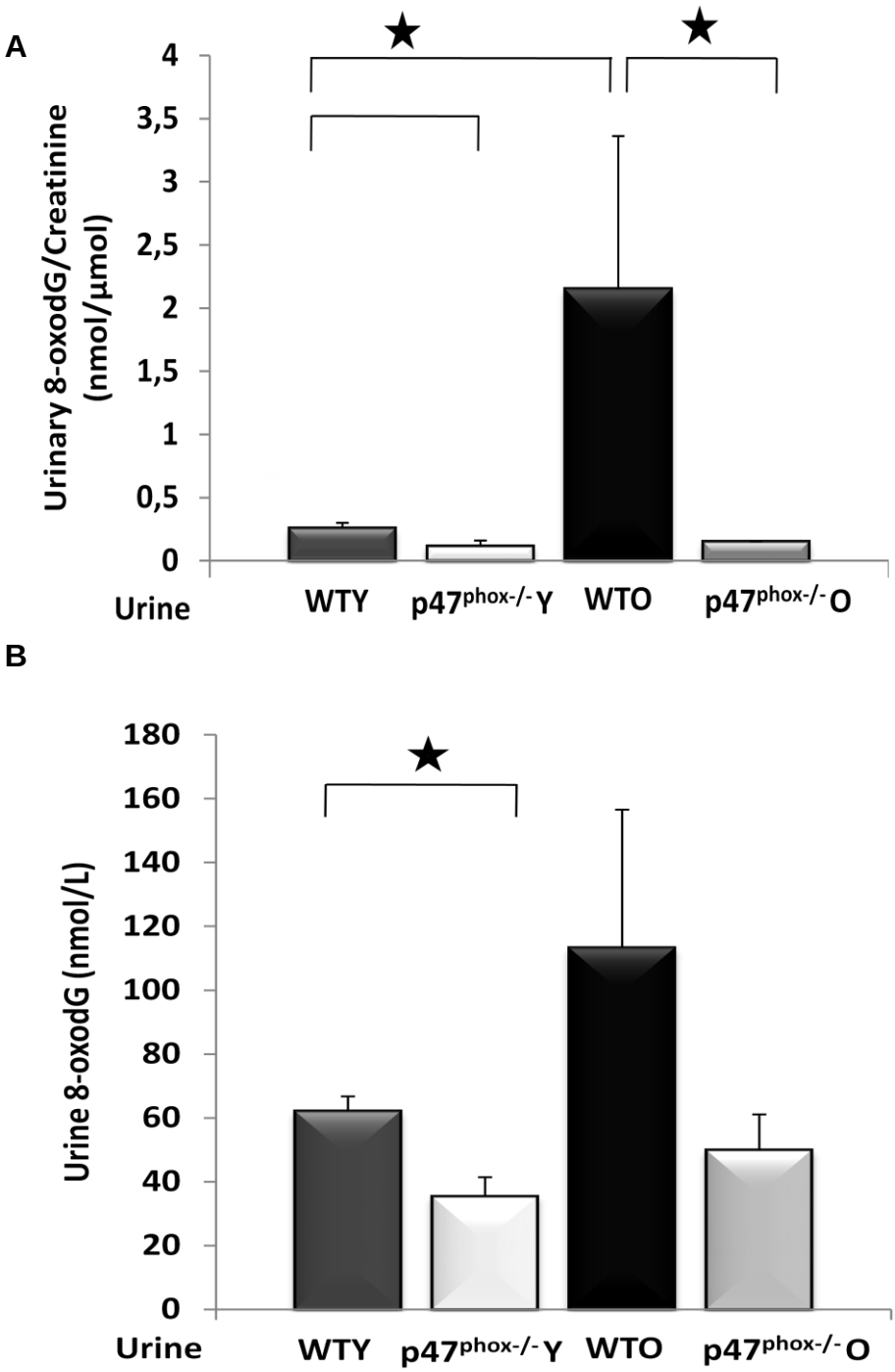

Figure 35: Oxidative modification of DNA by LC-MS/MS. **A)** mouse urinary 8-oxodG/creatinin(nmol/µmol) from WTY (n=6, female, 12-13 weeks), p47phox$^{-/-}$Y (n=6, female, 12-13 weeks), WTO (n=4, 2 male, 2 female, 52-53 weeks), p47phox$^{-/-}$O (n=2, female, 30 weeks); **B)** mouse urinary 8-oxodG/L from WTY (n=6, female, 12-13 weeks), p47phox$^{-/-}$Y (n=6, female, 12-13 weeks), WTO (n=4, 2 male, 2 female, 52-53 weeks), p47phox$^{-/-}$O (n=2, female, 30 weeks). n= number of samples analyzed; each urine sample contains cumulated two animals urine. WTY= wild type young; WTO= wild type old; p47$^{phox-/-}$Y= p47phox knockout mice young; p47$^{phox-/-}$O= p47phox knockout mice old. Values are expressed in mean ± SE; ★P≤ 0.05 considered significant.

We also analyzed the urinary 8-oxodG in young and old WT and p47phox$^{-/-}$ mice. Urinary 8oxodG measurement has received considerable attention as a biomarker of oxidative genomic damage. This adduct enables noninvasive sample gathering and it is, extremely stable in this matrix [111]. For accurate quantification of the urinary lesion, the newly developed LC-ESI-MS/MS method was used for simultaneous quantification of urinary 8-oxodG and creatinine for normalization. Significant differences were observed between WT and p47phox$^{-/-}$ mice in both age groups with WT mice showing higher values than phox mice (Figure 35 A and B). And there was a significant difference in young and old WT urinary 8-oxodG normalized with creatinine (Figure 35A).

4.2.2 Role of p47phox in the formation of lipid peroxidation products

Isoprostanes are a series of prostaglandin-like compounds produced by non-enzymatic peroxidation of arachidonic acid [112]. 8-iso-prostaglandin F2α is an indicator of lipid oxidation by free radicals and recognized as an excellent biomarker for oxidative stress damage [113]. Moreover, 8-isoPGF2α is stable and relatively abundant in biological fluids including plasma, urine and tissues as well as in lipid-rich foods [114].

We analyzed the urinary and plasma 8-isoPGF2α from young and old WT and p47phox$^{-/-}$ mice (Figure 36 and 37). The level of urinary 8-isoPGF2α/creatinine showed a significant difference between WT and p47phox$^{-/-}$ in the aged group (WT higher than p47phox$^{-/-}$ mice)(Figure 36), but not in the young group. Moreover, values were twenty fold higher in aged WT mice compared to young WT (Figure 36). The 8-isoPGF2α level in plasma showed a clear difference between WT and p47phox$^{-/-}$ mice in the old group. The level was significantly higher in old WT than young WT mice (Figure 37A). However, we did no see any difference in the young group.

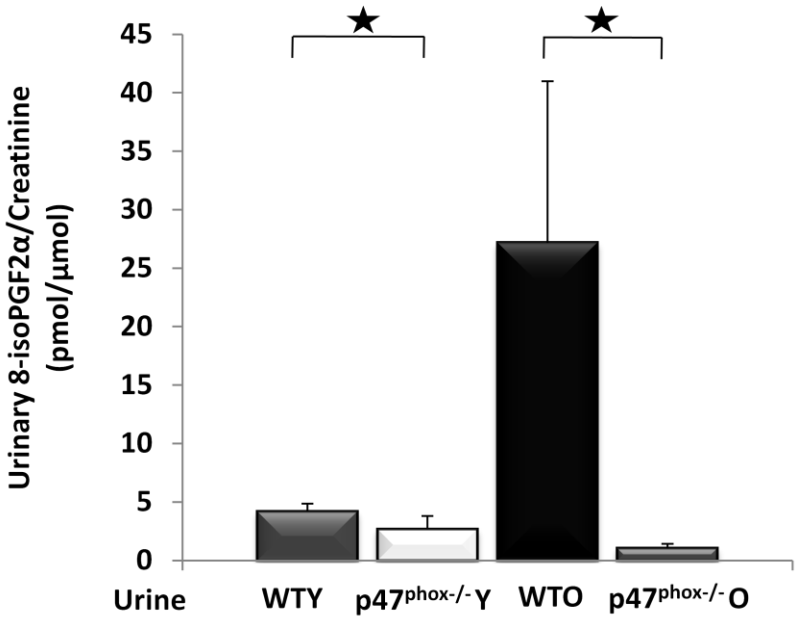

Figure 36: The oxidative lipid damage marker 8-isoPGF2α measured using LC-ESI-MS/MS in urine . Mouse urinary 8-isoPGF2α/creatinin (nmol/µmol) from WTY (n=6, female, 12-13 weeks), p47phox$^{-/-}$Y (n=6, female, 12-13 weeks), WTO (n=4, 2 male, 2 female, 52-53 weeks), p47phox$^{-/-}$ O (n=2, female, 30 weeks); n= number of samples analyzed; each urine sample contains cumulated two animals urine. WTY= wild type young; WTO= wild type old; p47$^{phox-/-}$Y= p47phox knockout mice young; p47$^{phox-/-}$O= p47phox knockout mice old. Values are expressed in mean ± SE; ★P≤ 0.05 considered significant.

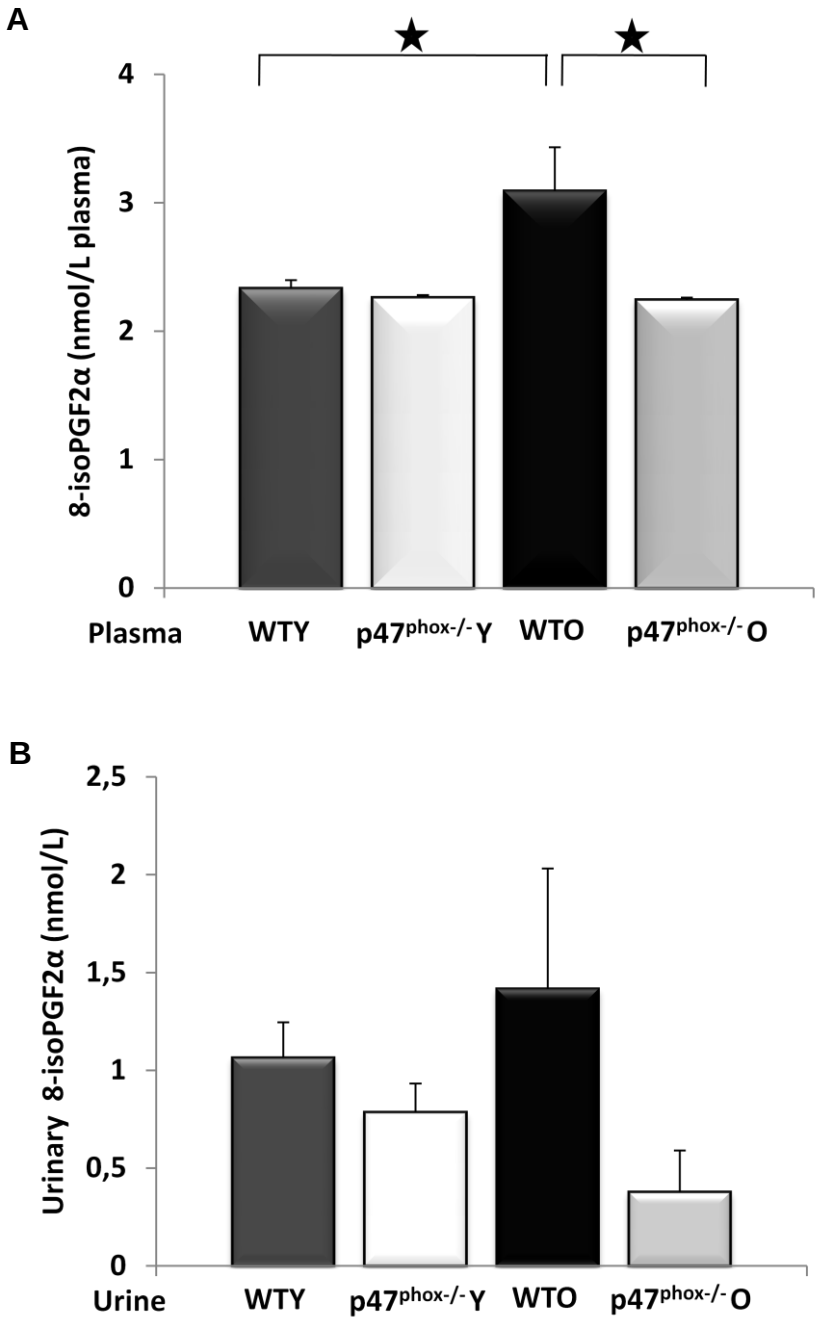

Figure 37: The oxidative lipid damage marker 8-isoPGF2α measured using LC-ESI-MS/MS in plasma. **A)** mouse plasma 8-isoPGF2α from WTY (n=4, female, 21-23 weeks), p47phox$^{-/-}$Y (n=3, female, 21-23 weeks), WTO (n=6, female, 52-53 weeks), p47phox-/-O (n=3, female, 30 weeks); **B)** mouse urinary 8-isoPGF2α/L from WTY (n=6, female, 12-13 weeks), p47phox$^{-/-}$Y (n=6, female, 12-13 weeks), WTO (n=4, 2 male, 2 female, 52-53 weeks), p47phox$^{-/-}$O (n=2, female, 30 weeks). n= number of samples analyzed; each urine sample contains cumulated two animals urine, each plasma sample contains plasma of two or more animals to achieve a volume which was sufficient for analysis. WTY= wild type young; WTO= wild type old; p47phox$^{-/-}$Y= p47phox knockout mice young; p47phox$^{-/-}$O= p47phox knockout mice old. Values are expressed in mean ± SE; ★P≤ 0.05 considered significant.

4.2.3 Influence of p47phox on oxidation of glutathione

An important oxidative stress marker is oxidized form of glutathione (GSSG). The increased ratio of GSSG/GSH indicates oxidative stress. To find the influence of p47phox on glutathione oxidation, we analyzed the GSSG and GSH level in plasma from young and old WT and p47phox$^{-/-}$mice. The GSSG/GSH ratio was significantly higher in WT mice than p47phox$^{-/-}$ mice in both the age groups (Figure 38). However, no difference in young and aged mice was seen in WT or p47phox$^{-/-}$ mice.

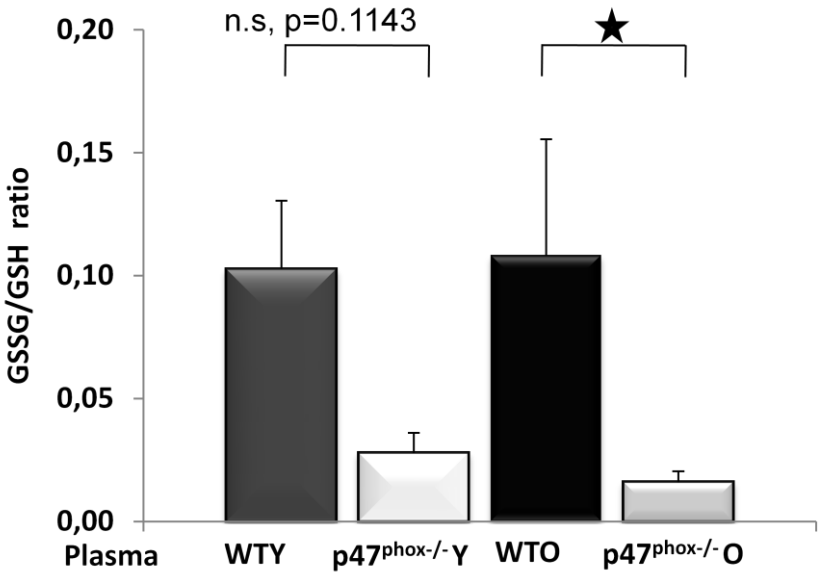

Figure 38: Mouse plasma GSSG/GSH ratio from WTY (n=4, female, 21-23 weeks),p47phox-/-Y (n=3, female, 21-23 weeks), WTO (n=6, female, 52-53 weeks), p47phox-/-O (n=3, female, 30 weeks); n= number of samples analyzed; each plasma sample contains plasma of two or more animals to achieve a volume which was sufficient for analysis. WTY= wild type young; WTO= wild type old; p47phox$^{-/-}$Y= p47phox knockout mice young; p47phox$^{-/-}$O= p47phox knockout mice old. Values are expressed in mean ± SE; ★P≤ 0.05 considered significant.

4.2.4 Is angiotensin II a key player in ageing?

The Renin-Angiotensin-Aldosterone-system (RAAS), is involved in the regulation of blood pressure and vasoconstriction. Binding of Ang II to its AT1 receptor and aldosterone via mineralocarticoid receptor mediates the generation of free radicals via NOX and that contributes damage to the tissues [65, 96, 106, 115, 116]. We were interested to study the role of p47phox in Ang II induced DNA and lipid damage during

ageing. Therefore we analyzed Ang II and related hormone Aldosterone from urine and plasma (Figure 39-43). The amount of urinary Ang II and aldosterone was about four and five fold higher in old than in young WT mice (Figure 39 A and 40A). Also level of Ang II showed a significant difference between WT and p47phox$^{-/-}$ mice in both young age groups but not in old. There was a significant correlation between the Ang II and the oxidative DNA damage marker urinary 8-oxodG as well as the oxidative lipid damage 8-isoPGF2α (Figure 41A and 42A). Aldosterone also showed a significant correlation between both oxidative DNA (Figure 41 B) and lipid damage (Figure 42B). However, the plasma concentration of Ang II and Aldosterone showed no significant difference between the groups.

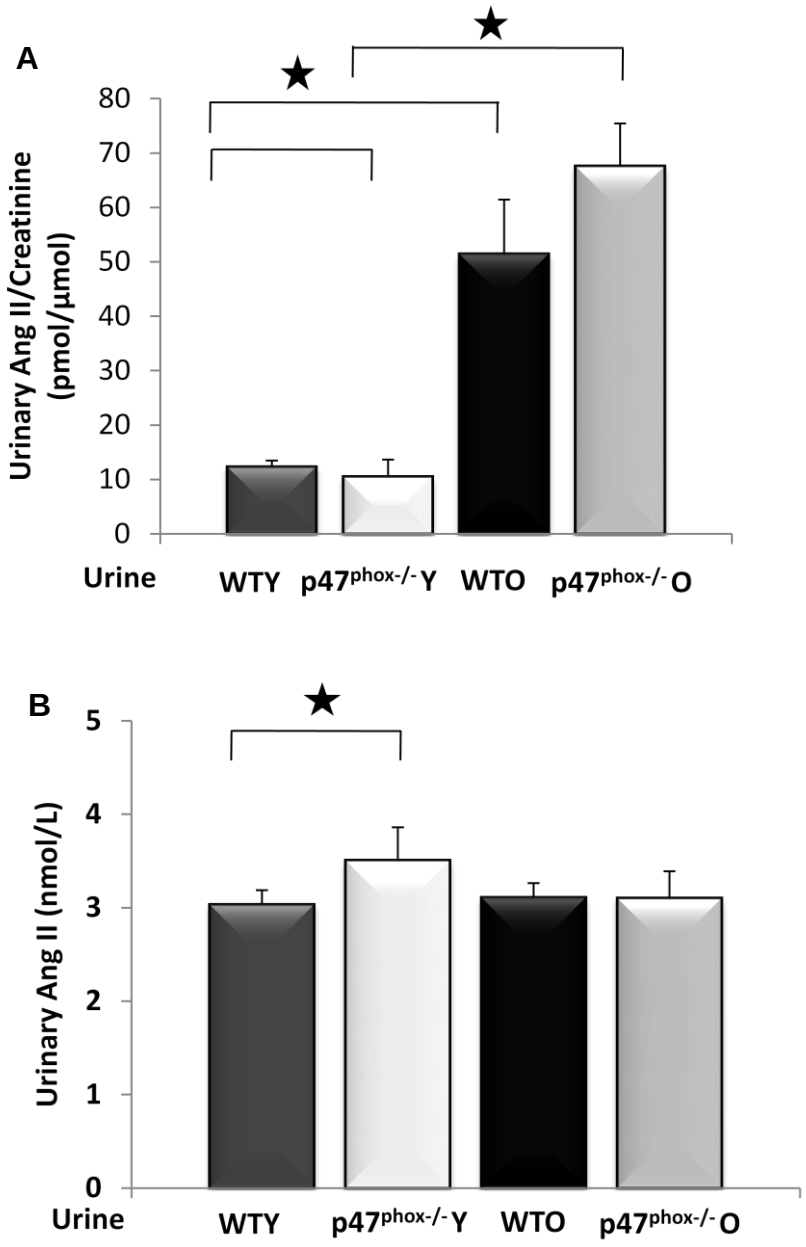

Figure 39: Ang II was analysed from urine and plasma by LC-ESI-MS/MS. **A)** mouse urinary Ang II/creatinin(pmol/µmol) from WTY (n=6, female, 12-13 weeks), p47phox$^{-/-}$Y (n=6, female, 12-13 weeks), WTO (n=4, 2 male, 2 female, 52-53 weeks), p47phox$^{-/-}$O (n=2, female, 30 weeks); **B)** mouse urinary Ang II/L from WTY (n=6, female, 12-13 weeks), p47phox$^{-/-}$Y (n=6, female, 12-13 weeks), WTO (n=4, 2 male, 2 female, 52-53 weeks), p47phox$^{-/-}$O (n=2, female, 30 weeks); n= number of samples analyzed; each urine sample contains cumulated two animals urine. WTY= wild type young; WTO= wild type old; p47phox$^{-/-}$Y= p47phox knockout mice young; p47$^{phox-/-}$O= p47phox knockout mice old. Values are expressed in mean ± SE; ★P≤ 0.05 considered significant.

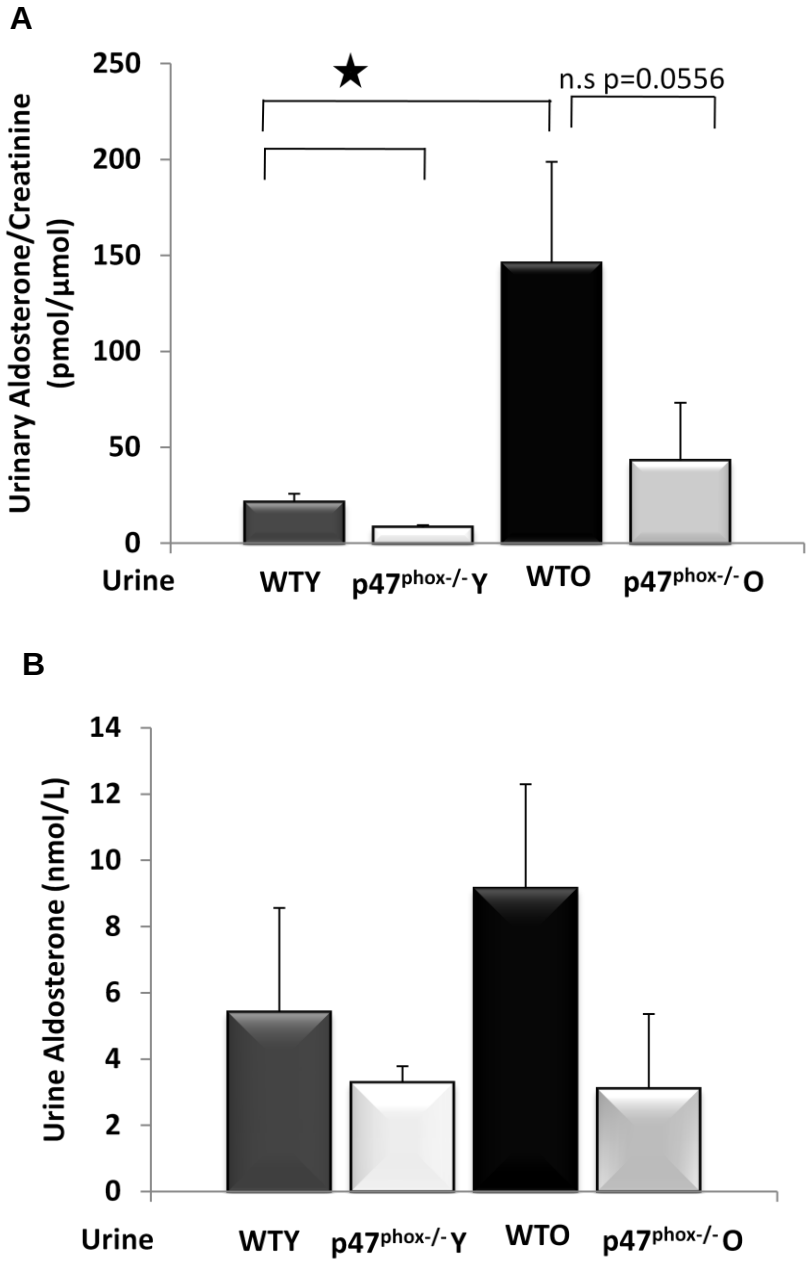

Figure 40: Aldosterone was analysed from urine and plasma by LC-ESI-MS/MS. **A)** mouse urinary aldosterone/creatinin(pmol/µmol) from WTY (n=6, female, 12-13 weeks), p47phox$^{-/-}$Y (n=6, female, 12-13 weeks), WTO (n=4, 2 male, 2 female, 52-53 weeks), p47phox$^{-/-}$O (n=2, female, 30 weeks); **B)** mouse urinary aldosterone/L from WTY (n=6, female, 12-13 weeks), p47phox$^{-/-}$Y (n=6, female, 12-13 weeks), WTO (n=4, 2 male, 2 female, 52-53 weeks), p47phox$^{-/-}$O (n=2, female, 30 weeks); n= number of samples analyzed; each urine sample contains cumulated two animals urine. WTY= wild type young; WTO= wild type old; p47$^{phox-/-}$Y= p47phox knockout mice young; p47$^{phox-/-}$O= p47phox knockout mice old. Values are expressed in mean ± SE; ★P≤ 0.05 considered significant.

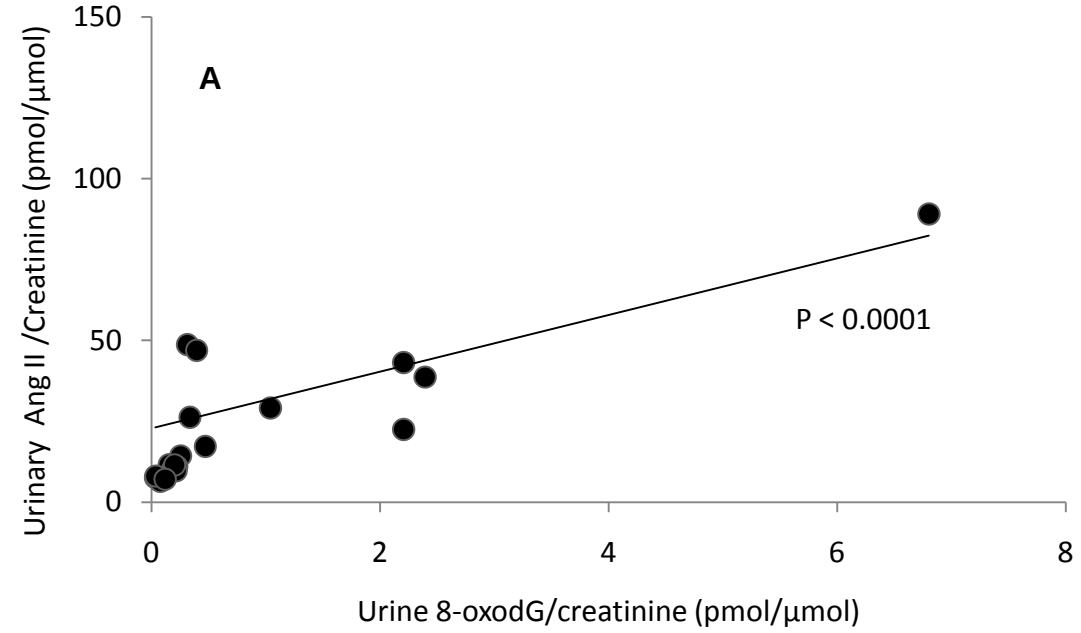
A
Urinary Ang II /Creatinine (pmol/µmol)
150
100
50
0
0
2
4
6
8
P < 0.0001
Urine 8-oxodG/creatinine (pmol/µmol)

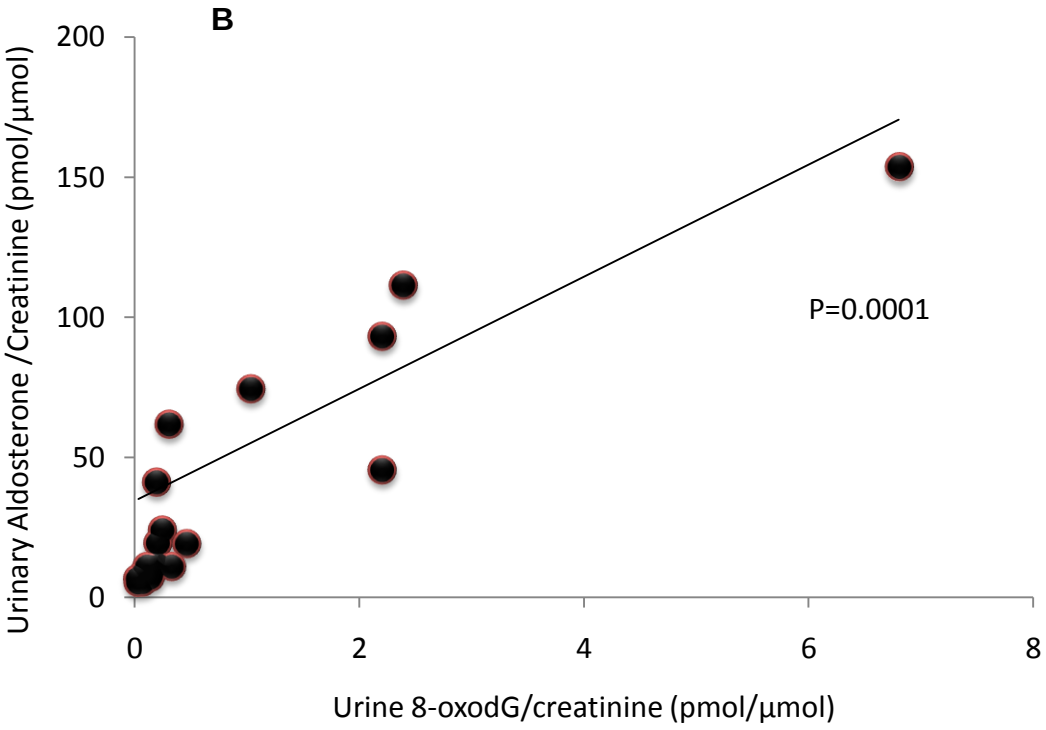
B
Urinary Aldosterone /Creatinine (pmol/µmol)
200
150
100
50
0
0
2
4
6
8
P=0.0001
Urine 8-oxodG/creatinine (pmol/µmol)

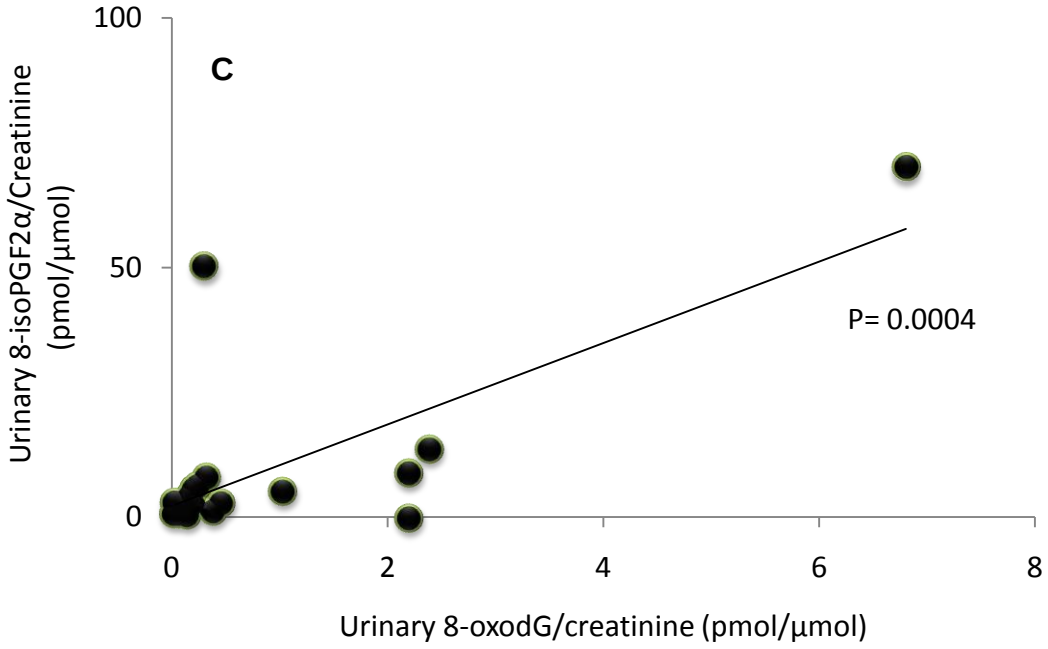

Figure 41: **A)** Correlation between urinary Ang II vs urinary 8-oxodG. **B)** Correlation between urinary aldosterone vs urinary 8-oxodG **C)** Correlation between urinary 8-isoPGF2α vs urinary 8-oxodG (p values from spearman rank correlation coefficient) P≤ 0.05 considered significant

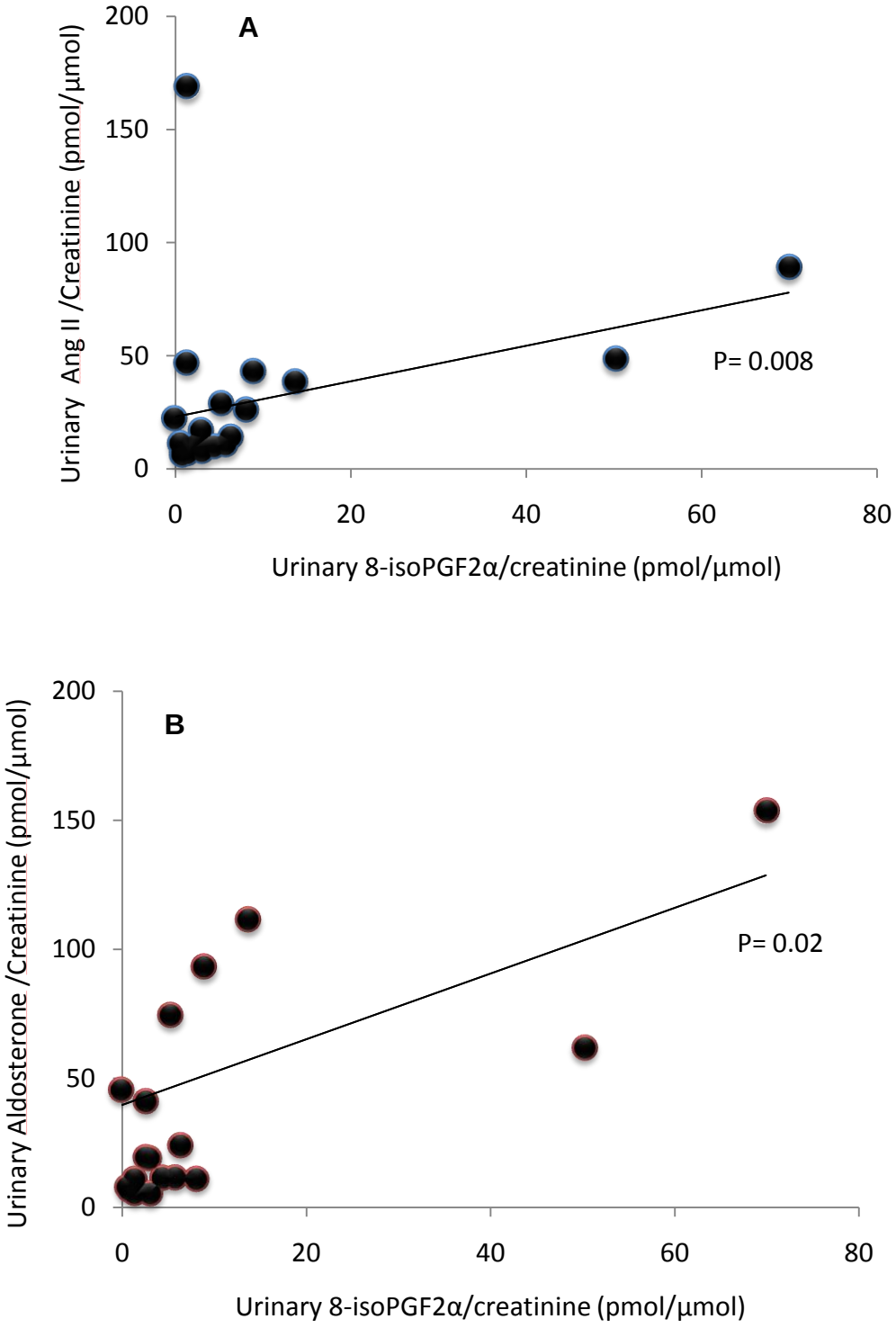

Figure 42: A) Correlation between urinary Ang II vs 8-isoPGF2α. **B)** Correlation between urinary aldosterone vs 8-isoPGF2α (p values from spearman rank correlation coefficient; P≤ 0.05 considered significant

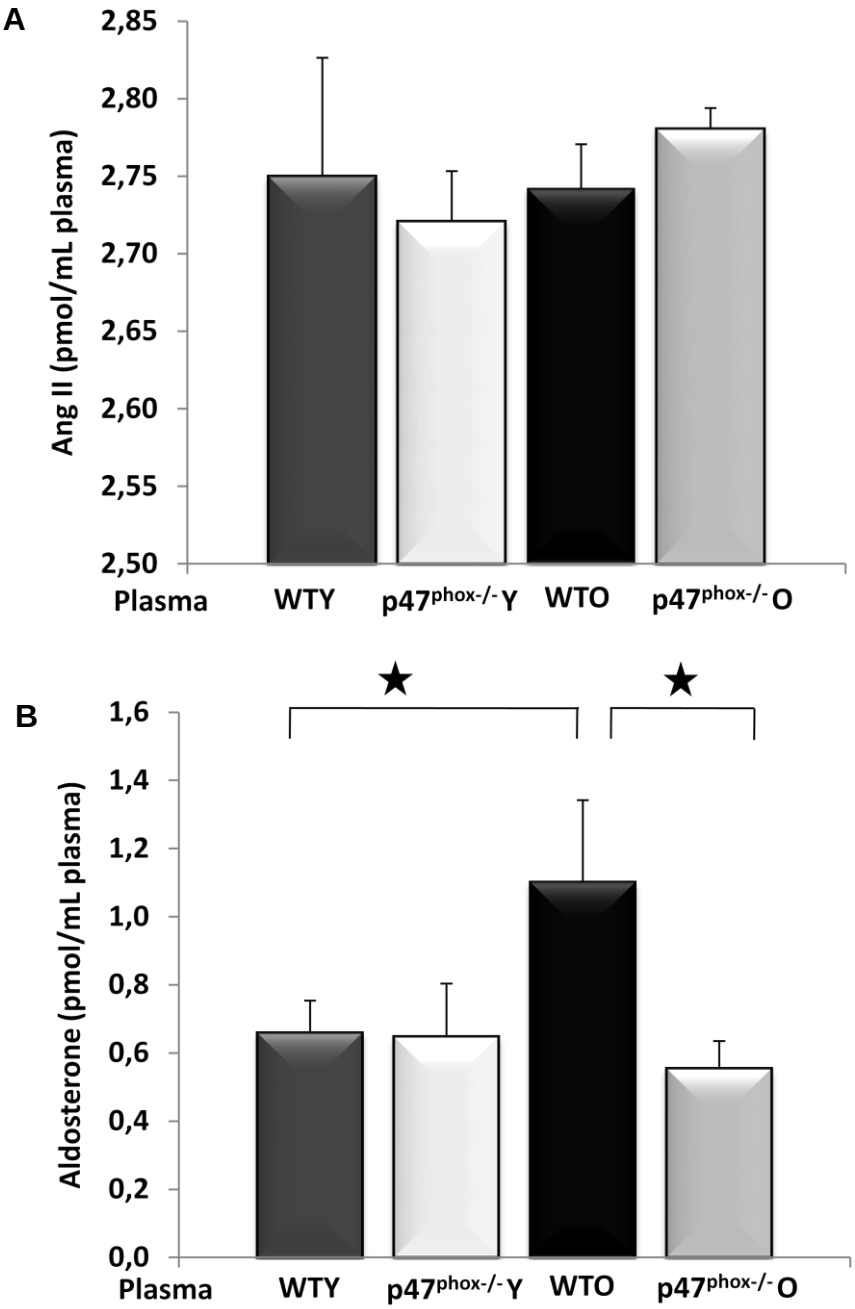

Figure 43: **A)** Mouse plasma Ang II from WTY (n=4, female, 21-23 weeks), p47phox$^{-/-}$Y (n=3, female, 21-23 weeks), WTO (n=6, female, 52-53 weeks), p47phox$^{-/-}$O (n=3, female, 30 weeks); **B)** Mouse plasma aldosterone from WTY (n=4, female, 21-23 weeks), p47phox$^{-/-}$Y (n=3, female, 21-23 weeks), WTO (n=6, female, 52-53 weeks), p47phox-/-O (n=3, female, 30 weeks); n= number of samples analyzed; each plasma sample contains plasma of two or more animals to achieve a volume which was sufficient for analysis. WTY= wild type young; WTO= wild type

old; p47phox$^{-/-}$Y= p47phox knockout mice young; p47phox$^{-/-}$O= p47phox knockout mice old. Values are expressed in mean ± SE; ★P≤ 0.05 considered significant.

Recently, we reported that Ang II induced oxidative stress and DNA damage in the pig kidney cell line LLC-PK1 [109]. Therefore, we studied the role of p47phox in Ang II induced DNA damage. DNA strand breaks were quantified using the comet assay in isolated kidney cells of young and old WT and p47phox$^{-/-}$ mice after Ang II treatment (200nM, 30min, in vitro incubation). We found a significant level of DNA damage in Ang II treated cells of WT compared with untreated cells (Figure 45), but no differences in cells from p47phox$^{-/-}$ mice.

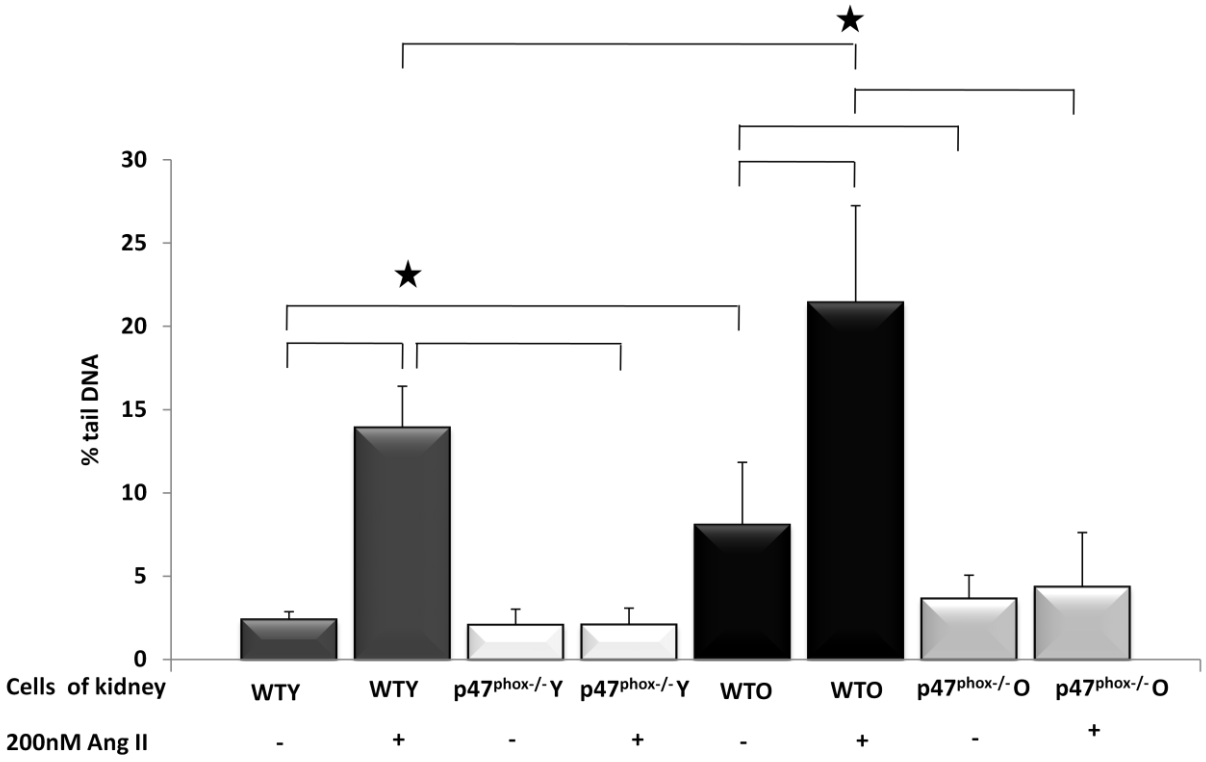

Figure 45: DNA damage measured by the comet assay in cell isolates from kidney and treated with or without 200nM Ang II. Mouse kidney cells from WTY (n=6, female, 21-23 weeks), p47phox$^{-/-}$Y (n=3, female, 21-23 weeks), WTO (n=6, 5 male, 4 female, 52-53 weeks), p47phox$^{-/-}$O (n=4, female, 30 weeks); n= number of samples analyzed; WTY= wild type young; WTO= wild type old; p47$^{phox-/-}$Y= p47phox knockout mice young; p47$^{phox-/-}$O= p47phox knockout mice old. Values are expressed in mean ± SE; ★P≤ 0.05 considered significant.

4.3 Rosuvastatin prevents angiotensin II–induced genotoxicity

4.3.1 Rosuvastatin prevents angiotensin II-induced superoxide formation

Superoxide formation can be observed with the superoxide sensitive dye dihydroethidium in LLC-PK1 cells after treatment with angiotensin II (Ang II) (Figure 45 A and B). This induction is significantly decreased after co-incubation with 1 µM rosuvastatin.

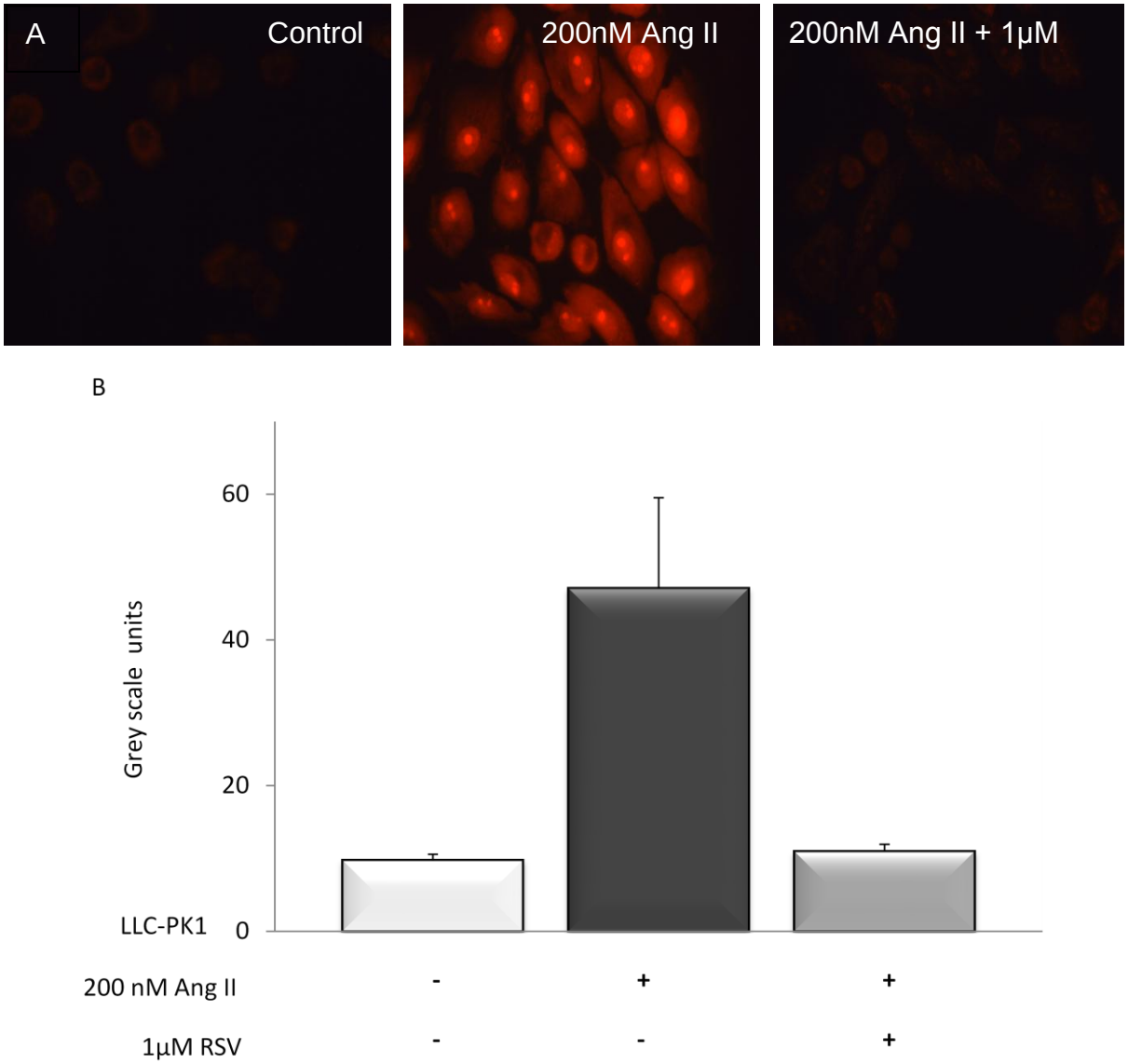

Figure 45: Formation of superoxide anions by angiotensin II (AngII) and its prevention by rosuvastatin. **A)** Dihydroethidium reacts with the superoxide radical anion and produces the fluorescent 2-hydroxyethidium. 1 µM Rosuvastatin (RSV) protects LLC-PK1 cells from the

superoxide anion radicals produced by Ang II; **B)** Quantification of the amount of superoxide anions (gray scale units). The experiment was done a single time, and 50cells were counted.

4.3.2 Rosuvastatin prevents angiotensin II-induced genomic damage

Ang II causes DNA strand breaks in LLC-PK1 cell dose dependently (Figure 46A). Rosuvastatin was able to prevent the genotoxicity of Ang II in LLC-PK1 cells. The DNA strand breaks, measures by the comet assay were significantly reduced already by 10 nM rosuvastatin (Figure 46B). No further reduction could be observed with the higher rosuvastatin concentration of 1 µM. Ang II causes micronuclei (subtype of chromosomal aberration) in LLC-PK1 cell dose dependently (Figure 47A). The frequency of micronuclei was also lowered significantly by rosuvastatin (Figure 47B). The putative mutagenic DNA base modification 8-oxodG, formed in cells incubated with Ang II, was quantified by LC-MS/MS (Figure 48). There was a dose dependent increase of 8-oxodG. Rosuvastatin was able to prevent the formation of this DNA lesion.

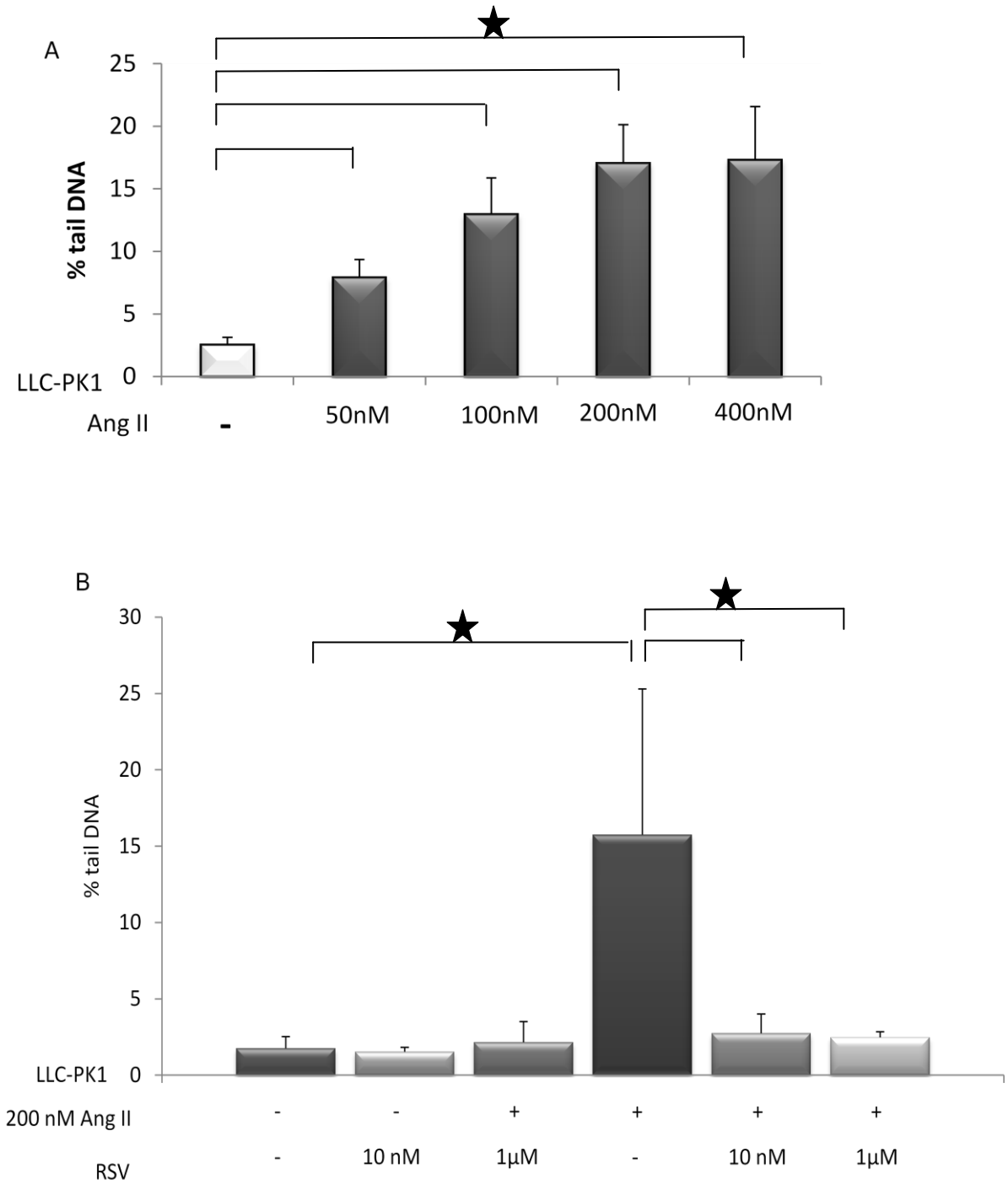

Figure 46: Rosuvastatin (RSV) prevents Ang II induced DNA damage. **A)** Ang II induced DNA damage monitored with the comet assay. LLC-PK1 cells were treated with Ang II in different concentrations and the percentage of DNA in tail was measured; **B)** Rosuvastatin (RSV) protects LLC-PK1 cells from DNA strand breaks caused by Ang II; Values are expressed in mean ± SD; ★P≤ 0.05 considered significant

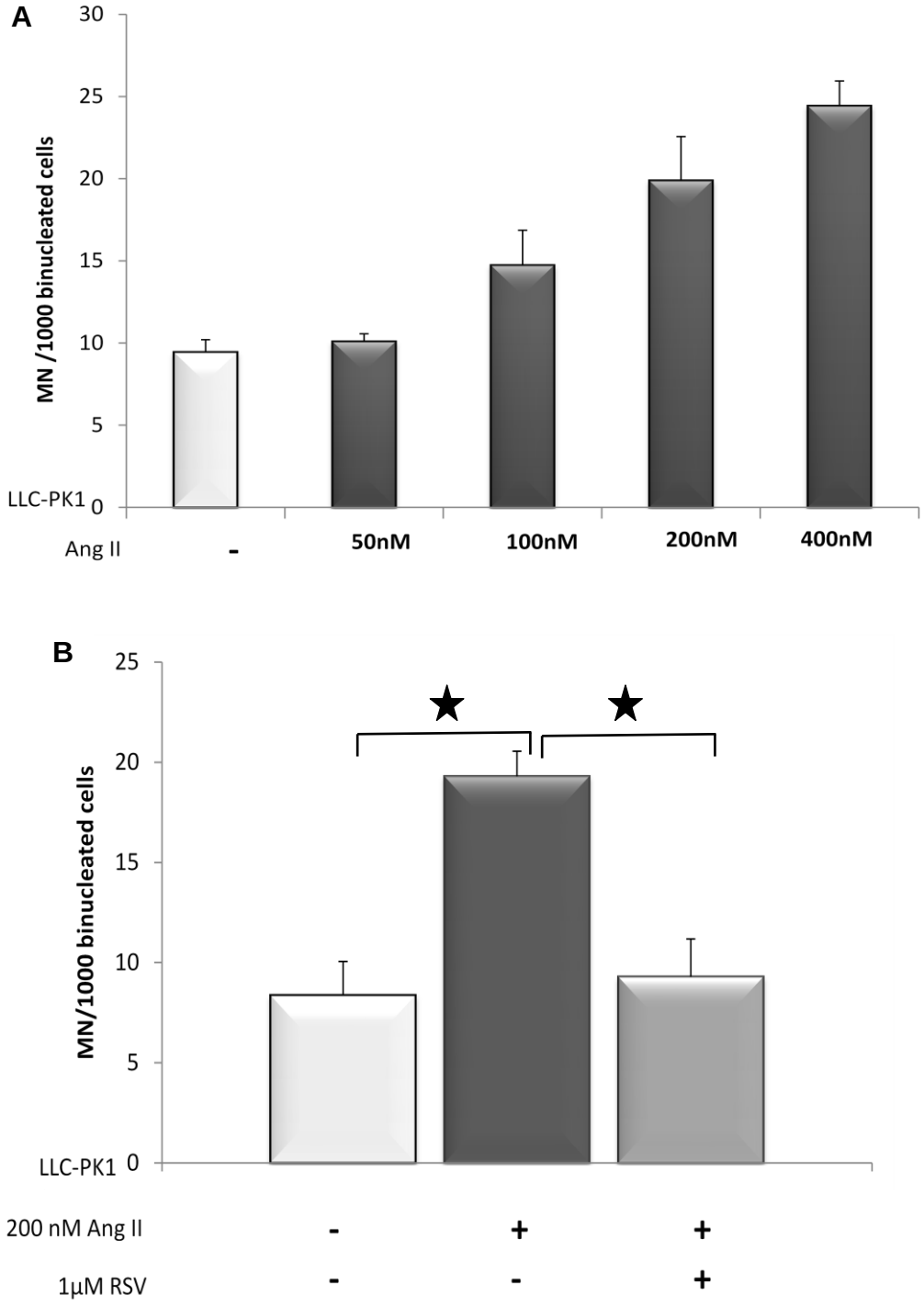

Figure 47: Rosuvastatin (RSV) prevents Ang II induced genomic damage. **A)** Micronucleus induction by Ang II in LLC-PK1cells, single time experiment and two slides were counted; **B)** Rosuvastatin (RSV) protects LLC-PK1 cells from micronuclei formation. Cells were treated with Ang II with/ without 1µM RSV for 4h, then cytochalasin B was added and incubated for 24 h. The micronucleus frequency was determined in binucleated cells. Values are expressed in mean ± SD; ★P≤ 0.05 considered significant

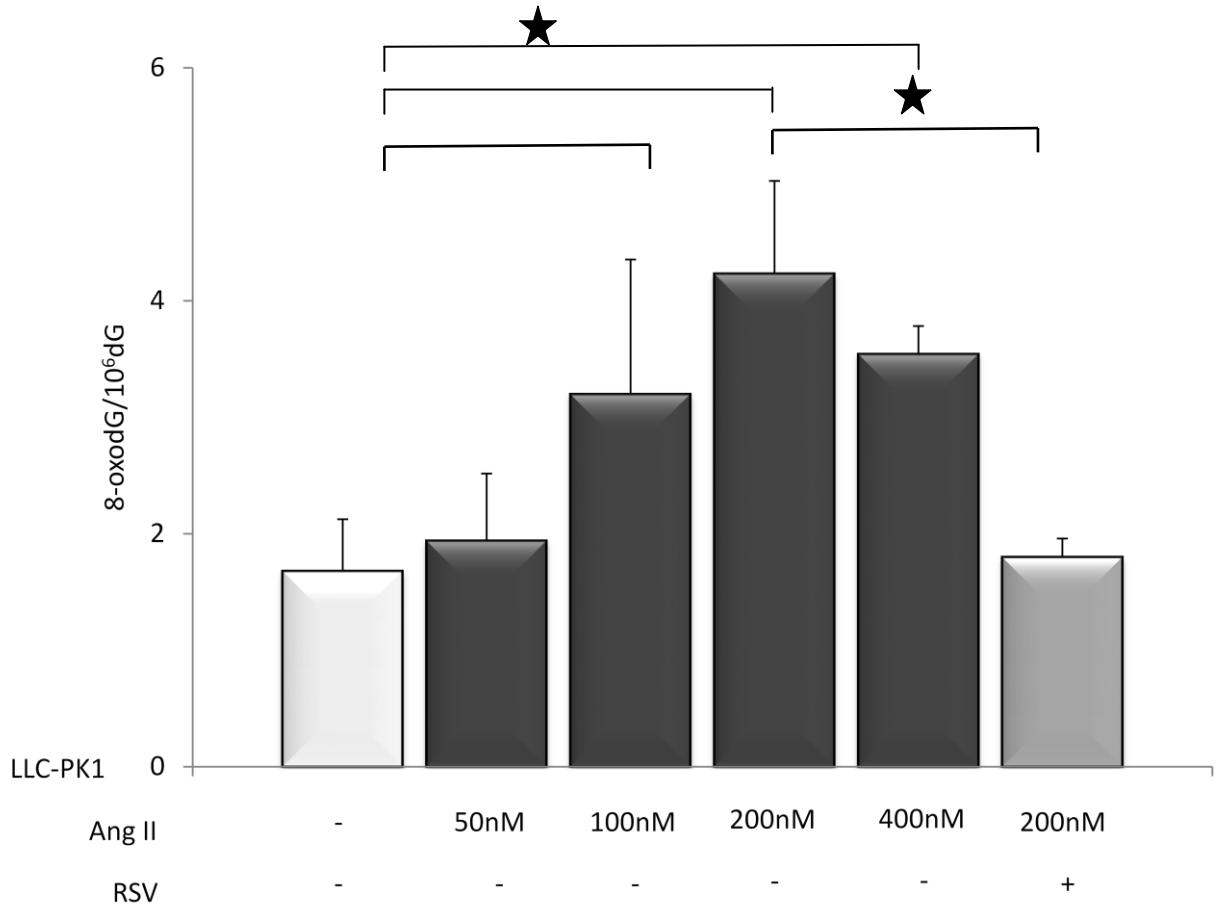

Figure 48: Rosuvastatin (RSV) prevents Ang II induced genomic damage. **A)** Ang II induced 8-oxodG in LLC-PK1 cells dose-dependently, which was analyzed by Isotope diluted LC-MS/MS method. Rosuvastatin protects LLC-PK1 cells from oxidative DNA damage caused by Ang II. Values are expressed in mean ± SD; ★P≤ 0.05 considered significant

4.3.3 Rosuvastatin increases glutathione levels and glutathione metabolising enzymes

The measurement of the total glutathione levels in LLC-PK 1 cells revealed the potential of rosuvastatin to increase the amount of this important redox state regulating molecule. Together with Ang II, which alone also induced a significant rise of the cellular glutathione amount, rosuvastatin showed a synergistic effect on glutathione levels. Compared to the control neither rosuvastatin nor Ang II were able to increase the cellular glutathione amount. When utilised together, the two substances provoked a significant rise of glutathione levels (Figure 49A).

Analysis of the expression of three genes involved in glutathione metabolism, glutathione synthase, glutathione reductase and glutathione peroxidase (Figure 49B), showed that they are all upregulated in LLC-PK1 cells incubated with rosuvastatin alone (Figure 49B). No significant upregulation could be detected in cells treated either with angiotensin II alone or with the combination of Ang II and rosuvastatin.

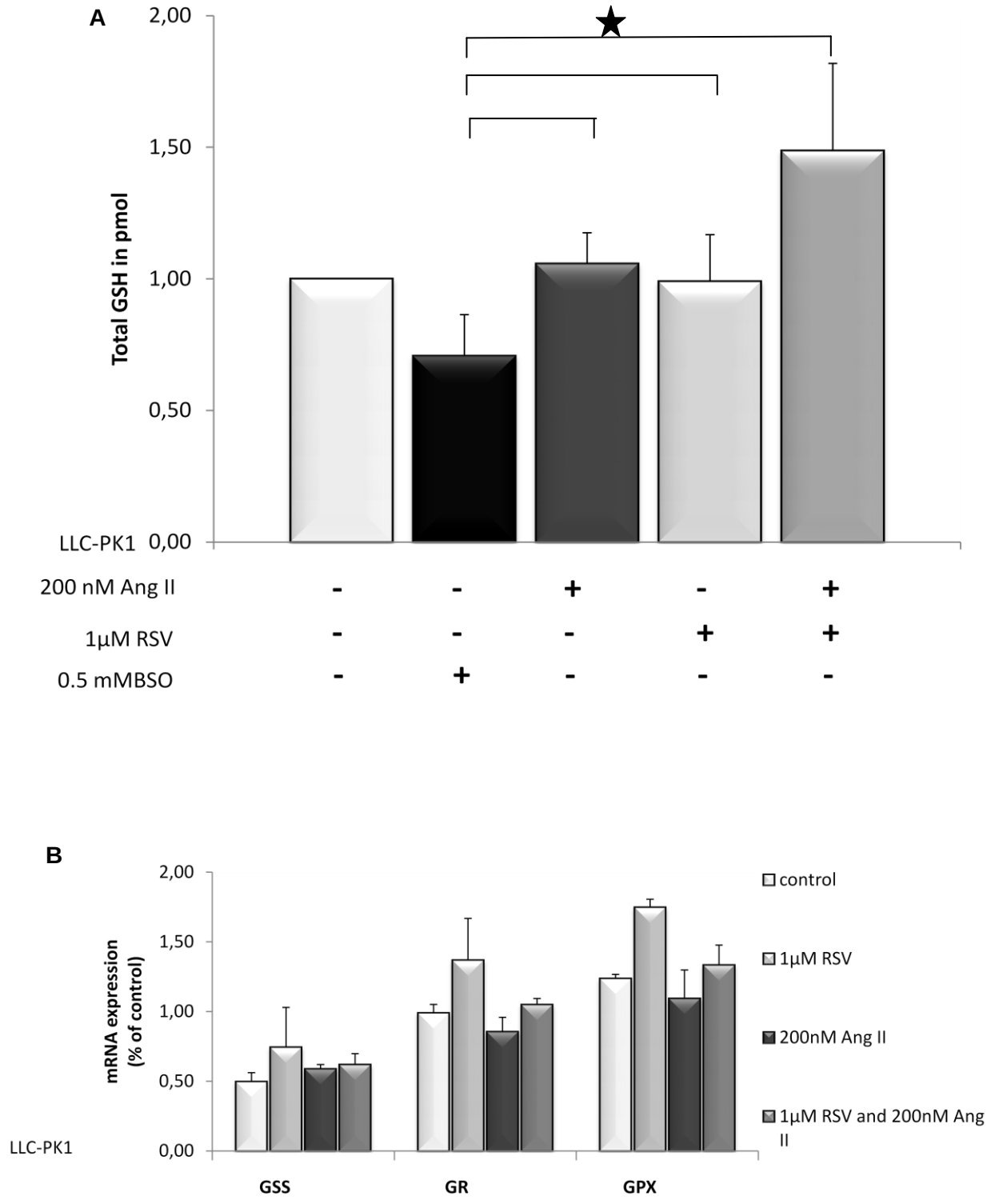

Figure 49: Rosuvastatin (RSV) increases glutathione and its metabolizing enzymes **A)** Total glutathione were analyzed in LLC-PK1 cells to check the protective effect of RSV against Ang II

B) Glutathione metabolic enzyme gene expression. GSS= glutathione synthetase; GR= glutathione reductase; GPX= glutathione peroxydase; BSO= dl-Buthionine-sulfoximine.

4.3.4 Rosuvastatin exerts its DNA-damage preventive effects independent of HMG-CoA reductase inhibition

To assess the impact of HMG-CoA reductase inhibition on the observed protective effects of rosuvastatin, intermediates of the cholesterol synthesis pathway were tested for their ability to reverse rosuvastatins actions. In the case of a HMG-CoA reductase inhibition-dependent effect, the effect would be reversed by a pathway intermediate. Since the addition of neither farnesol (FOH), farnesyl pyrophosphate (FPP) nor geranylgeraniol (GGOH) led to a significant increase of DNA damage again (Figure 50), the independence of rosuvastatins DNA damage preventive effect of HMG-CoA reductase inhibition was shown.

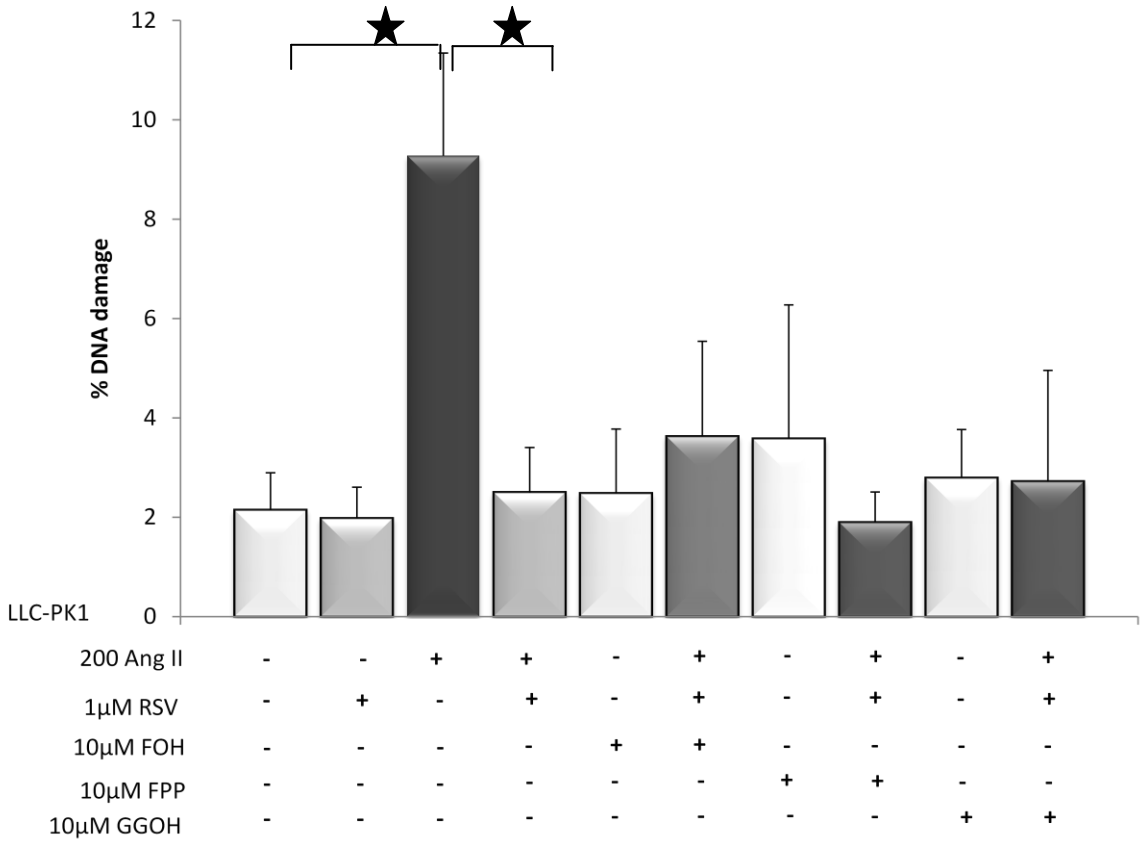

Figure 50: Rosuvastatin (RSV) protects LLC-PK1 cells from Ang II induced DNA damage independent of cholesterol sysnthesis. RSV=rosuvastatin; FOH=farnesol; FPP= farnesol pyrophosphate; GGOH= geranylgeraniol.

4.4 Parkinson's disease and oxidative DNA damage

Demographic and clinical data of the subjects enrolled in this study are presented in Table 7. The mean age of the control group was 68.8±4.9 and that of PD patients was 71.2± 3.2 years. All PD patients were treated with L-DOPA (188 – 1850 mg/day; Table 8) plus dopa decarboxylase inhibitor, either carbidopa (25 – 425 mg/day) or benserazide (47 – 187 mg/day) or both (142.18 – 462.5 mg/day). Nine PD patients also received the COMT inhibitor entacapone (600 – 1200 mg/day; Table 8). Nine patients were treated with a combination with the dopamine agonists pramipexol (1 – 3 mg/day), bromocriptin (8 mg/day) or piribedil (50 mg/day), the NMDA-antagonists amantadine (100mg/day) or budipin (10mg/day) or a combination within these classes of drugs (Table 8). Some patients were additionally treated with the monoamino oxidase B (MAO-B) inhibitors selegiline (10mg/day) or rasagiline (1mg/day), or the antipsychotic drugs quetiapin (25 – 250 mg/day) or clozapin (44mg/day; Table 8). Eleven patients also received other medications such as anti-diabetics, antihypertensive or thyroid management pharmaceuticals (Table 7). Like the PD patients, 7 out of 12 individuals of the control group suffered from typical health problems for this age group and took appropriate medications (Table 7). Gender distribution was unequal between the groups, with more females in the control group because they were life partners of the male PD patients. There was one smoker in each group and few individuals listed the intakes of antioxidant supplements.

Table 7: Characteristics of study participants

	PD patients	Control
Number of participant	18	12
Sex (male/female)	12/6	1/11
Smokers/non-smokers	1/17	1/11
Age at study (years)range	71.2 ± 3.2 (65-78)	68.8±4.9 (61-80)
Age at onset (years) range	61.0 ± 7.8(47-77)	Not applicable
Daily dose of L-Dopa (mg/day) range	808.68 ± 476.11 (188-1850)	Not applicable
Duration of Treatment (years) range (L-DOPA consumption)	9.8±5.2 (1.0 – 20)	Not applicable
Anti-oxidants/vitamin supplementation intake (yes/no)	3/16	2/10
Other medications (anti diabetics; antihypertensive; thyroid management; etc.) (yes/no)	11/8	7/5

The table with permission from Oli. R. G. et al. [104](copyright 2010, Springer).

Table 8: Anti-Parkinson's disease therapy

Combination therapy for PD patients	No of PD
L-DOPA (1200mg/day) + dopa decarboxylase inhibitor (300mg/day)	3
L-DOPA (600mg/day)+ dopa decarboxylase inhibitor (150mg/day) + COMT inhibitor (1000 mg/day)	2
L-DOPA (587.5mg/day) + dopa decarboxylase inhibitor (110.15 mg/day) + dopamine agonist (20.10mg/day)	3
L-DOPA (850mg/day) + dopa decarboxylase inhibitor (212.48mg/day) +antipsychotic (50mg/day)	1
L-DOPA (775mg/day) + dopa decarboxylase inhibitor (193.75mg/day) + COMT inhibitor (950mg/day) + dopamine agonist (2 mg/day)	4
L-DOPA (975mg/day) + dopa decarboxylase inhibitor (182.81 mg/day) + COMT inhibitor (800mg/day) +antipsychotic (106.25 mg/day)	3
L-DOPA (559.375mg/day) + dopa decarboxylase inhibitor (117.38mg/day) + MAO B inhibitors (5.5mg/day) + dopamine agonist (34.85 mg/day)	2

The table with permission from Oli. R. G. et al. [104](copyright 2010, Springer).

We analyzed the 8-oxodG in lymphocyte DNA and detected significantly elevated levels of this oxidative DNA-alteration in PD patients compared to the control group (Figure 51A). In the presence of elevated DNA-oxidization an increased amount of oxidative stress and a decreased antioxidative defense might be expected. Therefore, the antioxidant capacity of the plasma (FRAP-capacity) was determined (Figure 51 B). However, the FRAP values were significantly higher in PD patients than in controls. To investigate the biological consequences of the elevated DNA-oxidization we analyzed the micronucleus frequency in lymphocytes, but found no difference between the groups [104].

The daily dose of L-DOPA (188 - 1850 mg/day) correlated significantly with FRAP values in the plasma of PD patients (data not shown). When we analysed the antioxidant power of L-DOPA and dopamine in vitro in the FRAP assay, we found strong antioxidant capacities for both compounds in the cell free system (data not

shown). When we compared the biomarkers values (Figure 52A), treated without (9 patients) / with (9 patients) dopamine agonist within L-DOPA treated PD patients, the treatment with-dopamine agonist group showed positive correlations with 8-oxodG (Figure 52C), and MN (data not shown). After treatment of the neuronal cell line PC12 with 100 µM dopamine for 2 hours, we isolated the cellular DNA and measured the 8-oxodG content, which was elevated significantly (data not shown).

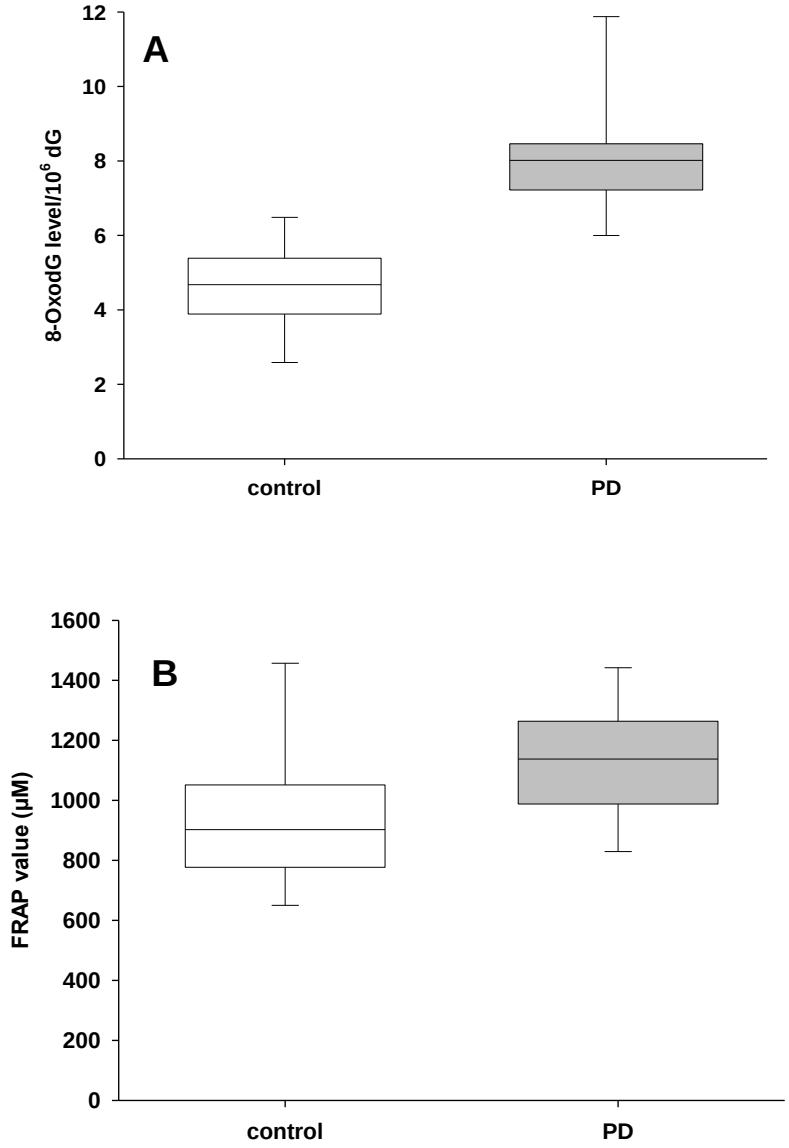

Figure 51: A). Oxidative stress biomarker 8-oxo-7,8-dihydro-2'-deoxyguanosine (8-oxodG) in peripheral lymphocyte DNA of healthy individuals and Parkinson disease (PD) patients after

chronic L-DOPA treatment. Shown are in box-plot with median values. **B).** Antioxidant capacity of plasma (Ferric Reducing Ability of Plasma- (FRAP) -Assay; µmol/L equivalents) of healthy individuals and PD patients after chronic L-DOPA treatment. Shown are in box-plot with median values. The figure with permission from Oli. R. G. et al. [104](copyright 2010, Springer).

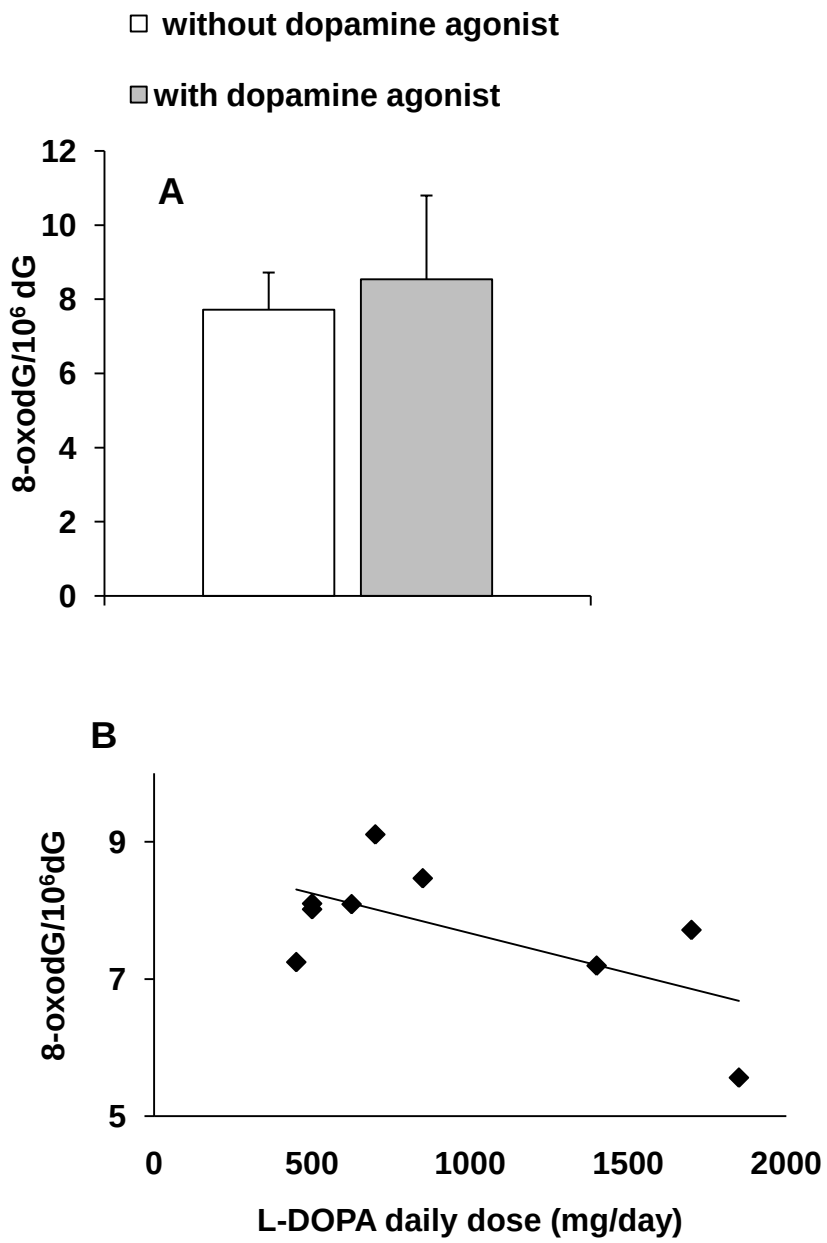

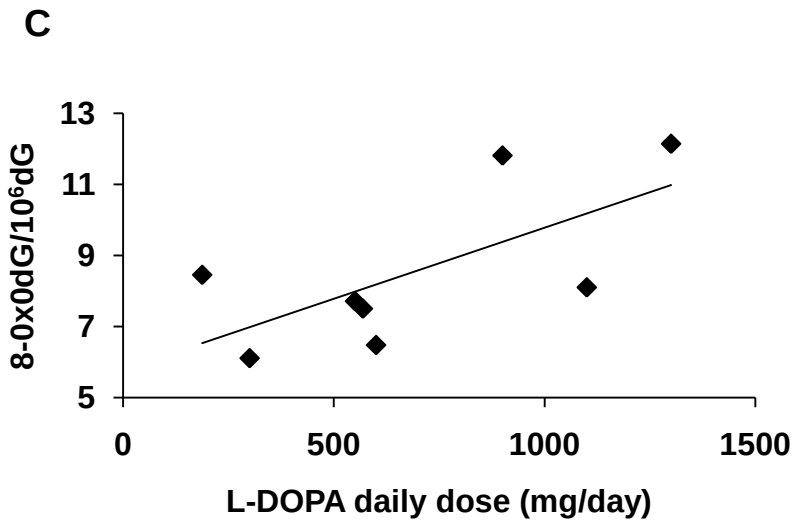

Figure 52: Oxidative stress biomarker 8-oxo-7,8-dihydro-2'-deoxyguanosine (8-oxodG) in peripheral lymphocyte DNA of Parkinson disease (PD) patients after chronic L-DOPA treatment without and with dopamine agonist . **A).** Shown are group averages with standard deviations. **B).** Correlation of the 8-oxodG and L-DOPA daily dose in without dopamine agonist therapy. **C).** Correlation of the 8-oxodG and L-DOPA daily dose in with dopamine agonist therapy. The figure with permission from Oli. R. G. et al. [104](copyright 2010, Springer).

5 Discussion

The increased oxidative stress causes DNA damage which leads to altered genomic information. As one pathway for increased ROS production, many endogenous (eg. angiotensin II (Ang II), aldosterone) and exogenous substances activate NADPH oxidase (NOX) enzyme and produce ROS (superoxide anion radicals, hydrogen peroxide, hydroxyl radicals). Rosuvastatin is a lipid lowering drug and shows pleotropic effect including antioxidant effect. Moreover, rosuvastatin reduces elevated level of angiotensin II type 1 receptor (AT1R), oxidative stress and protects the vascular system. Commonly, the oxidative stress is elevated in ageing and age related diseases (eg. Parkinson's disease (PD)). The oxidative stress and oxidative DNA damage was analyzed using newly developed isotope-diluted-LC-ESI-MS/MS methods.

5.1 Method development and validation: Analysis of oxidative stress markers and other analytes by LC-ESI-MS/MS

LC–MS/MS has proven one of the most effective tools in biochemical research. Particularly it is very useful for quantifying small amounts in complex biological matrices. LC–MS/MS based methods are generally characterized by high specificity, sensitivity and high-throughput potential [117]. The use of electrospray ionization (ESI) coupled with a triple quadrupole mass spectrometer [118] has already emerged as a powerful analytical tool in clinical biochemical genetics [119]. Several methods are available to measure 8-oxodG, 8-isoPGF2α, reduced and oxidized glutathione, dG, 8-nitroG, Ang II, aldosterone and creatinine in urine and plasma. But in our newly developed LC-ESI-MS/MS method we were able to measure all the analytes within a single run. This method was validated by us for C57BL/6J mouse urine and plasma samples. Most probably the method is applicable to samples from other animals and human samples.

Concerning urinary 8-oxodG analysis, there are several methods available [47, 120-125]. Recently the European Standards Committee for Urinary (DNA) Lesion Analysis (ESCULA; http://www.escula.org) was established to answer the issues associated with

the analysis of urinary DNA biomarkers of oxidative stress [46, 111, 126]. Many reports suggest that the commercially available 8-oxodG ELISA kits correlates with chromatographic techniques. It is an easier alternative to gold-standard techniques such as HPLC-ECD or LC-MS/MS. On the other hand, analysis of 8-oxodG by ELISA shows more variation within the technique than chromatography [111].

The new method shows a LOQ of 0.04pmol and a LOD of 0.01 pmol on the column with signal to noise ratio of >3 for 8-oxodG. The linearity was r=0.9917 and the accuracy in the low, middle and higher concentration range was within limits of the FDA guideline for both the 60 min and the 25 min method variations. With the satisfactory validation report, the analytical method was applied to analyze the markers from mouse urine and plasma for finding a possible role of p47phox in NOX derived DNA damage during aging.

A recently published method with simultaneous analysis of dG and 8-oxodG from cellular DNA using LC-MS/MS technique [43] prevented artifact formation of 8-oxodG during analysis by using online solid phase sample extraction. However, the resolution between 8-oxodG (RT: 7.4 min) and dG (RT: 7.8) was small. After analysis of a few samples the resolution became even smaller. Therefore, the artifact 8-oxodG peak appeared closer or merged with the original peak, which may often lead to wrong interpretation of the data. With our newly developed method the resolution between dG and 8-oxodG was more than 4 min. Probably the above discussed issue could be solved by replacing the analytical column and mobile phase, but without changing the extraction column.

Creatinine is a breakdown product of creatinine phosphate, and the amount depends on the muscle tissue in the body and the renal function. The creatinine rate of excretion is relatively constant over time. Therefore, most of the urinary markers are commonly normalized to creatinine [60]. Recently, the analysis of creatinine and urinary 8-oxodG was described in two different variations [60]. However, due to the limited urine volume from mice, it is very difficult to analyze creatinine by conventional calorimetric methods and it is time consuming to do the analysis of 8-oxodG and creatinine in two different methods. Therefore, we developed a simultaneous analysis of creatinine and 8-oxodG

together with other analytes. To the best of our knowledge this is the first report for simultaneous analysis of creatinine and 8-oxodG using a stable isotope dilution LC-ESI-MS/MS method.

Quantification of 8-isoPGF2α has been suggested as a reliable indicator of lipid peroxidation [54, 127]. There are several advantages of 8-iso-PGF2α analysis because of its chemical stability, its specific product during lipid oxidation, and because the levels are unaffected by diet, and there are quantitatively sufficient amounts for detection in the biological fluids such as plasma [128], serum [129] and urine [54, 128, 130, 131]. There are several traditional methods available for analysis of 8-isoPGF2α including ELISA and RIA. Chromatographic methods such as gas chromatographic (GC), or liquid chromatographic methods are also available; GC has high sensitivity and specificity but sample preparation is extensive [132-134].

Recently developed LC-MS/MS methods have a very good sensitivity, with LOQ of 5pg/ml and a LOD of 1pg/ml [135, 136]. With our newly developed simultaneous analysis of 8-iso-PGF2α and creatinine the LOQ was 1.2 fmol and less than 1 fmol for LOD on the column. This may be due to the gradient method and the mobile phase which we use in our method. The 8-iso-PGF2α elutes at about 30 min, at that time the gradient is about 90% methanol and 10% formic acid water. The organic modifier methanol increased the ESI performance significantly. Fortunately, 8-iso-PGF2α has a relatively high lipophilic nature; therefore, larger amounts of organic solvent were used for separation, which resulted in good sensitivity. The recovery of the analyte showed 107% and 71.77% for the lower and higher concentration range, respectively. Concerning accuracy, the %RSD is 14.2 for the low range, which is a bit higher than the recommended limit, but the middle and higher range were within the limit, and the method showed very good linearity. The newly developed stable isotope dilution LC-ESI-MS/MS method had very good sensitivity and enabled simultaneous analysis with creatinine for urinary 8-iso-PGF2α calculation. The method was applied to measure urinary and plasma 8-iso-PGF2α from WT and p47phox -/- mice.

GSH is the most abundant intracellular thiol molecule and plays an essential role in maintaining the redox environment. It exists in millimolar (1-10mM) concentrations in most cell types. On the other hand, the plasma concentration is in the micromolar range, which is approximately 0.4% of total blood GSH. The molar GSH: GSSG ratio exceeds 100:1, this ratio has been reported to decrease to values between 10:1 and even 1:1 in various disease models of oxidative stress [119, 137]. The measured concentrations of GSH and GSSG are highly variable among different reports [138-146]. Accurate measurement of reduced and oxidized glutathione from biological fluids is still very challenging because of the rapid oxidation of GSH to GSSG. Many sample preparation methods are used for determination of GSH in the biological samples, including deproteinization, derivatization and reduction.

Usually the protein precipitation has been carried out by acidification using trichloroacetic acid (TCA), perchloric acid, metaphosphoric acid, or sulfosalicylic acid, which yields a clear, protein-free supernatant after centrifugation. TCA is the a very useful protein precipitating agent and, about 3-4% oxidation of GSH occurs during sample preparation [147]. 10% Metaphosphoric acid yields about 1-2% GSH oxidation at 4°C for at least 24h [148]. However, the above mentioned reagents alone cannot eliminate the autoxidation of GSH. Chemical protection of the thiol group is necessary to prevent the GSH oxidation completely. This may be achieved by alkylating SH groups by addition of N-ethylmaleimide (NEM) which is a strong and fast alkylation agent (Figure 53).

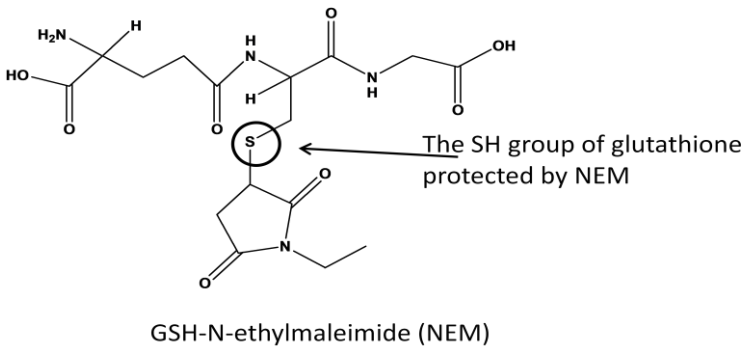

Figure 53: Protection of GSH form autoxidation by alkaylation at the SH group with N-ethylmaleimide (NEM).

Our sample preparation method, assures almost 100% protection of GSH from autoxidation by the use of the excess NEM. Therefore, the protected GSH and true GSSG of the sample can be extracted with solid phase extraction and quantified by LC-ESI-MS/MS technique. It is important that NEM is added immediately after collection of the samples (eg, whole blood or plasma) and that storage is done at -80°C until sample preparation for LC-ESI-MS/MS analysis.

Analysis of GSH and GSSG is possible with different methods, including spectrophotometer, HPLC-UV, HPLC-FL, HPLC-ECD, GC-MS, LC-MS, and LC-MS/MS. LC-MS has more advantages than all other methods because of ion suppression, ion enhancement matrix effect, and the use of stable isotope internal standards for accurate quantification. LC-MS is a powerful technique for the analysis of low-molecular thiols, including GSH [149]. Many groups published the simultaneous analysis of thiols and disulfides using LC-MS/MS methods [48,98,99,100] and recently Zhang et al reported a LC-MS/MS method for the analysis of GSH and GSSG in cultured cells treated with diethyl maleate (DEM), a GSH depleting agent [150]. Our newly developed LC-ESI-MS/MS method also has the advantage of simultaneous analysis of GSH and GSSG, with satisfactory recovery, accuracy and linearity. Moreover, by this method we separated diastereomers of the GSH-NEM adduct which appeared at 10.33 and 11.88 min. The separation pattern was similar to a recently reported one [151].

Various methods have been used for analysis of Ang II, including HPLC combined with radioimmunoassay [152-154]. The radioimmunoassay relies on specific antibodies for each peptide. Recently, LC-MS, LC-MS/MS [101] and nano-LC-MS [155, 156] methods have been developed for analysis of Ang II and related peptides in biological fluids. The above mentioned method has good accuracy and sensitivity. However, none of the methods used Ang II labeled internal standard for accurate quantification and to identify the specific Ang II peak in the complex biological samples. Therefore, in our LC-ESI-MS/MS method we used ^{15}N-^{13}C-Ang II which is ten mass higher than Ang II, as an internal standard. The mass transition 523.95 m/z [M+2H]2+ as a precursor ion and 263.10 m/z as product ion in the multiple reaction monitoring mode was employed for quantification of Ang II [155]. LOD for Ang II was less than 1fmol on column. Accuracy,

recovery and linearity of the method were satisfactory. In the sample collection or preparation step, we recommend to use a peptidase inhibitor (sodium metabisulfite, phosphoramidon, and thiorphan, final concentrations, 5mM, 0.1mM, and 10µM respectively) pre-coated tube for blood/urine collection [157] or a tube containing 50µL of 0.5M EDTA, 50µL of 0.5 M captopril (ACEi), trypsin inhibitor (0.15mg/mL blood) and aporotinin (2µg/mL blood). Both peptidase inhibitors are described to prevent degradation of peptides [109]. However, in our present study, we were not aware of the reagents at the time of sample collection. Therefore we could not use either reagent, but we recommend their use for further applications.

Accurate measurement of Ang II and Aldosterone concentrations may be essential for correct diagnosis of an elevated renin-angiotensin- aldosterone system. Therefore, our new method has the advantage of simultaneous analysis of Ang II and aldosterone in urine and plasma. There are many methods that can determine the aldosterone concentration in biological samples, including radioimmunoassay [158, 159], chemiluminescence-immunoassay [160, 161], GC-MS [162-164], LC-MS/MS [165-167] and LC-ESI-MS/MS [168]. The LC-MS/MS method provides a more reliable measurement of aldosterone than immunoassay and GC-MS and is becoming increasingly used in the clinical setting [167]. Our method has less than 1 fmol LOD and acceptable linearity for aldosterone. Both aldosterone and the internal standard d7-aldosterone were detected using negative mode ionization and quantified in the multiple reaction monitoring mode with following transitions 359.28 to 188.80 m/z and 366.15 to 192.80 m/z, respectively.

To the best of our knowledge, this is the first study where simultaneous analysis of 8-oxodG, 8-isoPGF2α, GSH and GSSG, dG, 8-nitroG, Ang II, aldosterone and creatinine were performed within a single run. The method is applicable to oxidative stress related pre-clinical, clinical, and basic research fields. In plasma, GSH, GSSH, 8-isoPGF2α, Ang II, aldosterone and creatine are quantifiable, where 8-oxodG, 8-nitroG and dG are not detected. In urine, 8-oxodG, GSH, GSSH, 8-isoPGF2α, Ang II, aldosterone, creatine and dG are quantifiable. But GSH, GSSG, and dG are not biological relevant and 8-

nitroG was not detectable amount in our study. In tissues, probably all the analytes are biological relevant and quantifiable.

5.2 Role of p47phox in Nox derived oxidative DNA and lipid damage

We applied the newly developed LC-ESI-MS/MS method to determine the amount of 8-oxodG, 8-isoPGF2α, GSH, GSSG, AngII, aldosterone, and creatinine in WT and p47phox$^{-/-}$ mice in different age groups.

In this study, we found that the oxidative DNA adducts 8-oxodG and the lipid oxidation product 8-isoPGF2α increasing with aged in WT mice, but not in p47phox$^{-/-}$ mice. Most probably the NOX derived ROS played an important role. To the best of our knowledge we report for the first time that the NOX organizer subunit p47phox plays a critical role in the formation of the mutagenic marker 8-oxodG.

A recent review describes the kidneys as very susceptible to damage by ageing, including morphological and functional changes [169]. We saw that DNA strand breaks were increased in kidneys of old WT mice compared with young WT. Also, strand breaks showed a clear difference appeared between old WT and p47phox$^{-/-}$ mice, and a slight but not significant difference in young kidneys. 8-oxodG was elevated in animal organs at older age in various animal models, including mice and rats. However, only few studies were able to achieve a background level of 8-oxodG within the limit of ESCODD values in which there is no artifact formation during analysis [23]. Our background value of about 3 adducts per 10^6 dG was within the range of ESCODD suggested values. The 8-oxodG level from young and old WT kidney DNA showed a significant difference and about 40% increased mean value with ageing.

Recently, Mikkelsen et. al., found an age dependent accumulation of 8-oxodG in WT mouse liver DNA analyzed by a chromatographic method, but no difference was observed in DNA strand breaks analyzed by comet assay [22]. We analyzed the DNA strand breaks in WT and p47phox$^{-/-}$ mouse liver in the young and old age group. There was a slightly elevated damage in old WT liver compared to p47phox$^{-/-}$. The background

damage in liver was about 50% less than in kidney. We saw a clear significant difference in old kidneys but only a small one in liver tissues. Ang II may activate NOX [170] and therefore, a relatively high amount of damage may be caused in the kidney where the renin-angiotensin-aldosterone system (RAAS) is locally involved with a relatively larger amount of Ang II [65]. Interestingly also the urinary 8-oxodG analyzed by LC-ESI-MS/MS was significantly higher in WT than p47phox$^{-/-}$ mice in both age groups. Some studies suggest that diet may manipulate the urinary 8-oxodG content [171-173], but ESCULA concluded that is not the case [47, 174-176]. Levels of urinary 8-oxodG vary with the different analysis techniques. The recent ESCULA validation report suggests that chromatography based MS or ECD methods have less within-technique-variation than ELISA [111]. Therefore the elevated urinary 8-oxodG in WT mice analyzed by LC-ESI-MS/MS can be considered to represent true oxidized lesion from p47phox dependent NOX derived ROS.

It is always important to measure more than one oxidative biomarker to elucidate the influence of oxidative stress. F2-Isoprostanes are the major products of lipid oxidation produced by the reaction of free radicals. Among all the 64 diastereoisomers of isoprostane, 8-isoPGF2α received most attention because it is not only a biomarker of oxidative stress but is also involved in renal and pulmonary vasoconstriction, various pathological conditions and also in the normal physiology of aging [53]. Urinary and plasma 8-isoPGF2α analyzed by LC-ESI-MS/MS increased with age in WT mice but not in p47phox$^{-/-}$ mice. After normalization to urinary creatinine, we still found that WT mice excreted more 8-isoPGF2α than old p47phox$^{-/-}$ mice, but there was no difference in young mice despite a LOD of less than 1 fmol on the column. However, since we had seen a difference in 8-oxodG we believe that the basal level production of NOX derived ROS is not capable of oxidizing lipid molecules but is sufficient for oxidizing DNA, especially guanine. This idea is supported by a study reporting iron-catalyzed DNA and lipid oxidation in-vitro, which also concluded that the presence of a low amount of free radicals is enough to damage the DNA but not the lipid molecules [177].

Another oxidative stress marker is oxidized glutathione. The analyzed GSSG/GSH ratio was significantly higher in WT than in p47phox$^{-/-}$ mice in both age groups. This was due

to elevated GSH in p47phox$^{-/-}$ mice rather than decrease in GSSG. The reason may be that p47phox$^{-/-}$ mice use less of GSH for ROS inactivation than WT mice. The increased amount of 8-oxodG and 8-isoPGF2α in WT mice may thus correspond to elevated level of GSSG/GSH.

Several reports suggest that Ang II activates NOX and produces ROS [61, 170]. Under normal physiological conditions, Ang II may regulate redox signaling pathways. However, overactivation of RAAS contributes to ageing [178-182] and age related diseases [183]. Therefore, we analyzed the urinary and plasma Ang II and aldosterone level by LC-ESI-MS/MS. We saw age dependent increases of urinary Ang II and aldosterone normalized to creatinine, supporting a RAAS contribution to ageing. It is not clear whether the plasma level of Ang II is age dependent but an age dependence has been reported for aldosterone. On the other hand, in the sample preparation we had neither added a general peptidase inhibitor nor selective ACE inhibitors to prevent the degradation of Ang II. This may also be the reason that we did not see an age dependent increase of Ang II in plasma. Interestingly, a study using 30 months saline treated rats showed an increased level of Ang II in cardiac tissue, but not in plasma. Probably the elevated level of Ang II in the cardiac tissues was due to the role of local RAAS involved in the heart [178]. To know more about the relation between Ang II and kidney ageing, one must analyze the Ang II content in WT mouse kidney in young and old groups, where we saw a significant elevation of the mutagenic DNA lesion 8-oxodG.

The creatinine normalized Ang II and Aldosterone showed a significant positive correlation with urinary 8-oxodG and 8-isoPGF2α. Modlinger et al [184] reported that urinary 8-isoPGF2α was increased in Ang II infused rats suggesting that Ang II contributes to increased lipid oxidation, which happens probably through NOX derived ROS. Ang II not only causes damage to lipids but also to the DNA, [109, 185, 186], which is described in more detail in a recent review [65]. Even 1nM Ang II was able to cause significant DNA damage in the isolated perfused mouse kidney [106]. We see significant age dependent DNA strand breaks caused by 200 nM Ang II treatment in isolated cells of WT mice and slightly but not significantly higher damage in p47phox-/- detected by comet assay. Based on the above results we believe that Ang II may play a

crucial role in age dependent damage to DNA at least in the kidney. However, aldosterone induced age dependent DNA damage to kidney needs to be investigated. Recently, we reported that aldosterone causes DNA strand breaks in the pig kidney cell line LLC-PK1 at nanomolar concentrations, and desoxycorticosterone acetate-salt (DOCA-salt), an aldosterone precursor, induced 8-oxodG in rats [108]. Moreover, we reported that aldosterone caused DNA strand breaks in immortalized mouse aortic endothelial WT cells (iMAEC with p47phox subunit) but not in iMAEC cells lacking p47phox (p47phox$^{-/-}$ cells) [65]. This suggests that Ang II and aldosterone probably influence the oxidative DNA damage and this action might be via NOX derived ROS.

Overall, the NOX organizer protein p47phox plays a crucial role in the formation of the oxidatively modified mutagenic base 8-oxodG in the kidney. Probably this effect is intensified with the action of Ang II and aldosterone.

5.3 Rosuvastatin protects angiotensin II–induced oxidative genomic damage

Statins are commonly used cholesterol lowering agents, acting through inhibition of 3-hydroxy-3-methylglutaryl-coenzyme A (HMG-CoA) reductase, which catalyses a rate limiting step in for cholesterol biosynthesis. Most of the statins including rosuvastatin have pleiotropic effects [187]. Among these, antioxidant properties of statins received much attention. It was hypothesized that statins protect from NOX induced ROS via upregulation of endogenous anti-oxidant enzymes [188]. Moreover, the antioxidant effect of statins appeared to be independent of cholesterol inhibition. Atorvastatin prevented the formation of Ang II induced free radicals in vascular smooth muscle cells by inhibiting Rac1 mediated NOX activity and down regulating AT1 receptor expression, both being independent of cholesterol inhibiting action [189]. Moreover, rosuvastatin protected DNA from oxidative stress in vitro [67, 109, 190], most probably via upregulation of glutathione sysnthesis [67].

Ang II caused oxidative stress, DNA damage and chromosomal aberrations in LLC-PK1 cells [109]. Ang II is an endogenous substance synthesized in the kidney and the

elevated amount causes oxidative stress and related diseases. Therefore, we selected Ang II and the pig kidney cell line LLC-PK1 to study the protective effect of rosuvastatin on DNA damage. At 10 nM rosuvastatin prevented DNA strand breaks analyzed by comet assay and at 1µM it protected from chromosomal aberration measured by micronuclei frequency assay. Furthermore, we also analyzed the oxidative mutagenic marker 8-oxodG in cells treated with Ang II alone and combined with rosuvastatin by LC-MS/MS. 1µM rosuvastatin was able to protect the LLC-PK1 cells from elevated oxidative DNA damage. The protective effect of rosuvastatin acts probably via inhibiting the activation of NOX enzyme which contributes to the DNA base modification. Further experimental evidence is required to prove that rosuvastatin inhibits NOX activity and expression of AT1 receptor in Ang II induced oxidative stress and DNA damage. However, it was already demonstrated that rosuvastatin attenuates Ang II induced cardiomyocyte hypertrophy via inhibition of AT1 receptor [191]. The increased amount of total glutathione in Ang II and rosuvastatin treated cells supported the idea that the protective effect of rosuvastatin was achieved via the antioxidant effect. Rosuvastatin alone upregulates the expression of glutathione synthase, glutathione reductase and glutathione peroxidase in LLC-PK1 cells which we also observed in HL-60 cell line [67]. The treatment of cells with cholesterol biosynthesis intermediates farnesol, farnesyl pyrophosphate, geranylgeraniol did not reverse the action of rosuvastatin. Therefore, rosuvastatin action was probably independent of cholesterol inhibition.

Overall, rosuvastatin protected the cells from Ang II induced oxidative stress, DNA and genomic damage in vitro. The protective effect of rosuvastatin is achieved via upregulation of glutathione and it is independent of cholesterol biosynthesis inhibition.

5.4 Parkinson's disease and oxidative DNA damage

In the present study, we demonstrated that the oxidative stress biomarker 8-oxodG was elevated in chronically L-DOPA-treated patients with PD, which agrees with previous reports using post-mortem brain tissue of PD patients [81, 82]. In our study the gender distribution was unequal between the groups, with more females in the control group because they were life partners of the male PD patients. While no data are available about a potential influence of gender on the 8-oxodG level in the DNA of peripheral

lymphocytes, we still cannot exclude a confounding effect of this gender difference, since reports stated that men excrete 29% [120] or 35% [122] more 8-oxodG than females in their urine, while others reported no differences [121, 123].

Among the five normal nucleotide bases, guanine is the most susceptible to oxidation, particularly the C8 position of deoxyguanosine is most effectively oxidized by hydroxyl radicals [192, 193]. In PD, several studies have examined whether the disease process is associated with a higher production or a lower detoxification of oxidants. Increased ROS production has been observed in peripheral blood monocyte cells (PBMC) after treatment with L-DOPA plus other medications used in a combined therapy (Prigione et al. 2006). Cerebrospinal fluid and plasma from PD patients showed higher oxidative stress in the form of lipoprotein oxidation after treatment with L-DOPA and dopamine agonists [194]. Vitte et al described that oxidative stress significantly increased in neutrophils from L-DOPA treated PD patients, but the role of additional medications or the disease itself remained unclear [195]. Antioxidant effects of additional medications, i.e. dopamine agonists, may be involved in some of the observed effects. Le et al reported that dopamine agonist showed antioxidant property independent of dopamine receptor activation [196]. Interestingly, a positive correlation was observed between 8-oxodG or MN amount of dopamine agonist within the subgroup of L-DOPA treated PD patients also receiving a dopamine agonist. This effect may be due to binding of D2 receptor by dopamine agonist. The cell might then recruit more dopamine inside the cell by activation of dopamine transporters (DAT). Once dopamine is inside, MAO converts it to metabolites and ROS which leads to formation of 8-oxodG, which can be prevented by the MAO inhibitor PCPA [104, 197].

Another endpoint for oxidative stress is the antioxidative capacity of plasma, measured as FRAP. Since low FRAP values indicate high oxidative stress or low antioxidant defense level, an inverse correlation with the levels of 8-oxodG might be expected. Instead, in our study the antioxidative capacity of plasma was higher in PD patients than in the control group. Elevated DNA oxidation should lead to increased genomic damage. However, micronucleus frequencies were not elevated compared to the controls. Opposite to that, Migliore et al reported an elevated micronucleus formation in

untreated PD patients [83]. A potential conclusion is that treatment with L-DOPA plus dopa decarboxylase inhibitors in our patients might have protected the patients from PD-related additional chromosomal damage. This assumption of a protective effect is supported by the correlation between antioxidant FRAP values and daily L-DOPA doses (plus dopa decarboxylase inhibitors). The dopa decarboxylase inhibitor carbidopa increases the plasma half-life of L-DOPA from 50 min to 80 min and decreases the plasma and urinary dopamine and its major metabolite homovanillic acid. When decarboxylation of L-DOPA is prevented by carbidopa, COMT becomes the major metabolizing enzyme for L-DOPA, catalyzing its metabolism to 3-methoxy-4-hydroxy-L-phenylalanine (3-OMD). When the COMT inhibitor entacapone is given together with L-DOPA and carbidopa, plasma levels of L-DOPA are greater and more sustained than after administration of L-DOPA and carbidopa alone [104].

Increased antioxidative capacity and no increase of micronuclei despite elevated 8-oxodG may be interpreted as a protective effect of L-DOPA therapy on genomic integrity. Our findings of an antioxidative capacity of L-DOPA and dopamine in a cell free in vitro system suggest a potential direct antioxidative effect of L-DOPA (and the small quantities of dopamine that are formed) in the serum. In support of this idea, a recent study employing the comet assay (single cell gel electrophoresis) as measure for DNA-damage detected that L-DOPA treatment reduced the DNA damage in peripheral blood cells from patients with PD [104, 198].

Peripheral blood lymphocytes express dopa decarboxylase (DDC) and L-type amino acid transporter (LAT1), and are able to uptake L-DOPA and convert it into dopamine. In addition, dopamine can enter via dopamine transporters (DAT) which has also been found on the lymphocyte plasma membrane [199-202]. Increased cytosolic levels of dopamine have been found to induce formation of ROS, and of semiquinones and quinones after catabolism and autooxidation [203]. In agreement with this, in our experiments with PC12 cells, dopamine caused oxidative stress leading to elevated 8-oxodG. Thus, the observed elevated 8-oxodG in the peripheral lymphocytes may be due to activities of dopamine inside the lymphocytes. Dopamine has been described to induce genomic damage in V79 cells, in the presence of metals like manganese,

copper, iron and cobalt, which could be effectively prevented by reduced glutathione [204]. We recently reported that dopamine caused genotoxicity in the rat neuronal PC12 cell, human lumpholastoid TK6 cells and rat kidney NRK cells, which was prevented by addition of antioxidants, dopamine type 2 receptor antagonists and DAT inhibitors [205]. Following chronic L-DOPA therapy, the amount of 8-oxodG formed in peripheral blood lymphocytes may be below a threshold for micronucleus induction, but it is not known whether it may result in an increased gene mutation frequency. In fact, dopamine has been described as mutagenic in a mammalian in vitro mutation assay [104, 206].

Major confounding factors for micronucleus frequency are generally age and gender. The age was not significantly different between groups here. Females are known to have higher frequencies than males [207]. Therefore, we cannot exclude that the micronucleus frequency would have been slightly elevated in the PD group, if gender distribution would have been equal. Antioxidant intake via supplements may influence the micronucleus frequency but was equal between patients and controls. Influences of other medications may be complex and are not well studied, but were similar between patients and controls [104].

Overall, medication with L-DOPA may upon conversion to dopamine inside of peripheral lymphocytes or other cells contribute to the oxidative stress burden in PD patients by increasing the intracellular 8-oxodG formation. But at the same time L-DOPA enhances the antioxidant level in the serum, thus protecting PD patients from increased oxidative stress. Other medications may add to these effects, and as an overall consequence, the genomic damage as seen as micronucleus frequency is not affected by L-Dopa therapy [104].

5.5 Conclusion

Overall, we have elucidated the role of ROS induced oxidative DNA damage in three models. The NOX organizer protein p47phox plays a crucial role in the formation of the oxidatively modified mutagenic marker 8-oxodG in the kidney. Rosuvastatin protected the pig kidney cell line LLC-PK1 from Ang II induced 8-oxodG in vitro. An increased 8-oxodG formation contributed to the oxidative stress burden in PD patients, which was compensated by antioxidant effect of L-DOPA.

6 Summary

When there is an imbalance between reactive oxygen species (ROS) and endogenous antioxidants (glutathione (GSH), superoxide dismutase (SOD), catalase etc.) the oxidative stress is increased and results in the oxidation of lipids, proteins and DNA. Although oxidation of lipids and proteins may also accumulates with age, only DNA oxidation leads to altered genomic information. As one pathway for increased ROS production, many endogenous and exogenous substances activate NADPH oxidase (NOX) enzyme and produce ROS. p47phox is a cytosolic organizer protein which plays an important role in NOX activation. Angiotensin II (Ang II) is an example for an endogenous compound which causes ROS through NOX activation. Rosuvastatin is an example for a drug with antioxidative capacity (upregulation of endogenous antioxidants). It is a lipid lowering drug which also reduces an elevated level of angiotensin II type 1 receptor (AT1R). Commonly, oxidative stress is elevated in ageing and age related diseases (eg. Parkinson's disease (PD)). The aim of the present study was to investigate the role of NOX derived ROS induced oxidative DNA damage and the influence of ROS in ageing and age related diseases, using different in vitro and in vivo models.

I) To quantify oxidative stress and oxidative DNA damage markers, we developed a new isotope-diluted-LC-ESI-MS/MS method and validated it to analyze 8-oxodG, 8-isoPGF2α, GSH, GSSG, Ang II, Aldosterone and creatinine in a single sample preparation. The analytes were monitored in the positive and negative multiple reaction monitoring (MRM) mode simultaneously. For optimum sensitivity, specific product ions and optimal instrument settings were obtained by infusion of authentic standards and using the quantitative optimization function of the Analyst 1.4.2 software. Two transitions per adduct were monitored. Peak areas of the most sensitive transitions were used for quantification. Creatinine, GSSG, GSH-NEM, dG, 8-nitroG, 8-oxodG and Ang II were analyzed using positive MRM mode. Aldosterone and 8-isoPGF2α were analyzed using negative MRM mode. The new method shows a LOD of 0.01 pmol on the column for 8-oxodG and 2.5 pmol for creatinine. To the best of our knowledge this is the first report for simultaneous

analysis of creatinine and 8-oxodG using a stable isotope dilution LC-ESI-MS/MS method. Quantification of 8-isoPGF2α has been suggested as a reliable indicator of lipid peroxidation. With our newly developed simultaneous analysis of 8-iso-PGF2α and creatinine the LOQ was 1.2 fmol and less than 1 fmol for LOD on the column. And the method had very good sensitivity and enabled simultaneous analysis with creatinine for urinary 8-iso-PGF2α calculation. The method was applied to measure urinary and plasma 8-iso-PGF2α.

GSH is the most abundant intracellular thiol molecule and it plays an essential role in maintaining the redox environment. It exists in millimolar (1-10mM) concentrations in most cell types. On the other hand, the plasma concentration is in the micromolar range, which is approximately 0.4% of total blood GSH. For analysis of GSH chemical protection of the thiol group is necessary to prevent GSH oxidation completely. This may be achieved by alkylating SH groups by addition of N-ethylmaleimide (NEM) which is a strong and fast alkylation agent. Our sample preparation method assures almost 100% protection of GSH from autoxidation by the use of excess NEM. Our newly developed LC-ESI-MS/MS method also has the advantage of simultaneous analysis of GSH and GSSG, with satisfactory recovery, accuracy and linearity.

Accurate measurement of Ang II and Aldosterone concentrations may be essential for correct diagnosis of an elevated renin-angiotensin-aldosterone system. Therefore, our new method has the advantage of simultaneous analysis of Ang II and aldosterone in urine and plasma.

This is the first study where simultaneous analysis of 8-oxodG, 8-isoPGF2α, GSH and GSSG, dG, 8-nitroG, Ang II, aldosterone and creatinine were performed within a single run. The method is applicable to oxidative stress related pre-clinical, clinical, and basic research fields. In plasma, GSH, GSSH, 8-isoPGF2α, Ang II, aldosterone and creatine are quantifiable, While 8-oxodG, 8-nitroG and dG are not detected. In urine, 8-oxodG, GSH, GSSH, 8-isoPGF2α, Ang II, aldosterone, creatine and dG are quantifiable. But GSH, GSSG, and dG are not biological

relevant and 8-nitroG was not detectable in our study. In tissues, probably all the analytes are biological relevant and quantifiable.

II) As an in vivo model for investigation of the role of NOX in oxidative DNA damage induction, we used the p47phox$^{-/-}$ mouse. The oxidative DNA base modification 8-oxodG of kidney DNA was significantly different between WT and p47phox$^{-/-}$ mice with WT mice showing more 8-oxodG in both young and old age groups. Ang II may activate NOX and therefore, a relatively high amount of damage may be caused in the kidney where the renin-angiotensin-aldosterone system (RAAS) is locally involved with a relatively larg amount of Ang II. Urinary 8-oxodG also showed significant differences between WT and p47phox$^{-/-}$ mice in both age groups with WT mice showing higher values than phox mice.

The oxidative stress marker urinary 8-isoPGF2α exhibited a significant difference between WT and p47phox$^{-/-}$ in the aged group (WT higher than p47phox$^{-/-}$ mice), but not in the young group. Moreover, values were twenty fold higher in aged WT mice compared to young WT. The 8-isoPGF2α level in plasma showed a clear difference between WT and p47phox$^{-/-}$ mice in the old group. The level was significantly higher in old WT than young WT mice. However, we did not see any difference in the young group. As another important oxidative stress marker, GSSG/GSH ratio was significantly higher in WT mice than p47phox$^{-/-}$ mice in both age groups. However, no difference between young and aged mice was seen in WT or p47phox$^{-/-}$ mice.

The amount of urinary Ang II and aldosterone was about four and five fold higher in old than in young WT mice. Ang II and Aldosterone showed significant correlation between urinary 8-oxodG and 8-isoPGF2α. However, the plasma concentration of Ang II and Aldosterone showed no significant difference between the groups. We found a significant level of DNA damage in Ang II treated kidney cell isolates of WT compared with untreated cells, but no differences in cells from p47phox$^{-/-}$ mice at least after short time (30 min) treatment in vitro. Under normal physiological conditions, Ang II may regulate redox signaling pathways via NOX activation and

ROS production. However, overactivation of RAAS seems to contribute to ageing and age related diseases.

This mouse knockout model demonstrated that the NOX organizer protein p47phox plays a crucial role in the formation of the oxidatively modified mutagenic marker 8-oxodG in the kidney.

III) The effect of an antioxidant drug was investigated in pig kidney LLC-PK1 cells. Ang II caused oxidative stress, DNA damage and chromosomal aberration in these cells. At 10 nM rosuvastatin prevented DNA strand breaks analyzed by comet assay and at 1µM it protected from chromosomal aberrations measured by the micronuclei frequency assay. Furthermore, 1µM rosuvastatin was able to protect LLC-PK1 cells from elevated oxidative DNA damage. The increased amount of total glutathione in Ang II and rosuvastatin treated cells supported the idea that the protective effect of rosuvastatin was achieved via the antioxidant effect. Rosuvastatin alone upregulated the expression of glutathione synthase, glutathione reductase and glutathione peroxidase in LLC-PK1 cells. The treatment of cells with the cholesterol biosynthesis intermediates farnesol, farnesyl pyrophosphate, geranylgeraniol did not reverse the action of rosuvastatin. Therefore, rosuvastatin action was probably independent of cholesterol biosynthesis inhibition.

Rosuvastatin protected the cells from Ang II induced oxidative stress, DNA and genomic damage in vitro. The protective effect of rosuvastatin was achieved via upregulation of glutathione and it was independent of cholesterol biosynthesis inhibition.

IV) As human disease for which ROS is often implied as contributor, Parkinson's disease was investigated. The oxidative stress biomarker 8-oxodG was elevated in chronically L-DOPA-treated patients with PD, which agrees with previous reports using post-mortem brain tissue of PD patients. The antioxidative capacity of plasma was measured as FRAP. Since low FRAP values indicate high oxidative stress or low antioxidant defense level, an inverse correlation with the levels of 8-oxodG might be expected. Instead, in our study the antioxidative capacity of plasma was higher in

PD patients than in the control group. Elevated DNA oxidation should lead to increased genomic damage. However, micronucleus frequencies were not elevated compared to the controls. A potential conclusion is that treatment with L-DOPA plus dopa decarboxylase inhibitors in our patients might have protected the patients from PD-related additional chromosomal damage.

Overall, the development of a new LC-ESI-MS/MS method enabled a sensitive quantification of several oxidative stress related alterations in our models. In combination with additional methods, this yielded the new information that the NOX organizer protein p47phox plays a crucial role in the formation of the oxidatively modified mutagenic marker 8-oxodG. Rosuvastatin protected the pig kidney cell line LLC-PK1 from Ang II induced oxidative stress, DNA and genomic damage in vitro in a cholesterol biosynthesis independent manner. An increased 8-oxodG formation contributed to the oxidative stress burden in PD patients, which was compensated by antioxidant effect of L-DOPA.

Further research will be needed to strengthen the relationship between these findings, which will then provide new disease prevention strategies.

7 Zusammenfassung

Bei einem Ungleichgewicht zwischen reaktiven Sauerstoffspezies (ROS) und endogenen Antioxidantien (Glutathion (GSH), Superoxiddismutase (SOD), Katalase etc.) ist der oxidative Stress erhöht, was zur Oxidation von Lipiden, Proteinen und DNA führt. Obwohl auch oxidierte Lipide und Proteine mit steigendem Alter akkumulieren können, führen nur DNA-Oxidationen zu veränderter genomischer Information. Ein möglicher Signalweg für gesteigerte ROS-Produktion ist die Aktivierung des Enzyms NADPH-Oxidase (NOX) und die damit verbundene Generierung von ROS durch viele endogene und exogene Substanzen. p47phox ist ein cytosolisches Protein, das eine wichtige Rolle bei der NOX-Aktivierung spielt. Angiotensin II (Ang II) ist ein Beispiel für eine endogene Verbindung, die über NOX-Aktivierung ROS produziert. Rosuvastatin ist ein Arzneistoff mit antioxidativen Eigenschaften (Hochregulation endogener Antioxidantien). Es gehört zur Gruppe der Cholesterinsenker und reduziert ausserdem erhöhtes Auftreten des Angiotensin-II-Typ-1-Rezeptors (AT1R). Normalerweise ist oxidativer Stress im Alter und bei Alterskrankheiten (z. B. Parkinson-Krankheit) erhöht. Das Ziel der vorliegenden Arbeit war, mit Hilfe unterschiedlicher Modelle in vitro und in vivo die Rolle von DNA-Schaden durch NOX-vermittelte ROS zu untersuchen und den Einfluss von ROS auf den Alterungsprozess und auf Alterskrankheiten zu bestimmen.

I) Um oxidativen Stress und oxidativen DNA-Schaden zu quantifizieren, entwickelten wir eine neue Isotopenverdünnungs-LC-ESI-MS/MS-Methode und validierten diese für eine Analyse von 8-oxodG, 8-isoPGF2α, GSH, GSSG, Ang II, Aldosteron und Kreatinin in einer einzigen Probe. Die Analyten wurden simultan im positiven und negativen Multiple-Reaction-Monitoring-Modus (MRM) erfasst. Zur Optimierung der Sensitivität wurden spezifische Ionisierungen und optimale Geräteeinstellungen durch Einsatz von Standardsubstanzen unter Verwendung quantitativer Optimierungsfunktionen der Software Analyst 1.4.2 erreicht. Je Addukt wurden zwei Übergänge detektiert. Die Peakflächen der sensitivsten Übergänge wurden zur Quantifizierung genutzt. Kreatinin, GSSG, GSH-NEM, dG, 8-nitroG, 8-oxodG und Ang II wurden im positiven MRM-Modus analysiert. Aldosteron und 8-

isoPGF2α wurden im negativen MRM-Modus analysiert. Mit der neuen Methode wurde eine Nachweisgrenze von 0,01 pmol auf der Säule für 8-oxodG und von 2,5 pmol für Kreatinin erreicht. Nach unserem Wissen ist dies der erste Bericht über eine simultane Analyse von Kreatinin und 8-oxodG mit einer Isotopenverdünnungs-LC-ESI-MS/MS-Methode. Die Quantifizierung von 8-isoPGF2α wurde als verlässlicher Indikator für Lipidperoxidation vorgeschlagen. Mit unserer neu entwickelten Methode zur simultanen Analyse von 8-iso-PGF2α und Kreatinin wurde eine Quantifizierungsgrenze von 1,2 fmol und eine Nachweisgrenze von weniger als 1 fmol auf der Säule erreicht. Die Methode weist eine hohe Sensitivität auf und ermöglicht die simultane Analyse von Kreatinin zur Berechnung des 8-iso-PFG2α im Urin. Die Methode wurde eingesetzt um 8-iso-PGF2α im Urin und im Plasma zu messen.

GSH ist das häufigste intrazelluläre Thiol-Molekül und spielt eine essentielle Rolle bei der Aufrechterhaltung desRedoxstatus. Es kommt in den meisten Zellarten in millimolaren (1 - 10 mM) Konzentration vor. Andererseits liegt die Plasma-Konzentration im mikromolaren Bereich, was einem Anteil von etwa 0,4 % des Gesamt-GSH im Blut entspricht. Zur Analyse von GSH ist es notwendig, die Thiol-Gruppe chemisch zu schützen um die Oxidation vollständig zu verhindern. Dies kann durch Alkylierung der SH-Gruppen mit Hilfe von N-Ethylmaleinimid (NEM), einem potenten und schnellen Alkylierungs-Agens, erreicht werden. Unsere Probenaufbereitungsmethode gewährleistet einen Schutz von GSH vor Autooxidation zu fast 100 % durch die Verwendung eines NEM-Überschusses. Unsere neue Methode hat darüber hinaus den Vorteil der simultanen Analyse von GSH und GSSG mit ausreichender Wiederfindungsrate, Genauigkeit und Linearität.

Die genaue Messung von Ang II und Aldosteron könnte ausschlaggebend für eine korrekte Erkennung eines aktivierten Renin-Angiotensin-Systems sein. Unsere Methode hat hier den Vorteil der simultanen Analyse von Ang II und

Aldosteron im Urin und im Plasma.

Die vorgelegte Methode ist die erste Methode zur simultanen Analyse von 8-oxodG, 8-isoPGF2α, GSH und GSSG, dG, 8-nitroG, Ang II, Aldosteronund Kreatinin in einem Lauf. Anwendungsfelder dieser Methode sind präklinische, klinische und Grundlagenforschungs-bezogene Fragestellungen im Zusammenhang mit oxidativem Stress. Im Plasma waren GSH, GSSH, 8-isoPGF2α, Ang II, Aldosteronund Kreatin quantifizierbar, während 8-oxodG, 8-nitroG und dG nicht detektiert wurden.Im Urin wurden 8-oxodG, GSH, GSSH, 8-isoPGF2α, Ang II, Aldosteron, Kreatin und dG quantifiziert.GSH, GSSG und dG sind jedoch biologisch nicht relevant und 8-nitroG wurde in unserer Studie nicht detektiert. Im Gewebe sind vermutlich alle Analyten relevant und quantifizierbar.

II) Zur Untersuchung der Rolle der NOX bei der Induktion oxidativen DNA-Schadens nutzen wir p47phox$^{-/-}$-Mäuse als in-vivo-Modell. Die oxidative DNA-Basenmodifikation 8-oxodG trat beim WT und bei p47phox$^{-/-}$-Mäusen in signifikant unterschiedlichem Maße auf, wobei der WT sowohl in der jungen als auch der alten Altersgruppe mehr 8-oxodG aufwies. Ang II könnte NOX aktivieren und daher könnte ein relativ hoher DNA-Schaden in der Niere auftreten, da hier das Renin-Angiotensin-Aldosteron-System (RAAS) lokal eine relativ hohe Menge an Ang II bereitstellt. Die Menge an 8-oxodG im Urin war ebenfalls signifikant unterschiedlich zwischen dem WT und p47phox$^{-/-}$-Mäusen in beiden Altersgruppen, wobei der WT höhere Werte zeigte als die phox-Mäuse.

Der Marker für oxidativen Stress 8-isoPGF2α im Urin war signifikant unterschiedlich ausgeprägt zwischen WT und p47phox$^{-/-}$-Mäusen in der alten Altersgruppe (WT höher als p47phox$^{-/-}$-Mäuse) aber nicht in der jungen Altersgruppe. Außerdem waren die Werte bei den alten WT-Mäusen im Vergleich zum jungen WTum das Zwanzigfache erhöht. Die 8-isoPGF2α-

Werte im Plasma zeigten einen klaren Unterschied zwischen WT und p47phox$^{-/-}$-Mäusen in der alten Gruppe. Die Werte waren signifikant höher in alten WT- als in jungen WT-Mäusen. Wir konnten jedoch keinen Unterschied innerhalb der jungen Gruppe beobachten. Ein weiterer wichtiger Marker für oxidativen Stress, das Verhältnis GSSG/GSH, war in beiden Altersgruppensignifikant höher bei WT-Mäusen als bei p47phox$^{-/-}$-Mäusen. Allerdings konnte kein Unterschied zwischen jungen und alten Mäusen festgestellt werden, weder im WT noch bei p47phox$^{-/-}$-Mäusen.

Die Menge an Ang II und Aldosteron im Urin war etwa um den Faktor vier bzw. fünf erhöht bei alten im Vergleich zu jungen WT-Mäusen. Ang II und Aldosteron zeigten signifikante Korrelationen mit 8-oxodG und 8-isoPGF2α im Urin. Die Konzentrationen von Ang II und Aldosteron im Plasma zeigten jedoch keine signifikanten Unterschiede zwischen den Gruppen. Wir konnten eine signifikante Höhe an DNA-Schaden in isolierten Ang-II-behandelten Nierenzellen des WT im Vergleich zu unbehandelten Zellen feststellen, jedoch zeigten sich keine Unterschiede bei Zellen von p47phox$^{-/-}$-Mäusen nach Behandlung für 30 min in vitro. Unter normalen physiologischen Umständen könnte Ang II Redox-Signalwege durch eine Aktivierung der NOX und einer Produktion von ROS regulieren. Eine Überaktivierung des RAAS scheint jedoch am Alterungsprozess und an Alterserkrankungen beteiligt zu sein.

Dieses Knockout-Modell zeigte, dass die NOX-Untereinheit p47phox eine entscheidende Rolle bei der Bildung des oxidativ modifizierten 8-oxodG, einem Marker für Mutagenität, in der Nierespielt.

III) Die Auswirkungen eines antioxidativen Arzneistoffes wurden in den Nierenzellen LLC-PK1 untersucht. Ang II verursachte oxidativen Stress, DNA-Schaden und chromosomale Aberrationen in diesen Zellen. In einer Konzentration von 10 nM verhinderte Rosuvastatin die Bildung von DNA-

Strangbrüchen (Comet Assay) und in einer Konzentration von 1 µM verhinderte es das Entstehen chromosomaler Aberrationen (Mikrokerntest). Weiterhin schützte Rosuvastatin in einer Konzentration von 1 µM die LLC-PK1-Zellen vor erhöhtem oxidativen DNA-Schaden. Die erhöhte Gesamtmenge an Glutathion in Ang-II- und Rosuvastatin-behandelten Zellen unterstützte die Hypothese, dass der schützende Effekt von Rosuvastatin durch antioxidative Wirkungen vermittelt wird. Rosuvastatin erhöhtealleindie Expression der Glutathionsynthase, der Glutathionreduktase und der Glutathionperoxidase in LLC-PK1-Zellen. Behandlung der Zellen mit den Cholesterinbiosynthese-Intermediaten Farnesol, Farnesylpyrophosphat und Geranylgeraniol machte die Wirkung von Rosuvastatin nicht rückgängig. Daher war die Wirkung von Rosuvastatin wahrscheinlich unabhängig von der Hemmung der Cholesterinbiosynthese.

Rosuvastatin schützte die Zellen in vitro vor durch Ang II verursachtem oxidativen Stress und DNA-Schaden. Der schützende Effekt von Rosuvastatin wurde durch eine Hochregulation von Glutathion erreicht und war unabhängig von der Hemmung der Cholesterinbiosynthese.

IV) Als Humanerkrankung, die oft mit ROS verbunden wird, wurde die Parkinson-Erkrankung untersucht. Der Marker für oxidativen Stress 8-oxodG war bei Parkinson-Patienten unter chronischer L-DOPA-Behandlung erhöht, dies stimmt mit früheren Berichten über post-mortem-Untersuchungen an Hirngewebe von Parkinson-Patienten überein. Die antioxidative Kapazität von Plasma wurde als FRAP gemessen. Da niedrige FRAP-Werte hohen oxidativen Stress bzw. niedrige antioxidative Abwehrmechanismen anzeigen, könnte eine inverse Korrelation mit der Höhe an 8-oxodG vermutet werden. Im Gegensatz dazu war in unserer Studie die antioxidative Kapazität des Plasmas bei Parkinson-Patienten höher als in der Kontrollgruppe. Erhöhte DNA-Oxidation sollte zu erhöhtem DNA-Schaden führen. Allerdings waren die Mikrokernraten im Vergleich zu Kontrollen nicht erhöht. Eine mögliche

Schlussfolgerung ist, dass die Behandlung mit L-DOPA und DOPA-Decarboxylasehemmern die Patienten vor zusätzlichen, Parkinson-assoziierten, chromosomalen Schäden geschützt haben könnte.

Insgesamt ermöglichte die Entwicklung einer neuen LC-ESI-MS/MS-Methode eine sensitive Quantifizierung mehrerer, mit oxidativem Stress verbundenen Modifizierungen in unseren Modellen. In Kombination mit zusätzlichen Methoden konnte so die neue Erkenntnis gewonnen werden, dass die NOX-Untereinheit p47phox eine essentielle Rolle bei der Bildung von oxidativ verändertem 8-oxodG, einem Marker für Mutagenität, spielt. Rosuvastatinschützte in vitro die Nierenzelllinie LLC-PK1 vor durch Ang II verursachtem DNA- und Genomschaden und oxidativem Stress unabhängig von der Cholesterinbiosynthese. Gesteigerte 8-oxodG-Bildung erhöhte den oxidativen Stress bei Parkinson-Patienten, was durch die antioxidativen Effekte von L-DOPA ausgeglichen wurde.

Weitere Untersuchungen sind notwendig, um den Zusammenhang zwischen diesen Befunden näher zu charakterisieren. Dies wird zu neuen Präventions-Strategien führen.

8 References

[1] Krause, K. H. Aging: a revisited theory based on free radicals generated by NOX family NADPH oxidases. *Exp Gerontol* **42:**256-262; 2007.

[2] Bedard, K.; Krause, K. H. The NOX family of ROS-generating NADPH oxidases: physiology and pathophysiology. *Physiol Rev* **87:**245-313; 2007.

[3] Brandes, R. P.; Weissmann, N.; Schroder, K. NADPH oxidases in cardiovascular disease. *Free Radic Biol Med* **49:**687-706; 2010.

[4] Schroder, K. Isoform specific functions of Nox protein-derived reactive oxygen species in the vasculature. *Curr Opin Pharmacol* **10:**122-126; 2010.

[5] Banfi, B.; Maturana, A.; Jaconi, S.; Arnaudeau, S.; Laforge, T.; Sinha, B.; Ligeti, E.; Demaurex, N.; Krause, K. H. A mammalian H+ channel generated through alternative splicing of the NADPH oxidase homolog NOH-1. *Science* **287:**138-142; 2000.

[6] Cheng, G.; Cao, Z.; Xu, X.; van Meir, E. G.; Lambeth, J. D. Homologs of gp91phox: cloning and tissue expression of Nox3, Nox4, and Nox5. *Gene* **269:**131-140; 2001.

[7] Gavazzi, G.; Banfi, B.; Deffert, C.; Fiette, L.; Schappi, M.; Herrmann, F.; Krause, K. H. Decreased blood pressure in NOX1-deficient mice. *FEBS Lett* **580:**497-504; 2006.

[8] Krause, K. H. Tissue distribution and putative physiological function of NOX family NADPH oxidases. *Jpn J Infect Dis* **57:**S28-29; 2004.

[9] Lambeth, J. D. Nox enzymes, ROS, and chronic disease: an example of antagonistic pleiotropy. *Free Radic Biol Med* **43:**332-347; 2007.

[10] Beckman, K. B.; Ames, B. N. The free radical theory of aging matures. *Physiol Rev* **78:**547-581; 1998.

[11] Banfi, B.; Malgrange, B.; Knisz, J.; Steger, K.; Dubois-Dauphin, M.; Krause, K. H. NOX3, a superoxide-generating NADPH oxidase of the inner ear. *J Biol Chem* **279:**46065-46072; 2004.

[12] Paffenholz, R.; Bergstrom, R. A.; Pasutto, F.; Wabnitz, P.; Munroe, R. J.; Jagla, W.; Heinzmann, U.; Marquardt, A.; Bareiss, A.; Laufs, J.; Russ, A.; Stumm, G.; Schimenti, J. C.; Bergstrom, D. E. Vestibular defects in head-tilt mice result from mutations in Nox3, encoding an NADPH oxidase. *Genes Dev* **18:**486-491; 2004.

[13] Nunoi, H.; Rotrosen, D.; Gallin, J. I.; Malech, H. L. Two forms of autosomal chronic granulomatous disease lack distinct neutrophil cytosol factors. *Science* **242:**1298-1301; 1988.

[14] Volpp, B. D.; Nauseef, W. M.; Clark, R. A. Two cytosolic neutrophil oxidase components absent in autosomal chronic granulomatous disease. *Science* **242:**1295-1297; 1988.

[15] Jones, S. A.; Hancock, J. T.; Jones, O. T.; Neubauer, A.; Topley, N. The expression of NADPH oxidase components in human glomerular mesangial cells: detection of protein and mRNA for p47phox, p67phox, and p22phox. *J Am Soc Nephrol* **5:**1483-1491; 1995.

[16] Jones, S. A.; O'Donnell, V. B.; Wood, J. D.; Broughton, J. P.; Hughes, E. J.; Jones, O. T. Expression of phagocyte NADPH oxidase components in human endothelial cells. *Am J Physiol* **271:**H1626-1634; 1996.

[17] Harman, D. Aging: a theory based on free radical and radiation chemistry. *J Gerontol* **11:**298-300; 1956.

[18] Lieber, M. R.; Karanjawala, Z. E. Ageing, repetitive genomes and DNA damage. *Nat Rev Mol Cell Biol* **5:**69-75; 2004.

[19] Imlay, J. A.; Linn, S. DNA damage and oxygen radical toxicity. *Science* **240:**1302-1309; 1988.

[20] Herrero, A.; Barja, G. 8-oxo-deoxyguanosine levels in heart and brain mitochondrial and nuclear DNA of two mammals and three birds in relation to their different rates of aging. *Aging (Milano)* **11:**294-300; 1999.

[21] Hamilton, M. L.; Van Remmen, H.; Drake, J. A.; Yang, H.; Guo, Z. M.; Kewitt, K.; Walter, C. A.; Richardson, A. Does oxidative damage to DNA increase with age? *Proc Natl Acad Sci U S A* **98:**10469-10474; 2001.

[22] Mikkelsen, L.; Bialkowski, K.; Risom, L.; Lohr, M.; Loft, S.; Moller, P. Aging and defense against generation of 8-oxo-7,8-dihydro-2'-deoxyguanosine in DNA. *Free Radic Biol Med* **47:**608-615; 2009.

[23] Moller, P.; Lohr, M.; Folkmann, J. K.; Mikkelsen, L.; Loft, S. Aging and oxidatively damaged nuclear DNA in animal organs. *Free Radic Biol Med* **48:**1275-1285; 2010.

[24] Dolle, M. E.; Snyder, W. K.; Dunson, D. B.; Vijg, J. Mutational fingerprints of aging. *Nucleic Acids Res* **30:**545-549; 2002.

[25] Brown, D. I.; Griendling, K. K. Nox proteins in signal transduction. *Free Radic Biol Med* **47:**1239-1253; 2009.

[26] Loft, S.; Poulsen, H. E. Cancer risk and oxidative DNA damage in man. *J Mol Med* **74:**297-312; 1996.

[27] Cooke, M. S.; Evans, M. D.; Dizdaroglu, M.; Lunec, J. Oxidative DNA damage: mechanisms, mutation, and disease. *FASEB J* **17:**1195-1214; 2003.

[28] Kasai, H.; Nishimura, S. Hydroxylation of guanine in nucleosides and DNA at the C-8 position by heated glucose and oxygen radical-forming agents. *Environ Health Perspect* **67:**111-116; 1986.

[29] Cadet, J.; Douki, T.; Ravanat, J. L. Oxidatively generated damage to the guanine moiety of DNA: mechanistic aspects and formation in cells. *Acc Chem Res* **41:**1075-1083; 2008.

[30] Bergeron, F.; Auvre, F.; Radicella, J. P.; Ravanat, J. L. HO* radicals induce an unexpected high proportion of tandem base lesions refractory to repair by DNA glycosylases. *Proc Natl Acad Sci U S A* **107:**5528-5533; 2010.

[31] Cadet, J.; Douki, T.; Ravanat, J. L. Oxidatively generated base damage to cellular DNA. *Free Radic Biol Med*; 2010.

[32] Joenje, H. Genetic toxicology of oxygen. *Mutat Res* **219:**193-208; 1989.

[33] Grollman, A. P.; Moriya, M. Mutagenesis by 8-oxoguanine: an enemy within. *Trends Genet* **9:**246-249; 1993.

[34] Singh, R.; Farmer, P. B. Liquid chromatography-electrospray ionization-mass spectrometry: the future of DNA adduct detection. *Carcinogenesis* **27:**178-196; 2006.

[35] Collins, A.; Cadet, J.; Epe, B.; Gedik, C. Problems in the measurement of 8-oxoguanine in human DNA. Report of a workshop, DNA oxidation, held in Aberdeen, UK, 19-21 January, 1997. *Carcinogenesis* **18:**1833-1836; 1997.

[36] Rodriguez, H.; Jurado, J.; Laval, J.; Dizdaroglu, M. Comparison of the levels of 8-hydroxyguanine in DNA as measured by gas chromatography mass spectrometry following hydrolysis of DNA by Escherichia coli Fpg protein or formic acid. *Nucleic Acids Res* **28:**E75; 2000.

[37] Ravanat, J. L.; Douki, T.; Duez, P.; Gremaud, E.; Herbert, K.; Hofer, T.; Lasserre, L.; Saint-Pierre, C.; Favier, A.; Cadet, J. Cellular background level of 8-oxo-7,8-dihydro-2'-deoxyguanosine: an isotope based method to evaluate artefactual oxidation of DNA during its extraction and subsequent work-up. *Carcinogenesis* **23:**1911-1918; 2002.

[38] ESCODD. Measurement of DNA oxidation in human cells by chromatographic and enzymic methods. *Free Radic Biol Med* **34:**1089-1099; 2003.

[39] Singh, R.; McEwan, M.; Lamb, J. H.; Santella, R. M.; Farmer, P. B. An improved liquid chromatography/tandem mass spectrometry method for the determination of 8-oxo-7,8-dihydro-2'-deoxyguanosine in DNA samples using immunoaffinity column purification. *Rapid Commun Mass Spectrom* **17:**126-134; 2003.

[40] Gedik, C. M.; Collins, A. Establishing the background level of base oxidation in human lymphocyte DNA: results of an interlaboratory validation study. *FASEB J* **19:**82-84; 2005.

[41] Roberts, D. W.; Churchwell, M. I.; Beland, F. A.; Fang, J. L.; Doerge, D. R. Quantitative analysis of etheno-2'-deoxycytidine DNA adducts using on-line immunoaffinity chromatography coupled with LC/ES-MS/MS detection. *Anal Chem* **73:**303-309; 2001.

[42] Koc, H.; Swenberg, J. A. Applications of mass spectrometry for quantitation of DNA adducts. *J Chromatogr B Analyt Technol Biomed Life Sci* **778:**323-343; 2002.

[43] Chao, M. R.; Yen, C. C.; Hu, C. W. Prevention of artifactual oxidation in determination of cellular 8-oxo-7,8-dihydro-2'-deoxyguanosine by isotope-dilution LC-MS/MS with automated solid-phase extraction. *Free Radic Biol Med* **44:**464-473; 2008.

[44] Gnana Oli, R.; Lutz, U.; Stopper, H.; Schupp, N.; Lutz, W. K. Optimization of 8-oxodG analysis of DNA from rat liver and cultured cells by control of artifactual contributions during DNA isolation and LC-tandem mass spectrometry. *Second Copenhagen Workshop on DNA Oxidation: Measurement and Meaning of DNA Oxidation*; 2009.

[45] Loft, S.; Hogh Danielsen, P.; Mikkelsen, L.; Risom, L.; Forchhammer, L.; Moller, P. Biomarkers of oxidative damage to DNA and repair. *Biochem Soc Trans* **36:**1071-1076; 2008.

[46] Cooke, M. S.; Henderson, P. T.; Evans, M. D. Sources of extracellular, oxidatively-modified DNA lesions: implications for their measurement in urine. *J Clin Biochem Nutr* **45:**255-270; 2009.

[47] Cooke, M. S.; Olinski, R.; Loft, S. Measurement and meaning of oxidatively modified DNA lesions in urine. *Cancer Epidemiol Biomarkers Prev* **17:**3-14; 2008.

[48] Monostori, P.; Wittmann, G.; Karg, E.; Turi, S. Determination of glutathione and glutathione disulfide in biological samples: an in-depth review. *Journal of chromatography. B, Analytical technologies in the biomedical and life sciences* **877:**3331-3346; 2009.

[49] Blair, I. A. Endogenous glutathione adducts. *Curr Drug Metab* **7:**853-872; 2006.

[50] Griffith, O. W. Biologic and pharmacologic regulation of mammalian glutathione synthesis. *Free radical biology & medicine* **27:**922-935; 1999.

[51] Griffith, O. W.; Mulcahy, R. T. The enzymes of glutathione synthesis: gamma-glutamylcysteine synthetase. *Adv Enzymol Relat Areas Mol Biol* **73:**209-267, xii; 1999.

[52] Wu, G.; Fang, Y. Z.; Yang, S.; Lupton, J. R.; Turner, N. D. Glutathione metabolism and its implications for health. *J Nutr* **134:**489-492; 2004.

[53] Spickett, C. M.; Wiswedel, I.; Siems, W.; Zarkovic, K.; Zarkovic, N. Advances in methods for the determination of biologically relevant lipid peroxidation products. *Free Radic Res* **44:**1172-1202; 2010.

[54] Montuschi, P.; Barnes, P. J.; Roberts, L. J., 2nd. Isoprostanes: markers and mediators of oxidative stress. *FASEB J* **18:**1791-1800; 2004.

[55] Comporti, M.; Signorini, C.; Arezzini, B.; Vecchio, D.; Monaco, B.; Gardi, C. F2-isoprostanes are not just markers of oxidative stress. *Free radical biology & medicine* **44:**247-256; 2008.

[56] Kadiiska, M. B.; Gladen, B. C.; Baird, D. D.; Germolec, D.; Graham, L. B.; Parker, C. E.; Nyska, A.; Wachsman, J. T.; Ames, B. N.; Basu, S.; Brot, N.; Fitzgerald, G. A.; Floyd, R. A.; George, M.; Heinecke, J. W.; Hatch, G. E.; Hensley, K.; Lawson, J. A.; Marnett, L. J.; Morrow, J. D.; Murray, D. M.; Plastaras, J.; Roberts, L. J., 2nd; Rokach, J.; Shigenaga, M. K.; Sohal, R. S.; Sun, J.; Tice, R. R.; Van Thiel, D. H.; Wellner, D.; Walter, P. B.; Tomer, K. B.; Mason, R. P.; Barrett, J. C. Biomarkers of oxidative stress study II: are oxidation products of lipids, proteins, and DNA markers of CCl4 poisoning? *Free radical biology & medicine* **38:**698-710; 2005.

[57] Hiraku, Y. Formation of 8-nitroguanine, a nitrative DNA lesion, in inflammation-related carcinogenesis and its significance. *Environ Health Prev Med*; 2009.

[58] Agnihotri, N.; Mishra, P. C. Formation of 8-nitroguanine due to reaction between guanyl radical and nitrogen dioxide: catalytic role of hydration. *J Phys Chem B* **114:**7391-7404; 2010.

[59] Tjan, H. L.; Tobias, G. J.; Levin, R.; Hopper, J., Jr. Creatinine clearance in clinical medicine. *Calif Med* **98:**121-128; 1963.

[60] Teichert, F.; Verschoyle, R. D.; Greaves, P.; Thorpe, J. F.; Mellon, J. K.; Steward, W. P.; Farmer, P. B.; Gescher, A. J.; Singh, R. Determination of 8-oxo-2'-deoxyguanosine and creatinine in murine and human urine by liquid

chromatography/tandem mass spectrometry: application to chemoprevention studies. *Rapid Commun Mass Spectrom* **23:**258-266; 2009.

[61] Garrido, A. M.; Griendling, K. K. NADPH oxidases and angiotensin II receptor signaling. *Mol Cell Endocrinol* **302:**148-158; 2009.

[62] Connell, J. M.; Davies, E. The new biology of aldosterone. *J Endocrinol* **186:**1-20; 2005.

[63] Marney, A. M.; Brown, N. J. Aldosterone and end-organ damage. *Clin Sci (Lond)* **113:**267-278; 2007.

[64] Schupp, N.; Queisser, N.; Wolf, M.; Kolkhof, P.; Barfacker, L.; Schafer, S.; Heidland, A.; Stopper, H. Aldosterone causes DNA strand breaks and chromosomal damage in renal cells, which are prevented by mineralocorticoid receptor antagonists. *Horm Metab Res* **42:**458-465; 2010.

[65] Queisser, N.; Fazeli, G.; Schupp, N. Superoxide anion and hydrogen peroxide-induced signaling and damage in angiotensin II and aldosterone action. *Biol Chem* **391:**1265-1279; 2010.

[66] Maron, D. J.; Fazio, S.; Linton, M. F. Current perspectives on statins. *Circulation* **101:**207-213; 2000.

[67] Schupp, N.; Schmid, U.; Heidland, A.; Stopper, H. Rosuvastatin protects against oxidative stress and DNA damage in vitro via upregulation of glutathione synthesis. *Atherosclerosis* **199:**278-287; 2008.

[68] Tian, X. Y.; Wong, W. T.; Xu, A.; Chen, Z. Y.; Lu, Y.; Liu, L. M.; Lee, V. W.; Lau, C. W.; Yao, X.; Huang, Y. Rosuvastatin Improves Endothelial Function of db/db Mice: Role of Angiotensin II Type 1 Receptors and Oxidative Stress. *British journal of pharmacology*; 2011.

[69] De Rijk, M. C.; Tzourio, C.; Breteler, M. M. B.; Dartigues, J. F.; Amaducci, L.; Lopez-Pousa, S.; Manubens-Bertran, J. M.; Alperovitch, A.; Rocca, W. A. Prevalence of parkinsonism and Parkinson's disease in Europe: The EUROPARKINSON collaborative study. *J. Neurol. Neurosurg. Psychiatry* **62:**10-15; 1997.

[70] Gerlach, M.; Double, K. L.; Youdim, M. B. H.; Riederer, P. Potential sources of increased iron in the substantia nigra of parkinsonian patients. *Journal of Neural Transmission-Supplement***:**133-142; 2006.

[71] Abou-Sleiman, P. M.; Muqit, M. M. K.; Wood, N. W. Expanding insights of mitochondrial dysfunction in Parkinson's disease. *Nature Reviews Neuroscience* **7:**207-219; 2006.

[72] Halliwell, B. Oxidative stress and neurodegeneration: where are we now? *Journal of Neurochemistry* **97:**1634-1658; 2006.

[73] McNaught, K. S. P.; Olanow, C. W. Protein aggregation in the pathogenesis of familial and sporadic Parkinson's disease. *Neurobiology of Aging* **27:**530-545; 2006.

[74] Gerlach, M.; Riederer, P.; Youdim, M. B. H. *Molecular mechanisms for neurodegeneration: Synergism between reactive oxygen species, calcium and excitotoxic amino acids.* Philadelphia: Lippincott-Raven; 1996.

[75] Mytilineou, C.; Han, S. K.; Cohen, G. Toxic and protective effects of L-dopa on mesencephalic cell cultures. *J Neurochem* **61:**1470-1478; 1993.

[76] Basma, A. N.; Morris, E. J.; Nicklas, W. J.; Geller, H. M. L-dopa cytotoxicity to PC12 cells in culture is via its autoxidation. *J Neurochem* **64:**825-832; 1995.

[77] Perry, T. L.; Yong, V. W.; Ito, M.; Foulks, J. G.; Wall, R. A.; Godin, D. V.; Clavier, R. M. Nigrostriatal dopaminergic neurons remain undamaged in rats given high doses of L-DOPA and carbidopa chronically. *J Neurochem* **43:**990-993; 1984.

[78] Zeng, B. Y.; Pearce, R. K.; MacKenzie, G. M.; Jenner, P. Chronic high dose L-dopa treatment does not alter the levels of dopamine D-1, D-2 or D-3 receptor in the striatum of normal monkeys: an autoradiographic study. *Journal of neural transmission* **108:**925-941; 2001.

[79] Quinn, N.; Parkes, D.; Janota, I.; Marsden, C. D. Preservation of the substantia nigra and locus coeruleus in a patient receiving levodopa (2 kg) plus decarboxylase inhibitor over a four-year period. *Mov Disord* **1:**65-68; 1986.

[80] Fahn, S.; Oakes, D.; Shoulson, I.; Kieburtz, K.; Rudolph, A.; Lang, A.; Olanow, C. W.; Tanner, C.; Marek, K. Levodopa and the progression of Parkinson's disease. *N Engl J Med* **351:**2498-2508; 2004.

[81] Alam, Z. I.; Jenner, A.; Daniel, S. E.; Lees, A. J.; Cairns, N.; Marsden, C. D.; Jenner, P.; Halliwell, B. Oxidative DNA damage in the parkinsonian brain: an apparent selective increase in 8-hydroxyguanine levels in substantia nigra. *J Neurochem* **69:**1196-1203; 1997.

[82] Nakabeppu, Y.; Tsuchimoto, D.; Yamaguchi, H.; Sakumi, K. Oxidative damage in nucleic acids and Parkinson's disease. *J Neurosci Res* **85:**919-934; 2007.

[83] Migliore, L.; Petrozzi, L.; Lucetti, C.; Gambaccini, G.; Bernardini, S.; Scarpato, R.; Trippi, F.; Barale, R.; Frenzilli, G.; Rodilla, V.; Bonuccelli, U. Oxidative damage and cytogenetic analysis in leukocytes of Parkinson's disease patients. *Neurology* **58:**1809-1815; 2002.

[84] Bonassi, S.; Norppa, H.; Ceppi, M.; Stromberg, U.; Vermeulen, R.; Znaor, A.; Cebulska-Wasilewska, A.; Fabianova, E.; Fucic, A.; Gundy, S.; Hansteen, I. L.; Knudsen, L. E.; Lazutka, J.; Rossner, P.; Sram, R. J.; Boffetta, P. Chromosomal aberration frequency in lymphocytes predicts the risk of cancer: results from a pooled cohort study of 22 358 subjects in 11 countries. *Carcinogenesis* **29:**1178-1183; 2008.

[85] Bonassi, S.; Znaor, A.; Ceppi, M.; Lando, C.; Chang, W. P.; Holland, N.; Kirsch-Volders, M.; Zeiger, E.; Ban, S.; Barale, R.; Bigatti, M. P.; Bolognesi, C.; Cebulska-Wasilewska, A.; Fabianova, E.; Fucic, A.; Hagmar, L.; Joksic, G.; Martelli, A.; Migliore, L.; Mirkova, E.; Scarfi, M. R.; Zijno, A.; Norppa, H.; Fenech, M. An increased micronucleus frequency in peripheral blood lymphocytes predicts the risk of cancer in humans. *Carcinogenesis* **28:**625-631; 2007.

[86] Burhans, W. C.; Weinberger, M. DNA replication stress, genome instability and aging. *Nucleic acids research* **35:**7545-7556; 2007.

[87] Myung, N. H.; Zhu, X.; Kruman, II; Castellani, R. J.; Petersen, R. B.; Siedlak, S. L.; Perry, G.; Smith, M. A.; Lee, H. G. Evidence of DNA damage in Alzheimer disease: phosphorylation of histone H2AX in astrocytes. *Age (Dordr)* **30:**209-215; 2008.

[88] Zawia, N. H.; Lahiri, D. K.; Cardozo-Pelaez, F. Epigenetics, oxidative stress, and Alzheimer disease. *Free radical biology & medicine* **46:**1241-1249; 2009.

[89] Cech, N. B.; Enke, C. G. Practical implications of some recent studies in electrospray ionization fundamentals. *Mass Spectrom Rev* **20:**362-387; 2001.

[90] Carlton, D. D., Jr.; Schug, K. A. A review on the interrogation of peptide-metal interactions using electrospray ionization-mass spectrometry. *Anal Chim Acta* **686:**19-39; 2011.

[91] Kitteringham, N. R.; Jenkins, R. E.; Lane, C. S.; Elliott, V. L.; Park, B. K. Multiple reaction monitoring for quantitative biomarker analysis in proteomics and metabolomics. *Journal of chromatography. B, Analytical technologies in the biomedical and life sciences* **877:**1229-1239; 2009.

[92] Kim, K.; Kim, Y. Preparing multiple-reaction monitoring for quantitative clinical proteomics. *Expert Rev Proteomics* **6:**225-229; 2009.

[93] Yocum, A. K.; Chinnaiyan, A. M. Current affairs in quantitative targeted proteomics: multiple reaction monitoring-mass spectrometry. *Brief Funct Genomic Proteomic* **8:**145-157; 2009.

[94] Pisitkun, T.; Hoffert, J. D.; Yu, M. J.; Knepper, M. A. Tandem mass spectrometry in physiology. *Physiology (Bethesda)* **22:**390-400; 2007.

[95] Liu, Q.; Cheng, L. I.; Yi, L.; Zhu, N.; Wood, A.; Changpriroa, C. M.; Ward, J. M.; Jackson, S. H. p47phox deficiency induces macrophage dysfunction resulting in progressive crystalline macrophage pneumonia. *Am J Pathol* **174:**153-163; 2009.

[96] Schupp, N.; Kolkhof, P.; Queisser, N.; Gartner, S.; Schmid, U.; Kretschmer, A.; Hartmann, E.; Oli, R. G.; Schafer, S.; Stopper, H. Mineralocorticoid receptor-mediated DNA damage in kidneys of DOCA-salt hypertensive rats. *The FASEB journal : official publication of the Federation of American Societies for Experimental Biology* **25:**968-978; 2011.

[97] Stopper, H.; Schinzel, R.; Sebekova, K.; Heidland, A. Genotoxicity of advanced glycation end products in mammalian cells. *Cancer letters* **190:**151-156; 2003.

[98] Harwood, D. T.; Kettle, A. J.; Winterbourn, C. C. Production of glutathione sulfonamide and dehydroglutathione from GSH by myeloperoxidase-derived oxidants and detection using a novel LC-MS/MS method. *Biochem J* **399:**161-168; 2006.

[99] Harwood, D. T.; Kettle, A. J.; Brennan, S.; Winterbourn, C. C. Simultaneous determination of reduced glutathione, glutathione disulphide and glutathione sulphonamide in cells and physiological fluids by isotope dilution liquid chromatography-tandem mass spectrometry. *J Chromatogr B Analyt Technol Biomed Life Sci* **877:**3393-3399; 2009.

[100] FDA. Guidance for Industry, Bioanalytical method validation. *http://www.fda.gov/cder/guidance/index.htm*; 2001.

[101] Cui, L.; Nithipatikom, K.; Campbell, W. B. Simultaneous analysis of angiotensin peptides by LC-MS and LC-MS/MS: metabolism by bovine adrenal endothelial cells. *Anal Biochem* **369:**27-33; 2007.

[102] Brink, A.; Lutz, U.; Volkel, W.; Lutz, W. K. Simultaneous determination of O6-methyl-2'-deoxyguanosine, 8-oxo-7,8-dihydro-2'-deoxyguanosine, and 1,N6-etheno-2'-deoxyadenosine in DNA using on-line sample preparation by HPLC column switching coupled to ESI-MS/MS. *J Chromatogr B Analyt Technol Biomed Life Sci* **830:**255-261; 2006.

[103] Benzie, I. F.; Strain, J. J. The ferric reducing ability of plasma (FRAP) as a measure of "antioxidant power": the FRAP assay. *Anal Biochem* **239:**70-76; 1996.

[104] Oli, R. G.; Fazeli, G.; Kuhn, W.; Walitza, S.; Gerlach, M.; Stopper, H. No increased chromosomal damage in L: -DOPA-treated patients with Parkinson's disease: a pilot study. *J Neural Transm*; 2010.

[105] Rasband, W. S. *ImageJ*; 1997-2008.

[106] Schmid, U.; Stopper, H.; Schweda, F.; Queisser, N.; Schupp, N. Angiotensin II induces DNA damage in the kidney. *Cancer Res* **68:**9239-9246; 2008.

[107] Schupp, N.; Schinzel, R.; Heidland, A.; Stopper, H. Genotoxicity of advanced glycation end products: involvement of oxidative stress and of angiotensin II type 1 receptors. *Ann N Y Acad Sci* **1043:**685-695; 2005.

[108] Schupp, N.; Kolkhof, P.; Queisser, N.; Gärtner, S.; Schmid, U.; Kretschmer, A.; Hartmann, E.; Oli, R. G.; Schäfer, S.; Stopper, H. Mineralocorticoid receptor-mediated DNA damage in kidneys of DOCA-salt rats. *FASEBJ (accepted)*; 2010.

[109] Schupp, N.; Schmid, U.; Rutkowski, P.; Lakner, U.; Kanase, N.; Heidland, A.; Stopper, H. Angiotensin II-induced genomic damage in renal cells can be prevented by angiotensin II type 1 receptor blockage or radical scavenging. *Am J Physiol Renal Physiol* **292:**F1427-1434; 2007.

[110] Giorgianni, F.; Cappiello, A.; Beranova-Giorgianni, S.; Palma, P.; Trufelli, H.; Desiderio, D. M. LC-MS/MS analysis of peptides with methanol as organic modifier: improved limits of detection. *Anal Chem* **76:**7028-7038; 2004.

[111] Evans, M. D.; Olinski, R.; Loft, S.; Cooke, M. S. Toward consensus in the analysis of urinary 8-oxo-7,8-dihydro-2'-deoxyguanosine as a noninvasive biomarker of oxidative stress. *FASEB J* **24:**1249-1260; 2010.

[112] Morrow, J. D.; Hill, K. E.; Burk, R. F.; Nammour, T. M.; Badr, K. F.; Roberts, L. J., 2nd. A series of prostaglandin F2-like compounds are produced in vivo in humans by a non-cyclooxygenase, free radical-catalyzed mechanism. *Proc Natl Acad Sci U S A* **87:**9383-9387; 1990.

[113] Teng, Y. H.; Wang, C. W.; Liao, Y. T.; Yang, M. W.; Liu, T. Y. Quantification of urinary 8-iso-prostaglandin F2alpha using liquid chromatography-tandem mass spectrometry during cardiac valve surgery. *J Clin Lab Anal* **24:**237-245; 2010.

[114] Wang, C. J.; Yang, N. H.; Liou, S. H.; Lee, H. L. Fast quantification of the exhaled breath condensate of oxidative stress 8-iso-prostaglandin F2alpha using on-line solid-phase extraction coupled with liquid chromatography/electrospray ionization mass spectrometry. *Talanta* **82:**1434-1438; 2010.

[115] Benigni, A.; Cassis, P.; Remuzzi, G. Angiotensin II revisited: new roles in inflammation, immunology and aging. *EMBO Mol Med* **2:**247-257; 2010.

[116] Queisser, N.; Oteiza, P. I.; Stopper, H.; Oli, R. G.; Schupp, N. Aldosterone induces oxidative stress, oxidative DNA damage and NF-κBactivation in kidney tubule cells. *J. Mol. Carcinogenesis (accepted)*; 2010.

[117] McLafferty, F. W. Tandem mass spectrometry. *Science* **214:**280-287; 1981.

[118] Fenn, J. B.; Mann, M.; Meng, C. K.; Wong, S. F.; Whitehouse, C. M. Electrospray ionization for mass spectrometry of large biomolecules. *Science* **246:**64-71; 1989.

[119] Iwasaki, Y.; Saito, Y.; Nakano, Y.; Mochizuki, K.; Sakata, O.; Ito, R.; Saito, K.; Nakazawa, H. Chromatographic and mass spectrometric analysis of glutathione in biological samples. *J Chromatogr B Analyt Technol Biomed Life Sci* **877:**3309-3317; 2009.

[120] Loft, S.; Vistisen, K.; Ewertz, M.; Tjonneland, A.; Overvad, K.; Poulsen, H. E. Oxidative DNA damage estimated by 8-hydroxydeoxyguanosine excretion in humans: influence of smoking, gender and body mass index. *Carcinogenesis* **13:**2241-2247; 1992.

[121] Yamamoto, T.; Hosokawa, K.; Tamura, T.; Kanno, H.; Urabe, M.; Honjo, H. Urinary 8-hydroxy-2'-deoxyguanosine (8-OHdG) levels in women with or without gynecologic cancer. *J Obstet Gynaecol Res* **22:**359-363; 1996.

[122] Loft, S.; Poulsen, H. E.; Vistisen, K.; Knudsen, L. E. Increased urinary excretion of 8-oxo-2'-deoxyguanosine, a biomarker of oxidative DNA damage, in urban bus drivers. *Mutat Res* **441:**11-19; 1999.

[123] Matsumoto, Y.; Ogawa, Y.; Yoshida, R.; Shimamori, A.; Kasai, H.; Ohta, H. The stability of the oxidative stress marker, urinary 8-hydroxy-2'-deoxyguanosine (8-OHdG), when stored at room temperature. *J Occup Health* **50:**366-372; 2008.

[124] Thanan, R.; Murata, M.; Pinlaor, S.; Sithithaworn, P.; Khuntikeo, N.; Tangkanakul, W.; Hiraku, Y.; Oikawa, S.; Yongvanit, P.; Kawanishi, S. Urinary 8-oxo-7,8-dihydro-2'-deoxyguanosine in patients with parasite infection and effect of antiparasitic drug in relation to cholangiocarcinogenesis. *Cancer Epidemiol Biomarkers Prev* **17:**518-524; 2008.

[125] Lee, K. F.; Chung, W. Y.; Benzie, I. F. Urine 8-oxo-7,8-dihydro-2'-deoxyguanosine (8-oxodG), a specific marker of oxidative stress, using direct, isocratic LC-MS/MS: Method evaluation and application in study of biological variation in healthy adults. *Clin Chim Acta* **411:**416-422; 2010.

[126] Garratt, L. W.; Mistry, V.; Singh, R.; Sandhu, J. K.; Sheil, B.; Cooke, M. S.; Sly, P. D. Interpretation of urinary 8-oxo-7,8-dihydro-2'-deoxyguanosine is adversely affected by methodological inaccuracies when using a commercial ELISA. *Free Radic Biol Med* **48:**1460-1464; 2010.

[127] Montuschi, P.; Barnes, P.; Roberts, L. J., 2nd. Insights into oxidative stress: the isoprostanes. *Curr Med Chem* **14:**703-717; 2007.

[128] Sircar, D.; Subbaiah, P. V. Isoprostane measurement in plasma and urine by liquid chromatography-mass spectrometry with one-step sample preparation. *Clin Chem* **53:**251-258; 2007.

[129] Dalaveris, E.; Kerenidi, T.; Katsabeki-Katsafli, A.; Kiropoulos, T.; Tanou, K.; Gourgoulianis, K. I.; Kostikas, K. VEGF, TNF-alpha and 8-isoprostane levels in exhaled breath condensate and serum of patients with lung cancer. *Lung Cancer* **64:**219-225; 2009.

[130] Roberts, L. J., 2nd; Moore, K. P.; Zackert, W. E.; Oates, J. A.; Morrow, J. D. Identification of the major urinary metabolite of the F2-isoprostane 8-iso-prostaglandin F2alpha in humans. *J Biol Chem* **271:**20617-20620; 1996.

[131] Zhang, B.; Saku, K. Control of matrix effects in the analysis of urinary F2-isoprostanes using novel multidimensional solid-phase extraction and LC-MS/MS. *J Lipid Res* **48:**733-744; 2007.

[132] Tsikas, D.; Schwedhelm, E.; Fauler, J.; Gutzki, F. M.; Mayatepek, E.; Frolich, J. C. Specific and rapid quantification of 8-iso-prostaglandin F2alpha in urine of healthy humans and patients with Zellweger syndrome by gas chromatography-tandem mass spectrometry. *J Chromatogr B Biomed Sci Appl* **716:**7-17; 1998.

[133] Tsikas, D. Application of gas chromatography-mass spectrometry and gas chromatography-tandem mass spectrometry to assess in vivo synthesis of prostaglandins, thromboxane, leukotrienes, isoprostanes and related compounds in humans. *J Chromatogr B Biomed Sci Appl* **717:**201-245; 1998.

[134] Carpenter, C. T.; Price, P. V.; Christman, B. W. Exhaled breath condensate isoprostanes are elevated in patients with acute lung injury or ARDS. *Chest* **114:**1653-1659; 1998.

[135] Syslova, K.; Kacer, P.; Kuzma, M.; Klusackova, P.; Fenclova, Z.; Lebedova, J.; Pelclova, D. Determination of 8-iso-prostaglandin F(2alpha) in exhaled breath condensate using combination of immunoseparation and LC-ESI-MS/MS. *J Chromatogr B Analyt Technol Biomed Life Sci* **867:**8-14; 2008.

[136] Montuschi, P. LC/MS/MS analysis of leukotriene B4 and other eicosanoids in exhaled breath condensate for assessing lung inflammation. *J Chromatogr B Analyt Technol Biomed Life Sci* **877:**1272-1280; 2009.

[137] Iwasaki, Y.; Hoshi, M.; Ito, R.; Saito, K.; Nakazawa, H. Analysis of glutathione and glutathione disulfide in human saliva using hydrophilic interaction chromatography with mass spectrometry. *J Chromatogr B Analyt Technol Biomed Life Sci* **839:**74-79; 2006.

[138] Mills, B. J.; Weiss, M. M.; Lang, C. A.; Liu, M. C.; Ziegler, C. Blood glutathione and cysteine changes in cardiovascular disease. *J Lab Clin Med* **135:**396-401; 2000.

[139] Lang, C. A.; Mills, B. J.; Mastropaolo, W.; Liu, M. C. Blood glutathione decreases in chronic diseases. *J Lab Clin Med* **135:**402-405; 2000.

[140] Papp, A.; Nemeth, I.; Karg, E.; Papp, E. Glutathione status in retinopathy of prematurity. *Free Radic Biol Med* **27:**738-743; 1999.

[141] Navarro, J.; Obrador, E.; Carretero, J.; Petschen, I.; Avino, J.; Perez, P.; Estrela, J. M. Changes in glutathione status and the antioxidant system in blood and in cancer cells associate with tumour growth in vivo. *Free Radic Biol Med* **26:**410-418; 1999.

[142] Samiec, P. S.; Drews-Botsch, C.; Flagg, E. W.; Kurtz, J. C.; Sternberg, P., Jr.; Reed, R. L.; Jones, D. P. Glutathione in human plasma: decline in association with aging, age-related macular degeneration, and diabetes. *Free Radic Biol Med* **24:**699-704; 1998.

[143] Navarro, J.; Obrador, E.; Pellicer, J. A.; Aseni, M.; Vina, J.; Estrela, J. M. Blood glutathione as an index of radiation-induced oxidative stress in mice and humans. *Free Radic Biol Med* **22:**1203-1209; 1997.

[144] Delmas-Beauvieux, M. C.; Peuchant, E.; Couchouron, A.; Constans, J.; Sergeant, C.; Simonoff, M.; Pellegrin, J. L.; Leng, B.; Conri, C.; Clerc, M. The enzymatic antioxidant system in blood and glutathione status in human immunodeficiency virus (HIV)-infected patients: effects of supplementation with selenium or beta-carotene. *Am J Clin Nutr* **64:**101-107; 1996.

[145] Sastre, J.; Asensi, M.; Gasco, E.; Pallardo, F. V.; Ferrero, J. A.; Furukawa, T.; Vina, J. Exhaustive physical exercise causes oxidation of glutathione status in blood: prevention by antioxidant administration. *Am J Physiol* **263:**R992-995; 1992.

[146] Gohil, K.; Viguie, C.; Stanley, W. C.; Brooks, G. A.; Packer, L. Blood glutathione oxidation during human exercise. *J Appl Physiol* **64:**115-119; 1988.

[147] Rossi, R.; Milzani, A.; Dalle-Donne, I.; Giustarini, D.; Lusini, L.; Colombo, R.; Di Simplicio, P. Blood glutathione disulfide: in vivo factor or in vitro artifact? *Clin Chem* **48:**742-753; 2002.

[148] Kand'ar, R.; Zakova, P.; Lotkova, H.; Kucera, O.; Cervinkova, Z. Determination of reduced and oxidized glutathione in biological samples using liquid chromatography with fluorimetric detection. *J Pharm Biomed Anal* **43:**1382-1387; 2007.

[149] Rellan-Alvarez, R.; Hernandez, L. E.; Abadia, J.; Alvarez-Fernandez, A. Direct and simultaneous determination of reduced and oxidized glutathione and homoglutathione by liquid chromatography-electrospray/mass spectrometry in plant tissue extracts. *Anal Biochem* **356:**254-264; 2006.

[150] Zhang, F.; Bartels, M. J.; Geter, D. R.; Jeong, Y. C.; Schisler, M. R.; Wood, A. J.; Kan, L.; Gollapudi, B. B. Quantitation of glutathione by liquid chromatography/positive electrospray ionization tandem mass spectrometry. *Rapid Commun Mass Spectrom* **22:**3608-3614; 2008.

[151] Horvati, K.; Bosze, S.; Hudecz, F.; Medzihradszky-Schweiger, H. A simple method for monitoring the cysteine content in synthetic peptides. *J Pept Sci* **14:**838-844; 2008.

[152] De Silva, P. E.; Husain, A.; Smeby, R. R.; Khairallah, P. A. Measurement of immunoreactive angiotensin peptides in rat tissues: some pitfalls in angiotensin II analysis. *Anal Biochem* **174:**80-87; 1988.

[153] Kohara, K.; Tabuchi, Y.; Senanayake, P.; Brosnihan, K. B.; Ferrario, C. M. Reassessment of plasma angiotensins measurement: effects of protease inhibitors and sample handling procedures. *Peptides* **12:**1135-1141; 1991.

[154] Kohara, K.; Brosnihan, K. B.; Chappell, M. C.; Khosla, M. C.; Ferrario, C. M. Angiotensin-(1-7). A member of circulating angiotensin peptides. *Hypertension* **17:**131-138; 1991.

[155] Lanckmans, K.; Stragier, B.; Sarre, S.; Smolders, I.; Michotte, Y. Nano-LC-MS/MS for the monitoring of angiotensin IV in rat brain microdialysates: limitations and possibilities. *J Sep Sci* **30:**2217-2224; 2007.

[156] Lanckmans, K.; Sarre, S.; Smolders, I.; Michotte, Y. Use of a structural analogue versus a stable isotope labeled internal standard for the quantification of angiotensin IV in rat brain dialysates using nano-liquid chromatography/tandem mass spectrometry. *Rapid Commun Mass Spectrom* **21:**1187-1195; 2007.

[157] Lortie, M.; Bark, S.; Blantz, R.; Hook, V. Detecting low-abundance vasoactive peptides in plasma: progress toward absolute quantitation using nano liquid chromatography-mass spectrometry. *Anal Biochem* **394:**164-170; 2009.

[158] Bayard, F.; Beitins, I. Z.; Kowarski, A.; Migeon, C. J. Measurement of plasma aldosterone by radioimmunoassay. *J Clin Endocrinol Metab* **31:**1-6; 1970.

[159] Bayard, F.; Beitins, I. Z.; Kowarski, A.; Migeon, C. J. Measurement of aldosterone secretion rate by radio-immunoassay. *J Clin Endocrinol Metab* **31:**507-511; 1970.

[160] Stabler, T. V.; Siegel, A. L. Chemiluminescence immunoassay of aldosterone in serum. *Clin Chem* **37:**1987-1989; 1991.

[161] Schirpenbach, C.; Seiler, L.; Maser-Gluth, C.; Beuschlein, F.; Reincke, M.; Bidlingmaier, M. Automated chemiluminescence-immunoassay for aldosterone during dynamic testing: comparison to radioimmunoassays with and without extraction steps. *Clin Chem* **52:**1749-1755; 2006.

[162] Siekmann, L. Determination of steroid hormones by the use of isotope dilution--mass spectrometry: a definitive method in clinical chemistry. *J Steroid Biochem* **11:**117-123; 1979.

[163] Breuer, H.; Siekmann, L. Mass fragmentography as reference method in clinical steroid assay. *J Steroid Biochem* **6:**685-688; 1975.

[164] Stockl, D.; Reinauer, H.; Thienpont, L. M.; De Leenheer, A. P. Determination of aldosterone in human serum by isotope dilution gas chromatography/mass spectrometry using a new heptafluorobutyryl derivative. *Biol Mass Spectrom* **20:**657-664; 1991.

[165] Fredline, V. F.; Taylor, P. J.; Dodds, H. M.; Johnson, A. G. A reference method for the analysis of aldosterone in blood by high-performance liquid chromatography-atmospheric pressure chemical ionization-tandem mass spectrometry. *Anal Biochem* **252:**308-313; 1997.

[166] Guo, T.; Taylor, R. L.; Singh, R. J.; Soldin, S. J. Simultaneous determination of 12 steroids by isotope dilution liquid chromatography-photospray ionization tandem mass spectrometry. *Clin Chim Acta* **372:**76-82; 2006.

[167] Taylor, P. J.; Cooper, D. P.; Gordon, R. D.; Stowasser, M. Measurement of aldosterone in human plasma by semiautomated HPLC-tandem mass spectrometry. *Clin Chem* **55:**1155-1162; 2009.

[168] Turpeinen, U.; Hamalainen, E.; Stenman, U. H. Determination of aldosterone in serum by liquid chromatography-tandem mass spectrometry. *J Chromatogr B Analyt Technol Biomed Life Sci* **862:**113-118; 2008.

[169] Martin, J. E.; Sheaff, M. T. Renal ageing. *J Pathol* **211:**198-205; 2007.

[170] Griendling, K. K.; Minieri, C. A.; Ollerenshaw, J. D.; Alexander, R. W. Angiotensin II stimulates NADH and NADPH oxidase activity in cultured vascular smooth muscle cells. *Circ Res* **74:**1141-1148; 1994.

[171] Cathcart, R.; Schwiers, E.; Saul, R. L.; Ames, B. N. Thymine glycol and thymidine glycol in human and rat urine: a possible assay for oxidative DNA damage. *Proc Natl Acad Sci U S A* **81:**5633-5637; 1984.

[172] Fraga, C. G.; Shigenaga, M. K.; Park, J. W.; Degan, P.; Ames, B. N. Oxidative damage to DNA during aging: 8-hydroxy-2'-deoxyguanosine in rat organ DNA and urine. *Proc Natl Acad Sci U S A* **87:**4533-4537; 1990.

[173] Park, E. M.; Shigenaga, M. K.; Degan, P.; Korn, T. S.; Kitzler, J. W.; Wehr, C. M.; Kolachana, P.; Ames, B. N. Assay of excised oxidative DNA lesions: isolation of 8-oxoguanine and its nucleoside derivatives from biological fluids with a monoclonal antibody column. *Proc Natl Acad Sci U S A* **89:**3375-3379; 1992.

[174] Gackowski, D.; Rozalski, R.; Roszkowski, K.; Jawien, A.; Foksinski, M.; Olinski, R. 8-Oxo-7,8-dihydroguanine and 8-oxo-7,8-dihydro-2'-deoxyguanosine levels in human urine do not depend on diet. *Free Radic Res* **35:**825-832; 2001.

[175] Cooke, M. S.; Evans, M. D.; Dove, R.; Rozalski, R.; Gackowski, D.; Siomek, A.; Lunec, J.; Olinski, R. DNA repair is responsible for the presence of oxidatively damaged DNA lesions in urine. *Mutat Res* **574:**58-66; 2005.

[176] Cooke, M. S.; Lunec, J.; Evans, M. D. Progress in the analysis of urinary oxidative DNA damage. *Free Radic Biol Med* **33:**1601-1614; 2002.

[177] Djuric, Z.; Potter, D. W.; Taffe, B. G.; Strasburg, G. M. Comparison of iron-catalyzed DNA and lipid oxidation. *J Biochem Mol Toxicol* **15:**114-119; 2001.

[178] Groban, L.; Pailes, N. A.; Bennett, C. D.; Carter, C. S.; Chappell, M. C.; Kitzman, D. W.; Sonntag, W. E. Growth hormone replacement attenuates diastolic dysfunction and cardiac angiotensin II expression in senescent rats. *J Gerontol A Biol Sci Med Sci* **61:**28-35; 2006.

[179] Wang, M.; Takagi, G.; Asai, K.; Resuello, R. G.; Natividad, F. F.; Vatner, D. E.; Vatner, S. F.; Lakatta, E. G. Aging increases aortic MMP-2 activity and angiotensin II in nonhuman primates. *Hypertension* **41:**1308-1316; 2003.

[180] Thompson, M. M.; Oyama, T. T.; Kelly, F. J.; Kennefick, T. M.; Anderson, S. Activity and responsiveness of the renin-angiotensin system in the aging rat. *Am J Physiol Regul Integr Comp Physiol* **279:**R1787-1794; 2000.

[181] Min, L. J.; Mogi, M.; Iwai, M.; Horiuchi, M. Signaling mechanisms of angiotensin II in regulating vascular senescence. *Ageing Res Rev* **8:**113-121; 2009.

[182] Benigni, A.; Corna, D.; Zoja, C.; Sonzogni, A.; Latini, R.; Salio, M.; Conti, S.; Rottoli, D.; Longaretti, L.; Cassis, P.; Morigi, M.; Coffman, T. M.; Remuzzi, G. Disruption of the Ang II type 1 receptor promotes longevity in mice. *J Clin Invest* **119:**524-530; 2009.

[183] de Cavanagh, E. M.; Inserra, F.; Ferder, M.; Ferder, L. From mitochondria to disease: role of the renin-angiotensin system. *Am J Nephrol* **27:**545-553; 2007.

[184] Modlinger, P.; Chabrashvili, T.; Gill, P. S.; Mendonca, M.; Harrison, D. G.; Griendling, K. K.; Li, M.; Raggio, J.; Wellstein, A.; Chen, Y.; Welch, W. J.; Wilcox, C. S. RNA silencing in vivo reveals role of p22phox in rat angiotensin slow pressor response. *Hypertension* **47:**238-244; 2006.

[185] Schmid, U.; Stopper, H.; Heidland, A.; Schupp, N. Benfotiamine exhibits direct antioxidative capacity and prevents induction of DNA damage in vitro. *Diabetes Metab Res Rev* **24:**371-377; 2008.

[186] Herbert, K. E.; Mistry, Y.; Hastings, R.; Poolman, T.; Niklason, L.; Williams, B. Angiotensin II-mediated oxidative DNA damage accelerates cellular senescence in cultured human vascular smooth muscle cells via telomere-dependent and independent pathways. *Circ Res* **102:**201-208; 2008.

[187] Liao, J. K.; Laufs, U. Pleiotropic effects of statins. *Annu Rev Pharmacol Toxicol* **45:**89-118; 2005.

[188] Christ, M.; Bauersachs, J.; Liebetrau, C.; Heck, M.; Gunther, A.; Wehling, M. Glucose increases endothelial-dependent superoxide formation in coronary arteries by NAD(P)H oxidase activation: attenuation by the 3-hydroxy-3-methylglutaryl coenzyme A reductase inhibitor atorvastatin. *Diabetes* **51:**2648-2652; 2002.

[189] Wassmann, S.; Laufs, U.; Baumer, A. T.; Muller, K.; Ahlbory, K.; Linz, W.; Itter, G.; Rosen, R.; Bohm, M.; Nickenig, G. HMG-CoA reductase inhibitors improve endothelial dysfunction in normocholesterolemic hypertension via reduced production of reactive oxygen species. *Hypertension* **37:**1450-1457; 2001.

[190] Ajith, T. A.; Riji, T.; Anu, V. In vitro anti-oxidant and DNA protective effects of the novel 3-hydroxy-3-methylglutaryl coenzyme A reductase inhibitor rosuvastatin. *Clinical and experimental pharmacology & physiology* **35:**625-629; 2008.

[191] Kang, B. Y.; Mehta, J. L. Rosuvastatin attenuates Ang II--mediated cardiomyocyte hypertrophy via inhibition of LOX-1. *J Cardiovasc Pharmacol Ther* **14:**283-291; 2009.

[192] Kasai, H.; Hayami, H.; Yamaizumi, Z.; SaitoH; Nishimura, S. Detection and identification of mutagens and carcinogens as their adducts with guanosine derivatives. *Nucleic acids research* **12:**2127-2136; 1984.

[193] Kasai, H.; Nishimura, S. Hydroxylation of deoxyguanosine at the C-8 position by ascorbic acid and other reducing agents. *Nucleic acids research* **12:**2137-2145; 1984.

[194] Buhmann, C.; Arlt, S.; Kontush, A.; Moller-Bertram, T.; Sperber, S.; Oechsner, M.; Stuerenburg, H. J.; Beisiegel, U. Plasma and CSF markers of oxidative stress are increased in Parkinson's disease and influenced by antiparkinsonian medication. *Neurobiol Dis* **15:**160-170; 2004.

[195] Vitte, J.; Michel, B. F.; Bongrand, P.; Gastaut, J. L. Oxidative stress level in circulating neutrophils is linked to neurodegenerative diseases. *J Clin Immunol* **24:**683-692; 2004.

[196] Le, W. D.; Jankovic, J.; Xie, W.; Appel, S. H. Antioxidant property of pramipexole independent of dopamine receptor activation in neuroprotection. *Journal of neural transmission* **107:**1165-1173; 2000.

[197] Fazeli, G.; Oli, R. G.; Schupp, N.; Stopper, H. The Role of the Dopamine Transporter in Dopamine-Induced DNA Damage. *Brain Pathol*; 2010.

[198] Cornetta, T.; Palma, S.; Aprile, I.; Padua, L.; Tonali, P.; Testa, A.; Cozzi, R. Levodopa therapy reduces DNA damage in peripheral blood cells of patients with Parkinson's disease. *Cell Biol Toxicol* **25:**321-330; 2009.

[199] Gaugitsch, H. W.; Prieschl, E. E.; Kalthoff, F.; Huber, N. E.; Baumruker, T. A novel transiently expressed, integral membrane protein linked to cell activation. Molecular cloning via the rapid degradation signal AUUUA. *The Journal of biological chemistry* **267:**11267-11273; 1992.

[200] Musso, N. R.; Brenci, S.; Setti, M.; Indiveri, F.; Lotti, G. Catecholamine content and in vitro catecholamine synthesis in peripheral human lymphocytes. *The Journal of clinical endocrinology and metabolism* **81:**3553-3557; 1996.

[201] Amenta, F.; Bronzetti, E.; Cantalamessa, F.; El-Assouad, D.; Felici, L.; Ricci, A.; Tayebati, S. K. Identification of dopamine plasma membrane and vesicular transporters in human peripheral blood lymphocytes. *Journal of neuroimmunology* **117:**133-142; 2001.

[202] Rajda, C.; Dibo, G.; Vecsei, L.; Bergquist, J. Increased dopamine content in lymphocytes from high-dose L-Dopa-treated Parkinson's disease patients. *Neuroimmunomodulation* **12:**81-84; 2005.

[203] Kostrzewa, R. M.; Kostrzewa, J. P.; Brus, R. Neuroprotective and neurotoxic roles of levodopa (L-DOPA) in neurodegenerative disorders relating to Parkinson's disease. *Amino Acids* **23:**57-63; 2002.

[204] Snyder, R. D.; Friedman, M. B. Enhancement of cytotoxicity and clastogenicity of l-DOPA and dopamine by manganese and copper. *Mutation research* **405:**1-8; 1998.

[205] Stopper, H.; Schupp, N.; Fazeli, G.; Dietel, B.; Queisser, N.; Walitza, S.; Gerlach, M. Genotoxicity of the neurotransmitter dopamine in vitro. *Toxicol In Vitro* **23:**640-646; 2009.

[206] McGregor, D. B.; Riach, C. G.; Brown, A.; Edwards, I.; Reynolds, D.; West, K.; Willington, S. Reactivity of catecholamines and related substances in the mouse lymphoma L5178Y cell assay for mutagens. *Environ Mol Mutagen* **11:**523-544; 1988.

[207] Fenech, M.; Neville, S.; Rinaldi, J. Sex is an important variable affecting spontaneous micronucleus frequency in cytokinesis-blocked lymphocytes. *Mutation research* **313:**203-207; 1994.

9 Acknowledgements

காலத்தி னாற்செய்த நன்றி சிறிதெனினும்
ஞாலத்தின் மாணப் பெரிது.

- திருவள்ளுவர்

A favour conferred in the time of need, though it be small (in itself),
is (in value) much larger than the world.

- Thiruvalluvar

Jean Baptiste Massieu, said *“Gratitude is the memory of the heart.”* My utmost gratitude goes to my mentor, Prof. Dr. Helga Stopper who accepted me as her PhD student. I greatly thank Prof. Stopper for guiding me always in the right direction, for her continuous encouragement, kindness, and most of all, for her patience. According to William Arthur Ward *"The mediocre teacher tells. The good teacher explains. The superior teacher demonstrates. The great teacher inspires."* Prof. Dr. Helga Stopper is the great teacher for me.

I am grateful to Dr. Nicole Schupp, who gave me healthy suggestions and discussions which provided great insight to my research. I express my immense gratitude to Dr. Schupp for timely corrections of all my abstracts and posters for various conferences.

My special thanks to the members of my advisory committee, PD Dr. Tcholpon Djuzenova and PD Dr. Alois Palmetshofer for their guidance and helpful discussions.

William Arthur Ward said *“Feeling gratitude and not expressing it is like wrapping a present and not giving it”.* I express my gratitude to Frau. Ursula Lutz, who introduced me the mass spectrometry technique by giving significant advice. A validation study on 8-oxodG analysis with Prof. Dr. Werner K. Lutz gave me an opportunity to learn more in the field of analysis of DNA lesions and made a good opening in the scientific field. I am thanking Prof. Lutz, very much forever, for all the immense help.

Henry Ward Beecher described, *"Gratitude is the fairest blossom which springs from the soul".* I warmly thank, Dr. Henning Hintzsche, for his friendly nature and timely help. I thank Henning for not only translating summary part (Zusammenfassung) of my thesis, also various applications for official purposes.

I would like to thank Nataly Bittner, for technical assistance in mass spectrometry, Simone Weissenberger and Miriam Kral for breeding p47phox-/- mice and also for helping in animal experiment together with Joana Sühlfleisch, Benjamin Weber and Marc Überschär. I thank Elisabeth Stein, Maria Scheurich and Thomas Büdel, for helping me in cell culture techniques. I also thank Dr. Gholamreza Fazeli for introducing me the comet assay.

I am most grateful to Dr. Nina Queisser and Nina Glaser for their friendliness and also introduced me the German cultural activities according to their local traditions. I also wish to thank Susanne Brand, Olga Schmal, Eman Maher-Sholkamy, Alexander Eckhardt for their nice cooperation.

I greatly express my gratitude to the GSLS, making me successful, not just as a graduate student but as a scientist.

I greatly thank the Indian Government for financial support for my PhD program. I also thank Gesellschaft für Umwelt-Mutationforschung e.V. (GUM), GSLS-Wuerzburg, GlaxoSmithKline Stiftung, for their travel awards.

My sincere thanks to Asst. Prof. Dr. Thangaraju Murugesan, Duke University Medical Center, USA, Asst. Prof. Dr. Baskaran Thyagarajan, University of Rochester Medical Center, USA and Dr. Lakshmanan Manikandan, Singapore for their continuous encouragement and guidance.

I am grateful to Mr and Mrs Kuttenkueller from Lengfeld, who stands by our side in time of need. I thank my parents and parents' in-law for their enormous support and I am happy to fulfill their desire. Last but not least, I thank my wife Swarna and my daughter Gemma for their moral supports.

Publications

1. Queisser. N, Oteiza. O. I, Stopper. H, **Rajaraman Gnana Oli**. Schupp. N, "*Aldosterone induces oxidative stress, oxidative DNA damage and NF-κBactivation in kidney tubule cells"* Mol.Carcinogenesis. **2011**, 50: 123-35.
2. Nicole Schupp, Peter Kolkhof, Nina Queisser, Sabine Gärtner, Ursula Schmid, Axel Kretschmer, Elke Hartmann, **Rajaraman Gnana Oli**, Stefan Schäfer, Helga Stopper, "*Mineralocorticoid receptor-mediated DNA damage in kidneys of DOCA-salt rats"* FASEB journal **2010,** 25(3):968-78.
3. Fazeli. G, **Rajaraman Gnana Oli**, Schupp. N, Stopper. H, "*The role of the dopamine transporter in dopamine-induced DNA damage"* Brain pathology. **2010** (doi: 10.1111/j.1750-3639.2010.00440.x.).
4. **Rajaraman Gnana Oli**, Fazeli G, Kuhn W, Walitza S, Gerlach M, Stopper H.; *"No increased chromosomal damage in L -DOPA-treated patients with Parkinson's disease: a pilot study".* J Neural Transm. **2010**, 117: 737- 746.
5. Walitza S, Kämpf K, **Rajaraman Gnana Oli**, Warnke A, Gerlach M, Stopper H., "*Prospective follow-up studies found no chromosomal mutagenicity of methylphenidate therapy in ADHD affected children".* Toxicol Lett. **2010**, 193(1):4-8.
6. Walitza S, Kämpf K, Artamonov N, Romanos M, **Rajaraman Gnana Oli**, Wirth S, Warnke A, Gerlach M, Stopper H. "*No elevated genomic damage in children and adolescents with attention deficit/hyperactivity disorder after methylphenidate therapy"*, Toxicol Lett. **2009**, 184(1):38-43.
7. **Rajaraman Gnana Oli**, Manikandan L, Swarna F. B, Manikandan P, Khosa R. L, "*Anti-inflammatory potential of Indigofera tinctoria in Rats"*, *Ind. J. Natural Products.* **2005** 21:12-15.
8. C. Selvam, Sanjay M. Jachak, **Rajaraman Gnana Oli**, Ramasamy Thilagavathi, Asit.K. Chakraborti, K.K. Bhutani, "*A new cyclooxygenase (COX) inhibitory pterocarpan from Indigofera aspalathoides: structure elucidation and determination of binding orientations in the active sites of the enzyme by molecular docking".* Tetrahedron Lett. **2004**, 45(22): 4311-4314.
9. **Rajaraman Gnana Oli** and Jachak S. M, "*Natural Products: An important Source for Anti-tubercular Drugs",CRIPS, 5*, 9-11, **2004**.

Presentations

Oral:

Rajaraman Gnana Oli, Schupp. N and Stopper. H, *"Critical role of the NADPH oxidase subunit p47phox in the formation of oxidative DNA damage"*, Analysis of free radicals, radical modifications and redox signaling, 18- 19, April, **2011**; Birmingham, UK. [Won the GlaxoSmithKline travel award]

Rajaraman Gnana Oli, Lutz U, Stopper H, Schupp N, Lutz W.K "*Optimization of 8-oxodGuo analysis of DNA from rat liver and cultured cells by control of artefactual contributions during DNA isolation and LC-tandem mass spectrometry "*Workshop on DNA Oxidation, 29 - 30 January **2009**, European Standards Committee on Oxidative DNA damage (ESCODD); Denmark.

Posters:

Rajaraman Gnana Oli, Schupp. N and Stopper. H, *"Critical role of the NADPH oxidase subunit p47phox in the formation of oxidative DNA damage"*, Analysis of free radicals and radical modifications and redox signalling, 18- 19, April, **2011**; Aston University, Birmingham, UK. [Won the GlaxoSmithKline travel award]

Rajaraman Gnana Oli, Schupp. N and Stopper. H, *"Critical role of the NADPH oxidase subunit p47phox in the formation of oxidative DNA damage"*, 17th Annual meeting of society of free radical biology and medicine" 17 - 21, November, **2010**; Orlando,FL, USA. [Won the poster award]

Rajaraman Gnana Oli, Schupp. N and Stopper. H, *"Critical role of the NADPH oxidase subunit p47phox in the formation of oxidative DNA damage"*, 26th Ernst Klenk Symposium in Molecular Medicine NOX Family NADPH Oxidases as Therapeutic Targets 04 - 06, November, **2010**; Koeln,Germany .

Rajaraman Gnana Oli, Schupp. N and Stopper. H. *"Rosuvastatin protects Angiotensin II induced oxidative stress and genomic damage"*, 10th International conference on environmental mutation, 20 - 25 August **2009**; Florence, Italy. [Won the GUM travel award]

Rajaraman Gnana Oli, Schupp. N and Stopper. H. *"Rosuvastatin protects from Angiotensin II induced DNA damage in LLC-PK1 cells"*, DGPT conference, 10 - 11 March **2009**; University of Mainz, Germany.

Rajaraman Gnana Oli, Schupp. N and Stopper. H. *"Rosuvastatin protects from Angiotensin II induced DNA damage in LLC-PK1 cells"*, 4th International symposium, Revolution Research, 26 - 27 March **2009**; students of the Graduate School of Life Sciences, University of Wuerzburg, Germany.

Rajaraman Gnana Oli, Lutz U, Stopper H, Schupp N, Lutz W.K "*Optimization of 8-oxodGuo analysis of DNA from rat liver and cultured cells by control of artefactual contributions during DNA isolation and LC-tandem mass spectrometry*

*"*Workshop on DNA Oxidation, 29 - 30 January **2009**, European Standards Committee on Oxidative DNA damage (ESCODD); Denmark.

Rajaraman Gnana Oli, Lutz. U, Schupp. N and Stopper. H. *"LC-MS/MS: A new technique for measuring oxidative DNA damage"*, International workshop on oxidative stress and genomic damage, 10th October **2008**; University of Wuerzburg, Germany.

Rajaraman Gnana Oli, Lutz. U, Schupp. N and Stopper. H. *"LC-MS/MS: A new technique for measuring oxidative DNA damage"*, The Graduate School of Life Sciences poster day, 5th September **2008**; University of Wuerzburg, Germany.

Patent

C. Selvam, Sanjay M. Jachak, **Rajaraman Gnana Oli**., K. K. Bhutani. 'New anti-inflammatory compounds from Indigofera aspalathoides', Indian WTO Application No. 1489/DEL/2003 dated 28-11-2003.

11 Affidavit

Affidavit

I hereby declare that my thesis entitled “Oxidative Stress: Role in genomic damage and disease" is the result of my own work. I did not receive any help or support from commercial consultants. All sources and / or materials applied are listed and specified in the thesis.

Furthermore, I verify that this thesis has not yet been submitted as part of another examination process neither in identical nor in similar form.

Würzburg……

Date Signature

Eidesstattliche Erklärung

Hiermit erkläre ich an Eides statt, die Dissertation “Oxidativer Stress: Bedeutung für genomische Schäden und Krankheit ” eigenständig, d.h. insbesondere selbstständig und ohne Hilfe eines kommerziellen Promotionsberaters, angefertigt und keine anderen als die von mir angegebenen Quellen und Hilfsmittel verwendet zu haben.
Ich erkläre außerdem, dass die Dissertation weder in gleicher noch in ähnlicher Form bereits in einem anderen Prüfungsverfahren vorgelegen hat.

Würzburg……

Datum Unterschrift